The reactivity of mononuclear molybdenum and rhenium alkyne complexes

Rumble, S. J.

Award date:
1994

Awarding institution:
University of Bath

THE REACTIVITY OF MONONUCLEAR MOLYBDENUM AND RHENIUM ALKYNE COMPLEXES.

submitted by S. J. Rumble for the degree of PhD of the University of Bath

1994

ProQuest LLC
789 East Eisenhower Parkway
P.O. Box 1346
Ann Arbor, MI 48106-1346

Abstract:

The formation and synthesis of molybdenum and rhenium mono- and bis-alkyne complexes and their subsequent reactivity form the basis of this thesis.

Chapter one deals with the synthesis of the two molybdenum propargyl complexes [Mo(η^2(2e)-MeC_2R)(σ,η^2(3e)-CH_2C_2R)(η–C_5H_5)] (R= Me, Ph) and the crystal structure determination of the phenyl-propyne system, as well as their reactivity towards carbon monoxide, leading to a novel cyclisation reaction. The X-ray structures of both cyclic complexes are discussed, and the reaction of the cyclic but-2-yne derived complex with $HBF_4.Et_2O$ with the X-ray structure of the resulting cationic bis-allyl complex.

Chapter 2 is concerned with the synthesis and characterisation of the rhenium butadienyl complex [BrRe{η^1,η^1,η^2(5e)=C(Ph)C(Ph)C(Ph)=CHPh}(η–C_5H_5)] and the evidence for a novel type of bent rhenium-carbon interaction between the metal and η^4(5e)-butadienyl fragment.

Chapter 3 deals with the synthesis of two rhenium-alkene complexes by reaction of the corresponding η^2–vinyl complexes with the electrophilic reagents trityl tetrafluoroborate and tetrafluoroboric acid, also a discussion of the evidence for η^2–stabilisation from the phenyl substituent of the alkene moiety to give a formal η^4(4e)-buta-1,3-diene.

Chapter 4 summarises the reactivity of several cyclopentadienyl-rhenium alkyne complexes towards phosphorous containing ligands, including a spin saturation transfer experiment on the η^2–vinyl complex [BrRe=C(Ph)CH(Ph){$P(OMe)_3$}(η–C_5H_5)].

Chapter 5 contains experimental detail and the appendix contains supplementary crystallographic data.

MEMORANDUM

The work described within this thesis was carried out by the author between October 1991 and October 1994 in the Department of Inorganic Chemistry at the University of Bath. Unless otherwise acknowledged it is the individual work of the author and has not been submitted for any other degree.

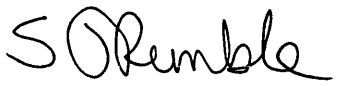

ACKNOWLEDGEMENTS

I would like to thank, first and foremost my Ph.D. supervisor Professor Michael Green, who has supplied endless advice and encouragement throughout the course of the work contained within this thesis.

Special thanks to Dr Carla Carfagna whose help has been invaluable in the completion of this work. Many of the results in this thesis could not have been presented without the assistance of many others. In particular, many thanks to Dr Mary Mahon who was responsible for the collection of the X-ray diffraction studies contained in this thesis, Dr R. J. Deeth for the theoretical studies and Dr R. Kinsman for his assistance with the spin-saturation transfer experiment. Also a big thank you to the rest of the technical staff within the department.

My fellow laboratory companions deserve a mention for putting up with my sense of humour, and special thanks to Jackie for keeping me sane.

I thank the Science and Engineering Research Council for their financial support in the form of a Research Studentship over the past three years.

Finally thanks to my parents for their continued support during the six years of my University life.

Abbreviations

M	:	metal atom
Re	:	rhenium
Mo	:	molybdenum
L	:	ligand
X	:	halide
Nu	:	nucleophile
R	:	alkyl group
Me	:	methyl
Ph	:	phenyl
Bu	:	butyl
detc	:	N,N,diethyldithiocarbamate
dmtc	:	N,N,dimethyldithiocarbamate
dppe	:	1,2-diphenylphosphinoethane
dppf	:	1,1`-bis(diphenylphosphino) ferrocene
arphos	:	1-diphenylphosphino 2-diphenylarsino ethane
s	:	secondary
t	:	tertiary
MO	:	molecular orbital
thf	:	tetrahydrofuran
Et_2O	:	diethyl ether
CH_2Cl_2	:	dichloromethane
TMS	:	tetramethylsilane
Cp, η–C_5H_5	:	η^5-cyclopentadienyl

Å	:	angstrom
i.r	:	infra-red
uv	:	ultra-violet
mol	:	mole
mmol	:	milli-mole
g	:	gram
mg	:	milli-gram

in relation to nmr data:

n.m.r	:	nuclear magnetic resonance
ppm	:	parts per million
J	:	scalar coupling constants in Hz
δ	:	chemical shift relative to TMS
s	:	singlet
d	:	doublet
t	:	triplet
q	:	quartet
m	:	multiplet
br	:	broad

in relation to infra-red data:

ν(CO)	:	frequency of carbonyl stretch in cm^{-1}

in relation to mass spectral data:

(M^+)	:	parent molecular ion

in relation to X-ray diffraction data:

a, b, c	:	unit cell edge lengths in Angstroms
Z	:	number of molecules per unit cell

CONTENTS **PAGE No.**

CHAPTER ONE:	Synthesis and reactions of molybdenum propargyl complexes.	1
1.1	Development of metal-alkyne chemistry.	2
1.2	Development of molybdenum alkyne chemistry.	6
1.3	Deprotonation of molybdenum bis-alkyne halides.	9
1.4	Reaction of [MoBr(η^2–PhC_2Me)$_2$(η–C_5H_5)] with Li[N($SiMe_3$)$_2$].	10
1.5	The X-ray structure of [Mo(σ,η^2–CH_2C_2Ph) (η^2–PhC_2Me)(η–C_5H_5)].	11
1.6	A Review of recent complexes containing the σ,η^2–propynyl ligand.	14
1.7	Structural aspects of [Mo(σ,η^2–CH_2C_2Ph) (η^2–PhC_2Me)(η–C_5H_5)].	18
1.8	Attempts at reversal of the dehydrohalogenation step.	20
1.9	Reactions of [Mo(σ,η^2–CH_2C_2R) (η^2–RC_2Me)(η–C_5H_5)] (R= Me, Ph) with carbon monoxide.	21
1.10	The X-ray structure of [Mo{η^2,η^3(5e)-C(Ph)C(O) C(Me)C(Ph)C-CH_2}(CO)(η–C_5H_5)].	23
1.11	The X-ray structure of [Mo{η^2,η^3(5e)-C(Me)C(O) C(Me)C(Me)C-CH_2}(CO)(η–C_5H_5)].	26
1.12	A proposed mechanism for the formation of [Mo{η^2,η^3(5e)-C(R)C(O)C(Me)C(R)C-CH_2}	28

	(CO)(η–C_5H_5)] (R= Me, Ph).	
1.13	The reaction of [Mo{η^2,η^3(5e)-C(Me)C(O) C(Me)C(Me)C-CH_2}(CO)(η–C_5H_5)] with $HBF_4.Et_2O$.	30
1.14	The X-ray structure of [Mo{η^3,η^3(6e)-C(Me)C(OH) C(Me)C(Me)C-CH_2}(CO)(η–C_5H_5)][BF_4].	31
CHAPTER 2:	The synthesis of a novel η^4(5e)-butadienyl: Evidence for a bent rhenium-carbon bond.	34
2.1	Development of η^2–vinyl chemistry.	35
2.2	The bonding of an η^2–vinyl to a metal centre.	38
2.3	The chemistry of metal bis-alkyne chemistry.	41
2.4	The development of η^4(5e)-butadienyl complexes.	44
2.5	The X-ray structure of [ReBr $(PhC_2Ph)_2$(η–C_5H_5)][PF_6].	48
2.6	Reaction of [ReBr($PhC_2Ph)_2$(η–C_5H_5)][PF_6] with $LiBHEt_3$.	51
2.7	The X-ray structure of [BrRe{η^1,η^1,η^2 (5e)=C(Ph)C(Ph)C(Ph)=CHPh}(η–C_5H_5)] **7**.	53
2.8	The nature of the unusual rhenium-carbon (Re-C7) interaction within complex **7**.	56
2.9	Evidence for the formation of an η^2–vinyl intermediate in the synthesis of complex **7**.	60
2.10	A proposed mechanism for the formation of the novel η^4(5e)-butadienyl complex **7**.	61
2.11	The formation of the rhenium bis-alkyne complex [ReBr($PhC_2Me)_2$(η–C_5H_5)][PF_6].	64

CHAPTER 3:	The synthesis of rhenium-alkene complexes: Evidence for η^2–stabilisation from a phenyl ring.	66
3.1	Transition metal-alkene chemistry.	67
3.2	Reaction of [BrRe=C(Ph)CH(Ph)(Ph_2MeP)(η–C_5H_5)] with trityl tetrafluoroborate.	70
3.3	Reaction of [BrRe=C(Ph)CH(Ph)(Ph_2MeP)(η–C_5H_5)] with tetrafluoroboric acid.	72
3.4	A Theoretical study on [BrRe=C(H)CH_2(PH_3)(η–C_5H_5)].	76
3.5	A proposed mechanism for the formation of the rhenium-alkene complex [ReBr{CH(Ph)=CPh(CPh_3)} (Ph_2MeP)(η–C_5H_5)][BF_4].	79
3.6	A proposed mechanism for the formation of the rhenium-alkene complex [ReBr{CH(Ph)=CH(Ph)} (Ph_2MeP)(η–C_5H_5)][BF_4].	82
3.7	Closing Comments.	83
CHAPTER 4:	The reactions of [$ReBr_2$(η^2-PhC_2R)(η–C_5H_5)] (R=Me, Ph) towards phosphorous containing ligands.	84
4.1	The reactivity of [$ReBr_2$(η^2-PhC_2Me)(η–C_5H_5)] towards mono-dentate phosphorous ligands.	85
4.2	The synthesis of rhenium alkyne di-cations by reaction of [$ReBr_2$(η^2-PhC_2R)(η–C_5H_5)] (R= Ph, Me) with bidentate phosphorous ligands.	87
4.3	The formation of the neutral η^2-vinyl complex [BrRe=C(Me)CH(Ph)(PPh_3)(η-C_5H_5)].	90
4.4	The synthesis of [BrRe=C(Ph)CH(Ph){$P(OMe)_3$} (η–C_5H_5)] and a spin saturation transfer experiment.	94

CHAPTER 5:	Experimental:	99
5.1	General practical details.	100
5.2	Characterisations.	100
5.3	Preparation of starting materials.	101
5.4 - 5.19	Preparation of novel complexes.	102
References:		118
Appendix:	Supplementary X-ray crystallographic data.	127

CHAPTER 1:

The synthesis and reactivity of molybdenum propargyl complexes.

1.1 Development of metal-alkyne chemistry.

Recently a considerable amount of research has been focused on the area of metal alkyne complexes. Only in recent times has the idea developed that an alkyne ligand could co-ordinate to a metal centre in a way other than the classical two electron σ donor/π acceptor as rationalised by the Dewar-Chatt-Duncanson model of transition metal alkyne bonding (fig 1).[1,2]

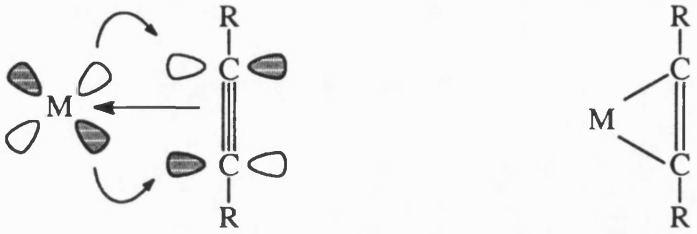

FIGURE 1

This model suggests that the alkyne is bonded by a combination of σ interaction, alkyne π to metal "dsp" and a π interaction metal d to alkyne π* (fig 1-A), or it can also be pictured in the extreme form consisting of two metal carbon bonds with complete re-hybridisation of the carbon atoms (fig 1-B). Examples of both these extremes are known, $[RhCl\{P(C_6H_5)_3\}_2C_4F_6]$ has the bonding mode shown as in fig 1-A whereas the platinum complex $[Pt\{P(C_6H_5)_3\}_2C_4F_6]$ has the bonding mode as shown in fig 1-B. The examples of metal alkyne complexes had tended to support this classical method of bonding, showing reactivity analogous to that which is seen in metal-alkene chemistry.[3,4,5,6] Evidence that suggested that alkynes could co-ordinate with a metal centre to a greater extent than as a two electron donor ligand came in 1963 when Tate and Augl published a communication containing the detailed synthesis of an tris-alkyne tungsten carbonyl complex (fig 2).[7,8]

$$[(CH_3CN)_3W(CO)_3] \xrightarrow{\Delta,\ \text{Hex-3-yne}} [W(CO)(EtC{\equiv}CEt)_3]$$

FIGURE 2

The proposed structure for this complex was pseudo tetrahedral (fig3). On examination of the spectroscopic data collected on this complex it was noted that all three alkyne ligands were equivalent.

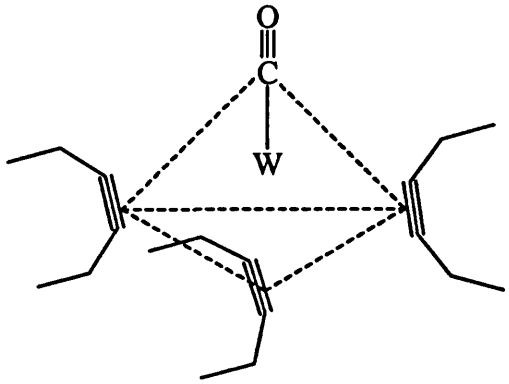

FIGURE 3

The effective atomic number for tungsten requires that to fully satisfy the eighteen electron rule the alkyne ligands must donate 10 electrons to the metal centre, their apparent equivalence suggesting that each alkyne ligand effectively donates "$3^1/_3$" electrons. This could be rationalised by two of the alkyne ligands donating both their π–electron pairs to the metal centre (similar to $[Pt(R_3P)_2ac]$ and $[ReCl(ac)_2]$[9,10]) and the third only one pair.

In 1968 King[11] published calculations which showed that it would be impossible for all three of the alkyne ligands contained within the complex to donate four electrons as only two sets of metal p and d orbitals are available to receive electron pairs by dative π–bonding from the alkyne ligands, the third ligand being able only to donate two electrons in the classical σ-donor/π-acceptor mode as seen previously. This leads to a total of ten electrons being donated by the three alkyne ligands, as required to satisfy the eighteen electron rule, the equivalence of the three ligands can be accommodated by fluxional switching of the alkyne bonding mode from two to four electrons within the spectroscopic time scale. In 1972, Laine and Bau[12] successfully established the X-ray crystal structure determination for the complex $[W(PhC_2Ph)_3(CO)]$. This showed that the molecule had a C_{3v} symmetry supporting the proposed pseudo-tetrahedral structure of Tate. The X-ray data showed that the alkyne ligand geometry had been grossly altered on co-ordination to the metal, the angle about the previously sp hybridised quaternary carbon atoms decreasing to 140°, an expected feature of metal alkyne complexes.[13,14]

Several papers that have been published since Kings' original calculation are all in broad agreement as to the nature of the bonding in the four electron donor alkyne co-ordinating to the metal centre (fig4).[17,18,19] The four electron donor properties arising when the two electrons in the alkyne π perpendicular orbitals supplement the π parallel bond, in order to alleviate the electron deficiency at the metal centre. These four electron alkynes can be identified using spectroscopic methods. Templeton and Ward published a communication in which they showed a correspondence between the carbon-13 chemical shifts of the alkyne ligands with the variable electron donation to a metal centre.[20] They observed a relationship between δ(ppm) and N(no of electrons donated) which can be illustrated by considering three molybdenum (II) alkyne complexes (fig5).

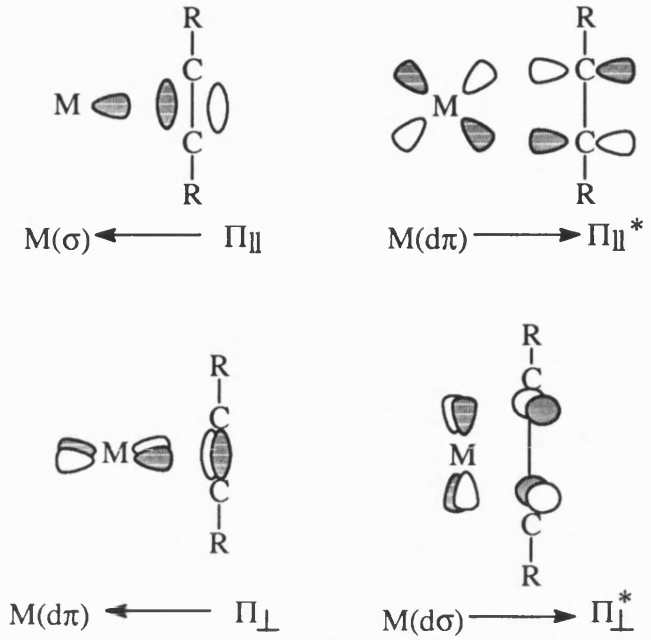

FIGURE 4

complex	δ–($R^{13}C_2R$)	δ–average	N
$(\pi\text{–}C_5H_5)_2Mo(HC_2H)$	117.7	117.7	2
$Mo(detc)_2(HC_2H)_2$	183.2, 177.1	180.2	3
$Mo(CO)(dmtc)_2(HC_2H)$	192.5, 187.4	190.0	4

FIGURE 5

The $^{13}C\text{-}\{^1H\}$ chemical shifts for these three complexes span a range of >80 ppm and reflects the relationship between δ and N, although a plot of δ vs N for known metal-alkyne complexes is not exactly linear it shows that δ is an observable piece of data that is highly sensitive to the nature of the metal-alkyne bonding mode, therefore providing experimental data which can allow the role of an alkyne ligand within a complex to be established.

1.2 Development of molybdenum alkyne chemistry.

In 1977 M. Green et al[21,22] observed that addition of silver tetrafluoroborate to a dichloromethane solution of the complex $[Mo_2(CO)_6(\eta^5\text{–}C_9H_7)_2]$ in the presence of an excess of an alkyne, led to a redox reaction resulting in the deposition of a silver mirror and a solution containing the cationic complex $[Mo(CO)(\eta^2\text{–}RC_2R)_2(\eta^5\text{–}C_9H_7)][BF_4]$ which was isolated after filtration and recrystallisation in excellent yields.[21,22]

The first reactions on these complexes showed that they were highly reactive towards trimethylphosphite giving access to the unusual blue to purple crystalline mono-alkyne complexes $[Mo\{P(OMe)_3\}_2(\eta^2\text{–}RC_2R')(\eta^5\text{–}C_9H_7)][BF_4]$; (R=R'=Me; R=R'=Ph; R=Bu^t, R'=H; R=Pr^i, R'=H). This chemistry was extended to the related η^5–cyclopentadienyl complexes, it was also discovered that the use of expensive silver salts could be avoided by forming the bis-alkyne complex by reaction of the easily synthesised complex $[Mo(NCMe)_2(CO)_2L]^+$ (L=$\eta^5\text{–}C_9H_7$ or $\eta^5\text{–}C_5H_5$) in the presence of an alkyne, which can readily replace the extremely labile acetonitrile ligands (fig6).[23]

These phosphite cations were expected to be reactive to the hydride sources $Na[BH_4]$ and $K[BHBu^s_3]$.[23,24] A smooth reaction was observed which led to the formation of a yellow crystalline η^3–anti-1-methyl allyl complex $[Mo\{P(OMe)_3\}_2(\eta^3\text{–anti } CH_2\ CH\ CHMe)(\eta\text{–}C_5H_5)]$. Possible mechanisms for the formation of the η^3–allyl involve either reaction of "H^-" directly with the quaternary alkyne carbon, or attack via the metal centre, this process being assisted by a switch in the alkyne bonding mode from 4 to 2 electrons.

There is also a third type of reaction possible which was observed by F. Feher.[25] That is namely a deprotonation reaction of the cations such as $[Mo\{P(OMe)_3\}_2(\eta^2\text{–}PhCH_2C_2Ph)(\eta\text{–}C_5H_5)][BF_4]$, which might be expected to form either an η^2–allenyl or a metallamethylenecyclopropene complex.

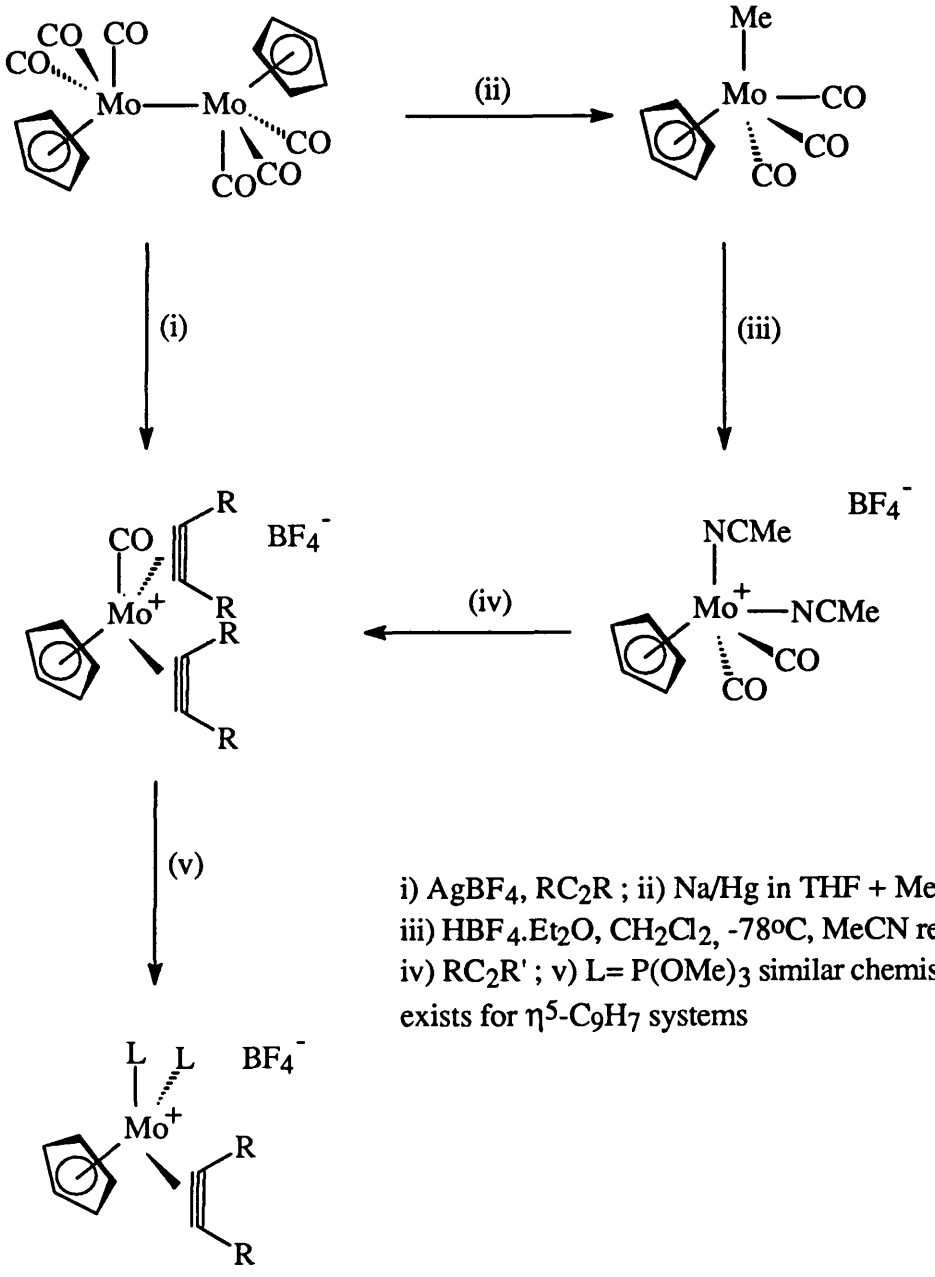

i) $AgBF_4$, RC_2R ; ii) Na/Hg in THF + MeI
iii) $HBF_4.Et_2O$, CH_2Cl_2, -78°C, MeCN reflux
iv) RC_2R' ; v) L= $P(OMe)_3$ similar chemistry exists for η^5-C_9H_7 systems

FIGURE 6

Reaction of $[Mo\{P(OMe)_3\}_2(\eta^2\text{–}PhCH_2C_2Ph)(\eta\text{–}C_5H_5)][BF_4]$ in diethyl ether in the presence of KH and a catalytic amount of Bu^tOH leads to the formation of a

neutral purple complex, identified as a mixture of two isomeric η^2–(3e) allenyl complexes, which differ with respect to the orientation of the phenyl and hydrogen on the γ carbon (fig7).

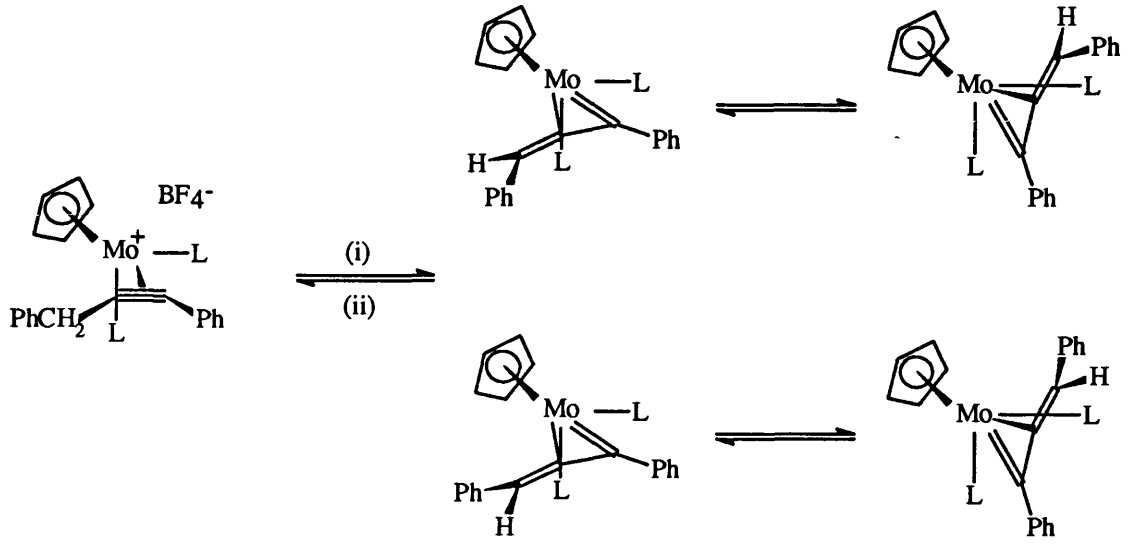

i) KH, Bu^{t}OH, Et_2O; ii) $HBF_4.Et_2O$

FIGURE 7

The η^2–allenyl fragment would be expected[26,27] to adopt planar geometry since the transformation of an η^1–(1e) allenyl to an η^2–(3e) allenyl must allow rotation to allow interaction between the metal and the C_α-C_β π system (fig8).

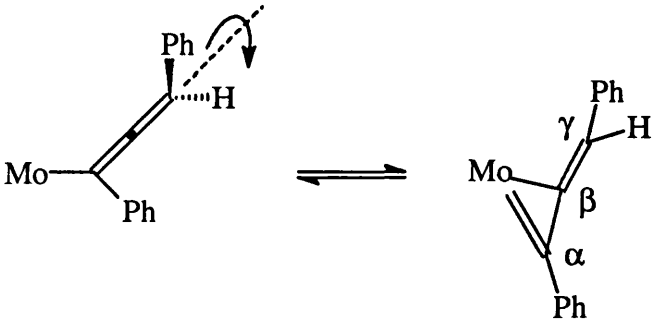

η^1(1e) η^2(3e)

FIGURE 8

The reverse of this reaction can be achieved by reaction of the η^2–allenyl with $HBF_4.Et_2O$ in dichloromethane.

1.3 Deprotonation of bis-alkyne molybdenum halides.

Complexes of the type $[MoBr(\eta^2\text{–}RC_2Me)_2(\eta\text{–}C_5H_5)]$ (R=Me, Ph) can be accessed by reaction of the corresponding acetonitrile complex with lithium bromide. Complexes of this type containing α-hydrogens might be expected to undergo a dehydrohalogenation reaction in the presence of a base such as $Li[N(SiMe_3)_2]$ (fig9) to form an η^2–(3e) allenyl species similar to the type of reaction seen previously with the complex $[Mo\{P(OMe)_3\}_2(\eta^2\text{–}PhCH_2C_2Ph)(\eta\text{–}C_5H_5)]$ (fig7).

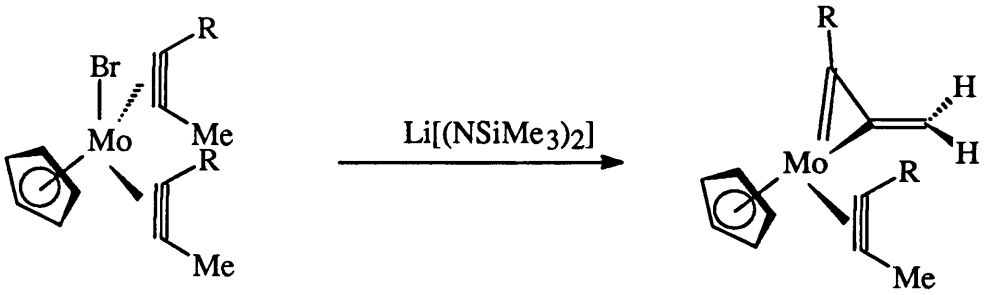

FIGURE 9

Preliminary attempts by C. Woolhouse on the but-2-yne complex $[MoBr(\eta^2\text{–}MeC_2Me)_2(\eta\text{–}C_5H_5)]$ proved inconclusive. Examination of the nmr data suggested that due to the lack of a low field $^{13}C\text{-}\{^1H\}$ molybdenum carbene bond a different type of reaction had occurred.[28] A reinvestigation into this area was undertaken to try and identify the product of this unexpected result.

1.4 Reaction of $[MoBr(\eta^2\text{–}PhC_2Me)_2(\eta\text{–}C_5H_5)]$ with $Li[N(SiMe_3)_2]$.

Treatment of $[MoBr(\eta^2\text{–}PhC_2Me)_2(\eta\text{–}C_5H_5)]$, (thf, -78°C) with one molar equivalent of the base $Li[N(SiMe_3)_2]$ afforded (70% yield) a red, crystalline, hydrocarbon soluble air sensitive compound (**1**). Although elemental analysis confirmed the expected molecular formula $[Mo(PhC_3H_2)(\eta^2\text{–}PhC_2Me)(\eta\text{–}C_5H_5)]$ for complex **1**, as in the previous but-2-yne example the absence in the $^{13}C\text{-}\{^1H\}$ nmr spectrum of a low field alkylidene α-carbon of the expected three electron η^2–allenyl fragment suggested that the sought for reaction had not in fact occurred. Examination of the ^1H nmr data also showed that the coupling constants for the two protons on the organic fragment were not consistent with that expected for an sp^2 hybridised carbon atom. Examination of the $^{13}C\text{-}\{^1H\}$ and coupled ^{13}C nmr spectra revealed resonances and coupling constants fully consistent with the suggested structure for **1** (fig10). Where a $Mo(\eta^5\text{–}C_5H_5)$ fragment is co-ordinated to a four electron η^2–bonded phenylpropyne and a three electron σ,η^2–prop-2-ynyl fragment. Thus the room temperature ^1H nmr spectrum exhibited a phenyl multiplet at δ7-8, an $\eta^5\text{–}C_5H_5$ resonance at δ4.88 and two doublets centred at δ5.01 and δ3.9 attributable to the two inequivalent propynyl hydrogens, which are coupled to each other with coupling constant $J(H^aH^b)$ 10.8Hz.

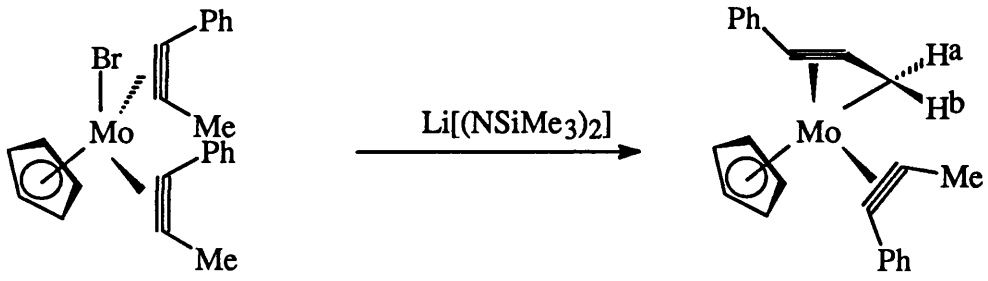

FIGURE 10

The ^{1}H nmr spectrum also showed a singlet at δ2.42 due to the methyl of a rotating four-electron η^2–bonded phenylpropyne ligand, its bonding mode is qualified by the ^{13}C-{^{1}H} nmr spectrum which shows two singlets at δ207.7 and δ197.0 attributable to the quaternary carbons of a four electron alkyne.[20] In the ^{1}H coupled ^{13}C nmr spectrum singlets at δ142.3 and δ124.86 are assigned to the quaternary propynyl carbons and are consistent with those values expected for a two electron donor alkyne ligand. The spectrum also shows a doublet of doublets at δ41.26 [J(CH^a) 158.6Hz; J(CH^b) 165.3Hz] due to the propynyl CH_2 group, the magnitude of the coupling constants being consistent with the proposed structure for **1**. After a great deal of effort X-ray quality crystals of complex **1** were grown, confirming the structure shown in fig10.

1.5 The X-ray structure of [Mo(σ,η^2–CH_2C_2Ph)(η^2–PhC_2Me)(η–C_5H_5)](**1**).

A single crystal determination for complex **1** was carried out to confirm the precise bonding within the propynyl ligand as one of two possible canonical forms was considered (fig11).

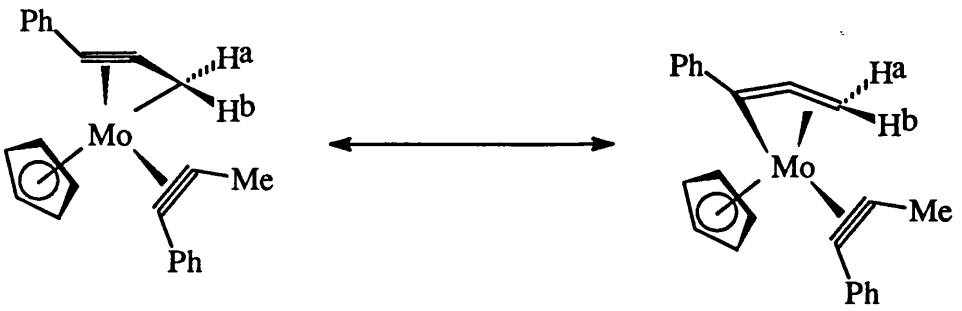

1a **1b**

FIGURE 11

Crystals of **1** were found to be orthorhombic belonging to the space group $P2_12_12_1$. The cell parameters were a=8.2346(7), b=10.667(2), c=20.604(2)Å and Z=4. Equivalent reflections were merged to give data and the structure was solved using Patterson methods using the SHELX[29] suite of programs. Hydrogen atoms were included at calculated positions except in the case of H171 (H^a) and H172 (H^b) which were located in an advanced difference Fourier and refined at a fixed distance of 1.08Å from C17. Final residuals after 10 cycles of least squares were R=0.0267, Rw=0.0292 full tables of the X-ray data can be found in the appendix.
Figure 12 shows the geometry of the molecule and the atomic numbering scheme used, selected bond lengths and angles are shown in table 1.

Bond Lengths/Å		Bond Angles/°	
Mo-C15	2.105	C6-C7-C8	141.4
Mo-C16	2.164	C15-C16-C17	146.1
Mo-C17	2.278		
C15-C16	1.281		
C16-C17	1.404		

TABLE 1

The crystal structure confirms that the molybdenum centre is bonded to an η^2–phenylpropyne and a σ,η^2–phenylpropynyl ligand, supported by the spectroscopic data discussed in the previous section. The propynyl fragment is seen to be σ-bonded to the metal via C17 and π-bonded via the alkyne triple bond between C15 and C16. The bond lengths confirm that the bond between C16-C17 is typical of a carbon-carbon single bond and that the bond between C15-C16 typical of a triple bond.

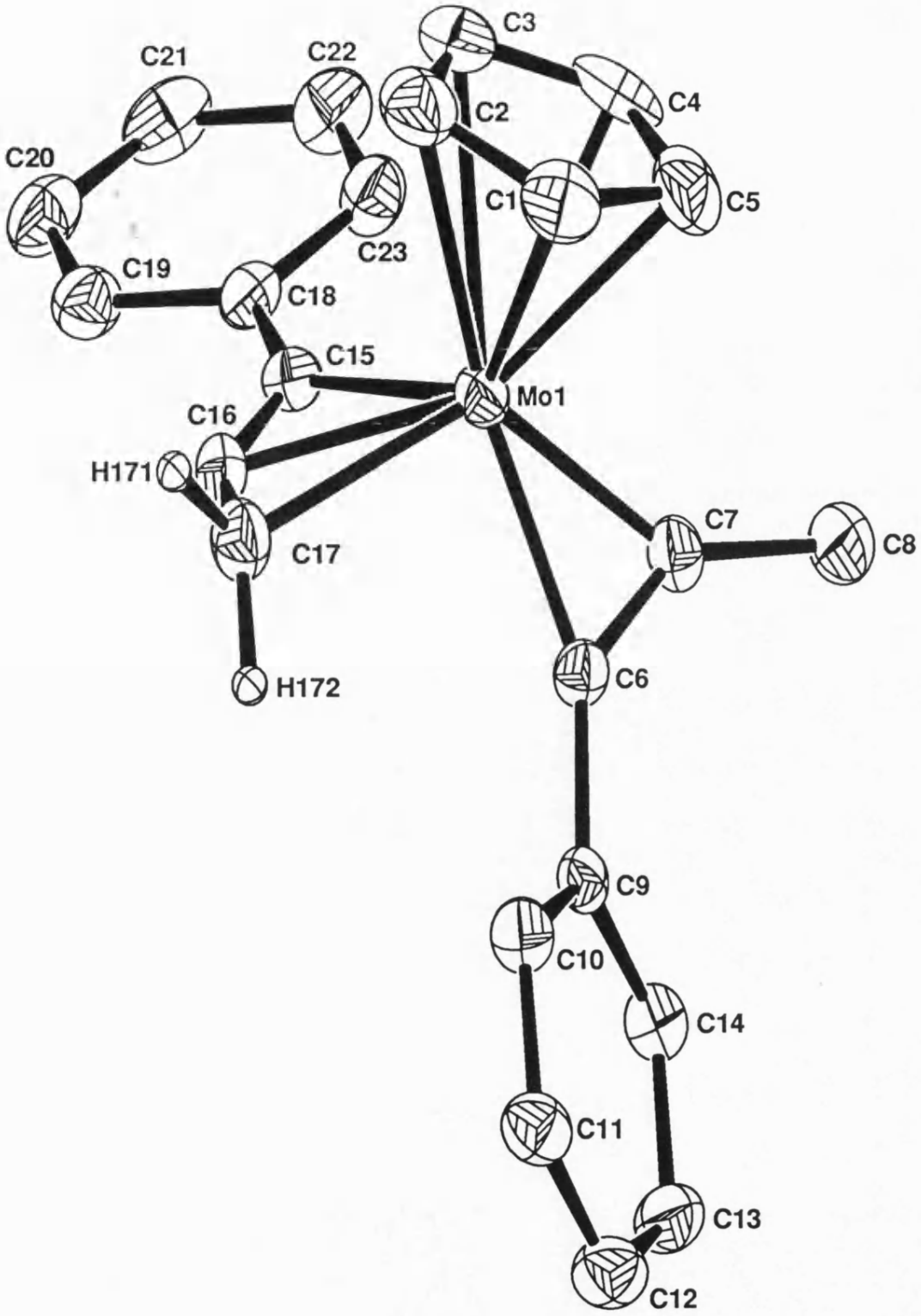

FIGURE 12

X-ray structure of [Mo(σ,η^2–CH_2C_2Ph)(η^2–PhC_2Me)(η–C_5H_5)] **1** phenyl and cyclopentadienyl hydrogens omitted for clarity.

The lack of any significant delocalisation across the propynyl ligand suggesting that the canonical form **1a** shown in figure 11 is that adopted by the molecule. The synthesis of **1** constitutes the first synthesis of a three electron σ,η^2–propynyl complex by deprotonation of a three or four electron η^2–alkyne complex.
Complex **1** is another example within a growing family of structures which contain this unusual σ,η^2–propynyl type of ligand.

1.6 A review of recent publications of complexes containing the σ,η^2–propynyl ligand.

Recently there has been several examples of three electron σ,η^2–propynyl complexes of Fe[30,31],Ru[32,33,34],Os[35] and W[36] carrying a =CHR group attached to the propynyl terminus i.e. σ,η^2–RC_2C=CHR, and shown to be formed in alkynyl-vinylidene coupling reactions. One of the first examples of an unsubstituted system was published in 1991.[37] It was found that uv irradiation of tricarbonyl molybdenum-arene complexes in the presence of prop-2-yn-1-ol and $HBF_4.Et_2O$ in a diethyl-ether solution yields stable complexes containing the previously unknown η^3–C_3H_3 ligand (fig13).

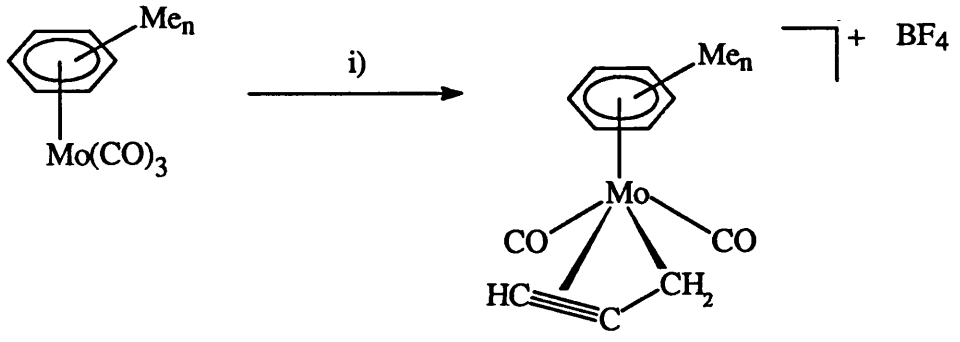

n=3,5,6 i) $HC{\equiv}CCH_2OH$, HBF_4Et_2O, uv irradiation <10^{0}C

FIGURE 13

These complexes were characterised by IR, ^{1}H and $^{13}C-\{^{1}H\}$ nmr spectroscopy and by single crystal X-ray structure analysis, which were carried out for the pentamethylbenzene derivative. In this molecule as in the π-allyl complexes $[Mo(\eta^3-C_3H_5)(CO)_2(\eta-C_5H_5)]$[38] and $[Mo(\eta^3-C_3H_5)(CO)Cl_2(\eta-C_5H_5)]$[39] the three carbon atoms are at bonding distances from the Mo atom (2.282-2.340Å). However, in contrast to these allyl complexes wherein the central carbon atom is considerably (ca. 0.7Å) displaced from the plane passing through the metal atom, within the propynyl complex it was found that the MoC_3 fragment was planar to within 0.014Å. It was also noted that the alkyne bond length (1.236Å) is somewhat shorter than in most transition metal complexes with co-ordinated alkynes, 1.269Å in $[Mo(\eta^2-PhC_2Ph)(\eta-C_5H_5)_2]$[40], 1.277Å in $[Mo(CO)(\eta^2-MeC_2Me)_2(\eta-C_5H_5)][BF_4]$.[41] As discussed previously the complex can be considered as one of two canonical forms (fig11) where the propynyl form contributes considerably more than the other.

Another recent example of a complex with this novel type of ligand was published by C. P. Casey.[42] After a recent publication where it was shown that hydride extraction of the rhenium-propene complex $[Re(CO)_2(CH_2=CHCH_3)(\eta-C_5H_5)]$ with trityl hexafluorophosphate (commonly used for the abstraction of a hydride) gave the η^3–allyl rhenium complex $[Re(CO)_2(\eta^3-CH_2CHCH_2)(\eta-C_5H_5)][BF_4]$[43] this type of abstraction was extended to include rhenium alkyne complexes. It was shown that hydride abstraction of the rhenium alkyne complex $[Re(\eta^2-MeC_2Me)(CO)_2(\eta-C_5Me_5)]$ produced the σ,η^2–propargyl complex $[Re(CO)_2(\eta^3-CH_2C_2CH_3)(\eta-C_5Me_5)][PF_6]$ (fig14). The spectroscopic data for the propargyl complex is comparable with that seen for the systems discussed in section 1.3. The alkyne ligand within $[Re(\eta^2-MeC_2Me)(CO)_2(\eta-C_5Me_5)]$ is acting as a two electron donor and the reaction was the first example for synthesis of a η^3–propargyl via hydride abstraction from a rhenium-alkyne complex.

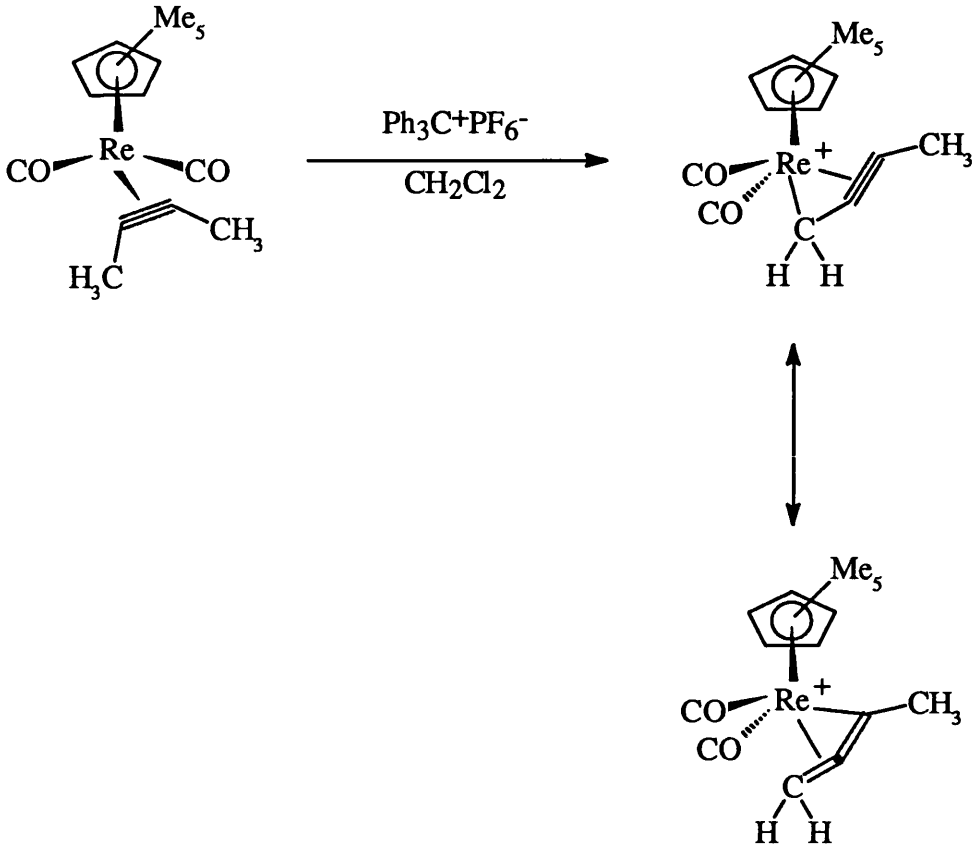

FIGURE 14

These two examples are of cationic propargyl complexes, but recently another publication containing an example of a neutral complex containing this type of ligand was released.[44] This paper deals with the synthesis of two neutral zirconium complexes, $Cp_2Zr(CH_3)(\eta^3\text{–}C(Ph)=C=CH_2)$ **A** and $Cp_2Zr(CH_2CCPh)_2$ **B**, the CH_2 resonance in the ^1H nmr of **A** is downfield of that expected for an η^3–phenylpropargyl[45,46] and upfield of that expected for an η^1–phenylallenyl ligand[44], but are comparable with the two examples previously discussed.[37,42] However, the $^{13}C\text{-}\{^1H\}$ nmr chemical shifts of the CH_2CC unit were not in agreement with those shifts reported for η^1–propargyl[45,46], η^3–propargyl[37,42], or η^1–allenyl[46,47,48] complexes. An X-ray crystal study revealed that this complex does indeed contain the unusual phenylallenyl ligand, this bonding description is qualified by

looking at the carbon-carbon bond lengths within the phenylallenyl moiety. In contrast to those shown in table 1 where the fragment shows triple bond character, this complex contains double bond character within the moiety and has the alternative resonance shown in figure 15.

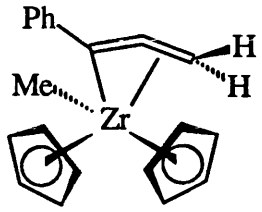

FIGURE 15

The second complex discussed in this paper, complex **B** is of interest as the ^1H nmr data shows fluxionality, which when frozen out reveals that the complex contains one η^1–propargyl and one η^3–allenyl fragment, which at ambient temperature interconvert as illustrated in figure 16. This represents the first example where both the proposed resonances for the propargyl ligand are seen within one complex.

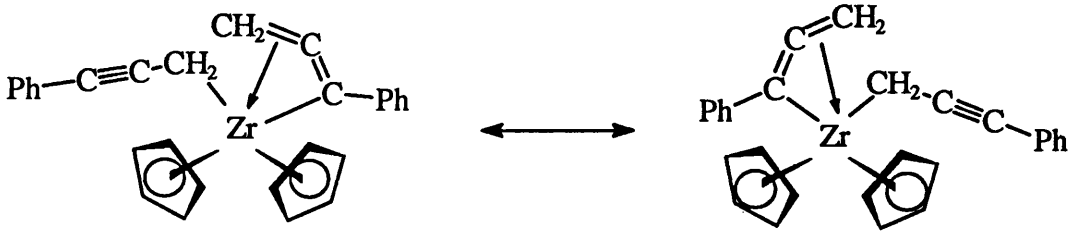

FIGURE 16

1.7 Structural aspects of [Mo(σ,η^2–CH_2C_2Ph)(η^2–PhC_2Me)(η–C_5H_5)] (**1**).

In the light of the unexpected formation of a propynyl ligand in the reaction of [MoBr(η^2–$PhC_2Me)_2$(η–C_5H_5)] with Li[N(SiMe$_2$)$_2$], and not the expected η^2–allenyl complex, a proposed mechanism for the formation of **1** is shown in figure 17. It is believed that the expected η^2–allenyl complex is formed originally in the reaction, but undergoes a rearrangement to form the η^1–allenyl, which then becomes bent allowing co-ordination to the molybdenum centre and therefore satisfying the eighteen electron rule. As shown previously this is in fact one of the canonical forms possible for an σ,η^2–propynyl ligand known to be formed in the reaction. This rearrangement may occur in this instance due to the presence of an extra alkyne in comparison to the phosphite ligands seen in the work of F. Feher, this extra alkyne may help to stabilise the 16 electron η^1–allenyl intermediate. An interesting structural aspect of this complex is that it can be seen as containing two co-ordinated alkynes, one adopting the usual U configuration *i.e* the phenyl-propyne ligand. However, the other alkyne contained within the propynyl fragment is held in an unusual Z configuration, due to the sigma bond from the CH_2 group to the metal centre. In principal either of these two alkynes could function as the four electron donor, but as shown by the nmr data it is in fact the normal U-alkyne which adopts this role in the complex, whereas the formal Z-alkyne is acting as the two electron donor. There is no evidence of a fluxional change of the bonding mode within the molecule as previously seen in the bis-alkyne systems.

Importantly the plane in which the three electron σ,η^2–propynyl ligand lies is not perpendicular to that of the η–C_5H_5 ligand, it would be expected that in the static state the four electron donor alkyne (phenyl-propyne) would lie parallel to the Mo-CH_2 vector in order to maximise backbonding as is seen in the crystal structure.

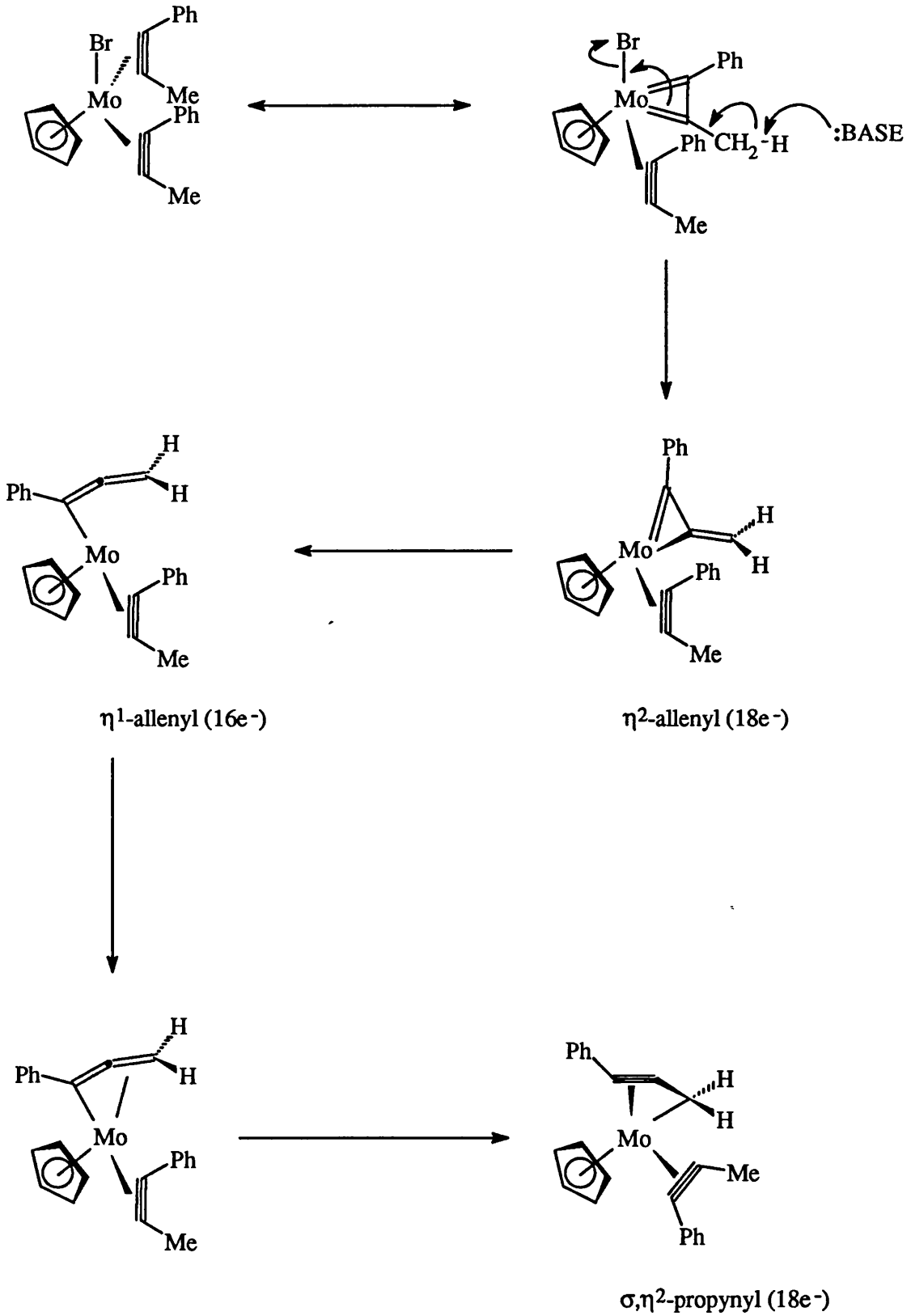
Ph
Br
Mo
Me
Ph
Me
Br
Ph
Mo
Ph
CH2
H
:BASE
Me
H
Ph
H
Mo
Ph
Me
Ph
H
H
Mo
Ph
Me
η1-allenyl (16e-)
η2-allenyl (18e-)
H
Ph
H
Mo
Ph
Me
Ph
H
H
Mo
Me
Ph
σ,η2-propynyl (18e-)

FIGURE 17

These neutral four electron η^2–alkyne, three electron σ,η^2–propynyl complexes are obviously of interest from the standpoint of reactivity, this is discussed further in section 1.9.

1.8 Attempts at reversal of the dehydrohalogenation step.

The reverse of this reaction may have been expected to produce a complex containing two effective "three" electron alkynes where the previously formal Z-alkyne had kept its configuration. However, protonation with trifluoroacetic acid [49] showed that the reaction reversed with the alkynes adopting the U-U configuration seen in the starting material, the reaction was repeated and followed by a low temperature nmr study in an attempt to show some evidence for the formation of an intermediate containing an alkyne held in the Z configuration, no such intermediate however, could be identified.

The protonation reaction would be expected to be charge controlled so a theoretical calculation was performed to discover which carbon atom in the σ,η^2–propynyl ligand carried the largest negative charge. The calculation was carried out by Miss J. McInnes and Dr. R. J. Deeth using the standard Extended Huckel Molecular Orbital (EHMO) method on the theoretical propargyl complex [Mo(σ,η^2-CH_2C_2H)(HC_2Me)(C_5H_5)], based on the X-ray structure and bond parameters for complex **1**, the hydrogen atoms were located 1.1Å from the parent atoms.[50] Table **2** shows the net charges for the propynyl ligand.

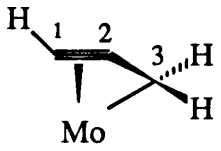

C1 -0.316	C2 +0.102	C3 -0.165

TABLE 2

These results suggest that protonation would attack C1 within the propynyl ligand, but it is known from the reaction that protonation proceeds via C3 to give the expected bis-alkyne complex. The negative charges seen on the two terminal carbons of the fragment are of similar magnitude, this suggests in the light of these results that other factors are directing the protonation reaction to proceed via C3 rather than the predicted reaction on C1, for example, there may be some electronic effect from the phenyl ring which is not seen in the theoretical study. A repeat of the calculation with the phenyl ring included indeed showed that the charge on C1 decreased to -0.206 and increased to -0.175 on C3. These two figures are much closer than in the unsubstituted system and possibly due to the steric hindrance of the phenyl ring the incoming HBF_4 attacks the less favourable carbon C3.

1.9 Reactions of $[Mo(\sigma,\eta^2\text{-}RC_2CH_2)(\eta^2\text{-}RC_2Me)(\eta\text{-}C_5H_5)][R=Ph, Me]$.

These two propynyl complexes can be viewed as eighteen electron systems each containing a 4e alkyne and 3e propynyl fragments. Both these types of ligands are able to switch their bonding modes, alkyne (4e-2e) and propynyl (3e-1e). This implies that in their 16 electron form they should be reactive towards two electron donor ligands.

Preliminary studies carried out by C. Woolhouse on the but-2-yne system showed that a reaction took place with carbon-monoxide and this led to the incorporation of two molecules of CO into the molecule, spectroscopically identified as one terminal and one acyl carbonyl, although the data did not fully establish the structure of the

resultant complex. A reinvestigation into this and the new phenylpropyne systems was carried out in an attempt to clarify the product of this reaction.

Reaction of carbon-monoxide bubbled through a solution of [Mo(σ,η^2–PhC_2CH_2)(η^2–PhC_2Me)(η–C_5H_5)] **1** at room temperature resulted in a colour change from red to yellow and the formation in good yield of an orange-yellow crystalline complex believed to be analogous to the but-2-yne system previously studied. This was confirmed spectroscopically by the presence of both a terminal carbonyl (ν_{co} 1925cm^{-1}) and acyl carbonyl (ν_{co} 1603cm^{-1}). The spectroscopic data for both these systems did not fully establish the structure of the products of the reaction and in fact suggested that a new type of reaction had occurred. This was confirmed by a single crystal X-ray diffraction study on crystals of both systems, revealing (fig18) that a new type of reaction had indeed occurred, leading to the formation of a novel alicyclic C_5 ligand with exocyclic oxygen and CH_2 groups. The inequivalence of the two exocyclic methylene hydrogens R=Me [δ3.27, d, 1H, J(H^aH^b) 2.2Hz; δ2.94, d, 1H, J(H^aH^b) 2.2Hz] and R=Ph [δ3.91, d, 1H, J(H^aH^b) 1.83 Hz; δ3.33, d, 1H, J(H^aH^b) 2.02Hz] and the acyl IR C-O stretch at 1595 cm^{-1} (R=Me) and 1603 cm^{-1} (R=Ph) suggest that canonical form A is of greater importance. The X-ray data for these two complexes are discussed in sections 1.10 and 1.11.

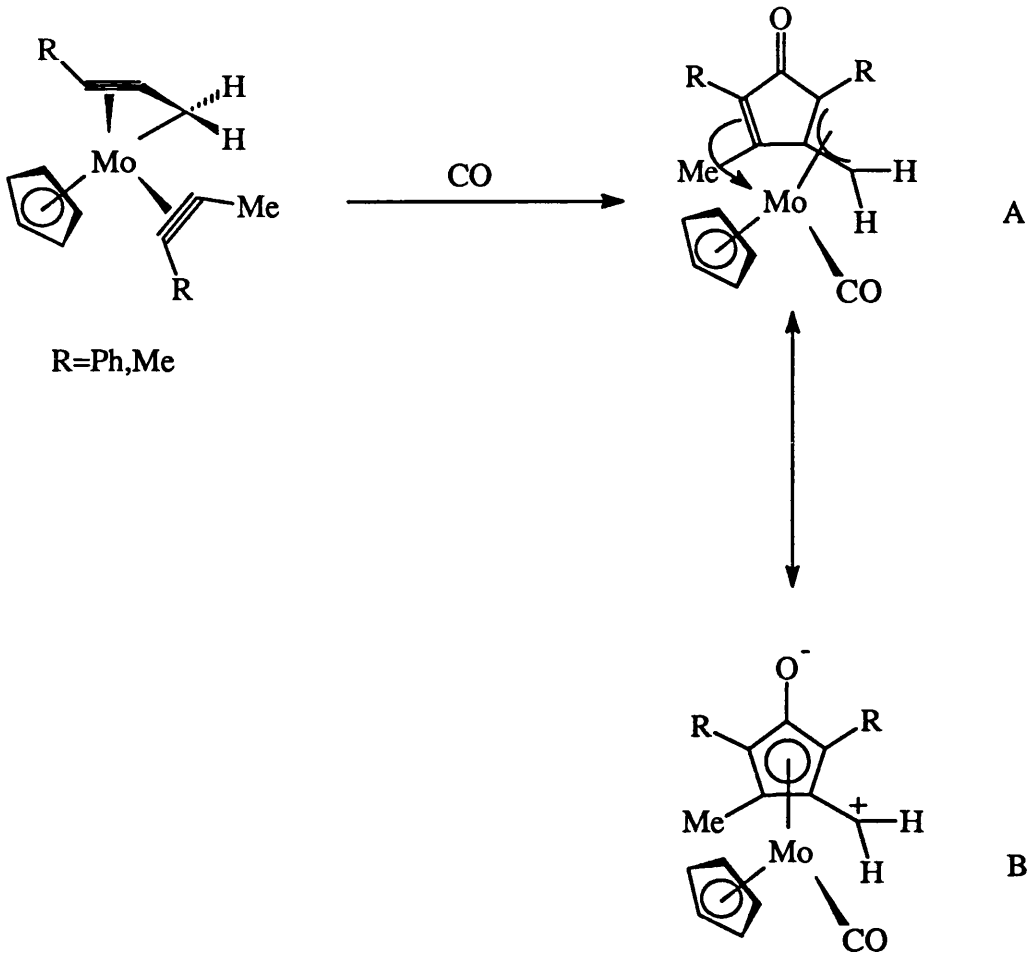

FIGURE 18

1.10 The X-ray structure of [Mo{$\eta^2\eta^3$(5e)-C(Ph)C(O)C(Me)C(Ph)C-CH_2}(CO)(η-C_5H_5)] (2).

A single crystal determination of complex **2** was carried out in order to define the stereochemistry of the unusual cyclic fragment. Crystals of **2** were found to be monoclinic belonging to the space group Pcab, the unit cell parameters are a=13.239(1), b=15.908(2), c=18.038(2)Å and Z=8. Equivalent reflections were merged to give 1760 data and the structure solved by Patterson methods using the SHELX[29] suite of programs. In the final least squares cycle all atoms were allowed to

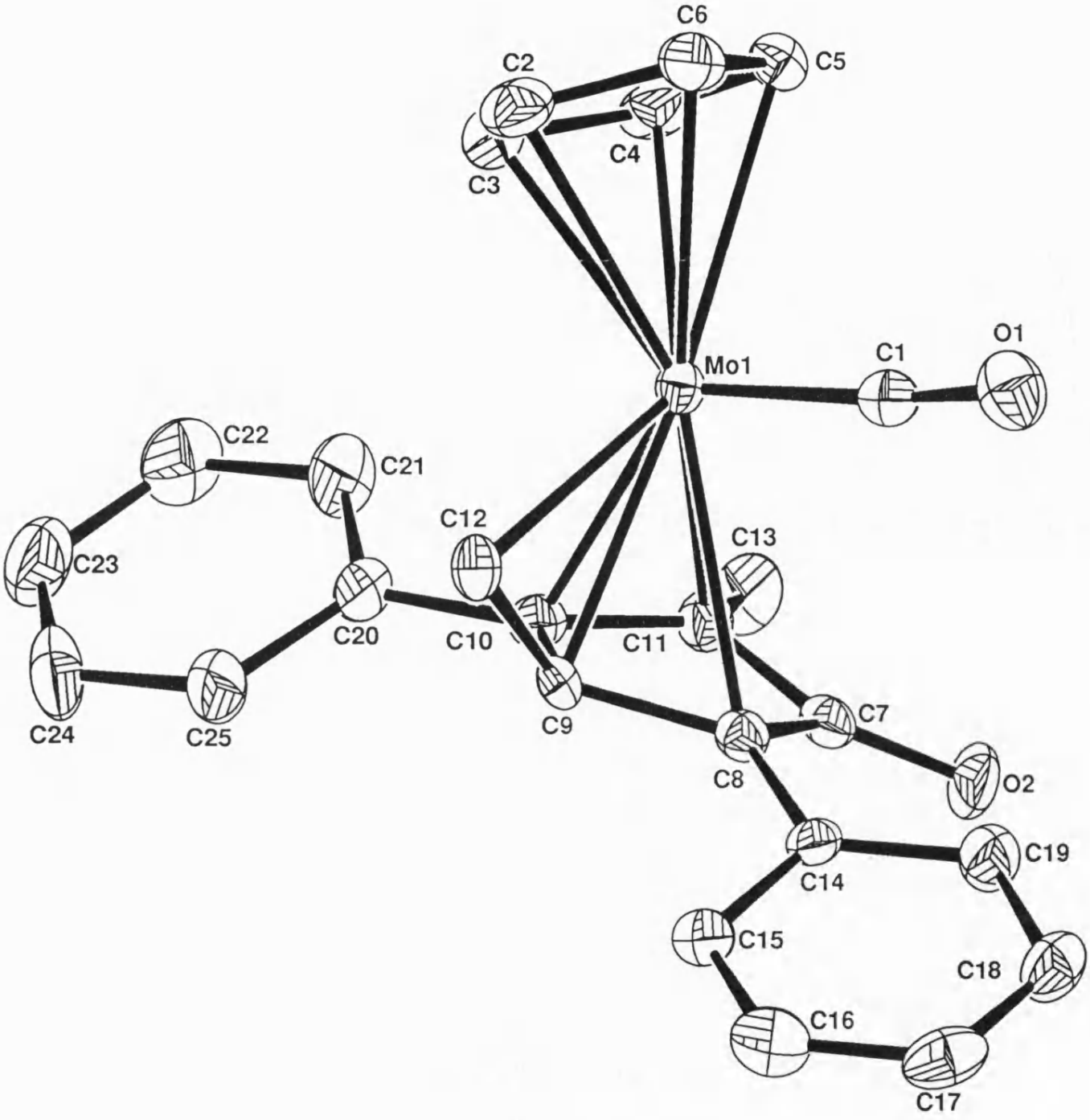

FIGURE 19

The X-ray structure of [Mo{$\eta^2\eta^3$(5e)-C(Ph)C(O)C(Me)C(Ph)C-CH_2}(CO)(η-C_5H_5)] (**2**) hydrogen atoms omitted for clarity.

vibrate anisotropically. Hydrogen atoms were included at calculated positions except for the two methylene hydrogens (attached to C12), which were located in an advanced difference Fourier and refined at a distance of 0.96Å from the parent atom. Final residuals after 10 cycles of least squares were R=0.0402, Rw=0.0416. Figure 19 shows the geometry of the molecule and the numbering scheme used. Full tables can be found in the appendix, selected bond lengths and angles can be found in table **3**.

Bond Lengths/Å				Bond Angles/°	
Mo-C7	2.664	C7-C8	1.471	C8-C9-C12	118.2
Mo-C8	2.368	C8-C9	1.458	C12-C9-C10	119.0
Mo-C9	2.162	C9-C10	1.448		
Mo-C10	2.247	C10-C11	1.435		
Mo-C11	2.407	C9-C12	1.412		
Mo-C12	2.284	C7-02	1.243		

TABLE 3

The carbon-carbon bond lengths within the new ligand suggest some delocalisation and hence a contribution from canonical form B (fig18), however the C-O bond length of 1.243Å is of the magnitude expected for a carbon-oxygen double bond, also the distance between the metal centre and the carbonyl carbon is longer than would be expected if the ligand was delocalised, and hence flat. This is confirmed by the fact that the methylene carbon, C12 lies 0.84Å above the plane defined by C8-C11. The bond angle of 118.2° between C8-C9-C12 is consistent with an allyl fragment. It is interesting to note that only one isomer is formed in the reaction such that the two phenyl rings lie either side of the allyl fragment instead of the alternative where they

would lie adjacent to the carbonyl, the mechanism for the formation of complex **2** is discussed in section 1.12.

1.11 The X-ray structure of [Mo{$\eta^2\eta^3$(5e)-C(Me)C(O)C(Me)C(Me)C-CH_2}(CO)(η-C_5H_5)](**3**).

Crystals of complex **3** were found to be monoclinic and cut from a multi twinned wedge, belonging to space group $P2_1/n$. The unit cell parameters are a=7.826(1), b=15.098(3), c=21.635(4)Å; β=95.14° and Z=8. Equivalent reflections were merged to give 2686 data and the structure solved by Patterson methods and refined using the SHELX suite of programs.[29] The asymmetric unit consisted of 2 molecules which were seen to be optical enantiomers which were treated as separate blocks. In the final least squares cycles all atoms were allowed to vibrate anisotropically. Hydrogen atoms were included at calculated positions in all cases except for C13 and C'13 where the relevant hydrogens were located in the penultimate difference Fourier and refined at fixed distances of 1.08Å from the parent atoms and R=Rw=0.0351. Figure 20 shows the geometry of the molecule and the atomic numbering scheme used. Full Tables can be found in the appendix. Selected bond lengths and angles are shown in table **4**.

Bond Lengths/Å				Bond Angles/°	
Mo-C7	2.637	C7-C8	1.466	C8-C9-C13	117.4
Mo-C8	2.332	C8-C9	1.454	C13-C9-C10	121.1
Mo-C9	2.150	C9-C10	1.444		
Mo-C10	2.251	C10-C11	1.406		
Mo-C11	2.39	C9-C13	1.435		
Mo-C13	2.335	C7-02	1.268		

TABLE 4

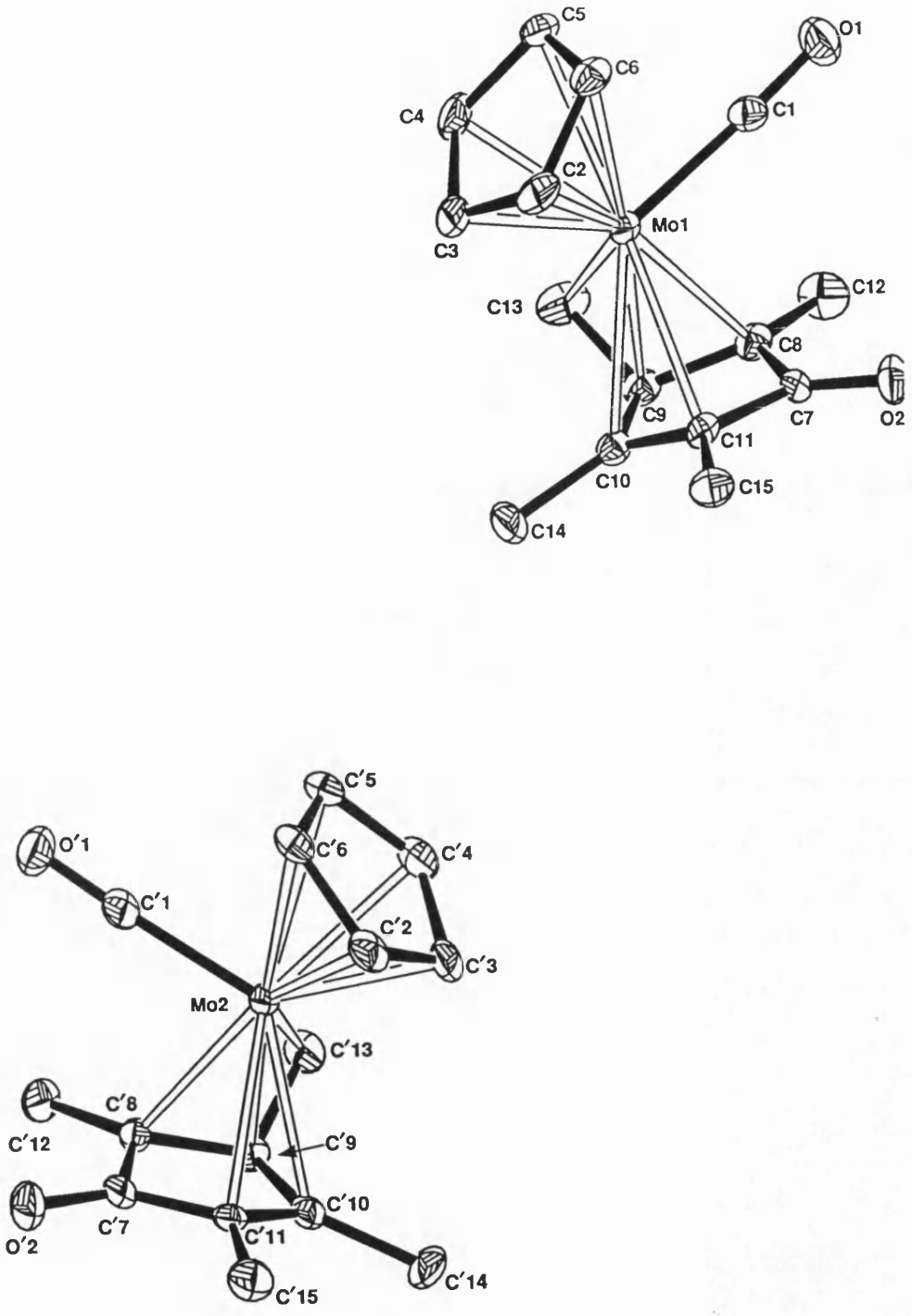

FIGURE 20

The X-ray structure of [Mo{$\eta^2\eta^3$(5e)-C(Me)C(O)C(Me)C(Me)C-CH_2}(CO)(η–C_5H_5)](**3**) hydrogens omitted for clarity.

The carbon-carbon bond lengths within the cyclic ligand suggest some delocalisation as seen previously, but as for complex **2** the C-O bond length in complex **3** of 1.268Å is of the magnitude expected for a carbon-oxygen double bond. Also C13 lies 0.92Å above the plane defined by C8-C11 and the bond angle of 117.4° between C8-C9-C13 is again consistent with an allyl fragment, the mechanism for the formation of complex **3** is discussed in section 1.12.

In a sense both these complexes (**2** and **3**) can be viewed as related to the electron rich molecule $[Mo(CO)(\eta-C_5H_5)_2]$ and therefore might be expected to be reactive towards electrophilic reagents.

1.12 A proposed mechanism for the formation of $[Mo\{\eta^2\eta^3(5e)\text{-}C(R)C(O)C(Me)C(R)C\text{-}CH_2\}(CO)(\eta-C_5H_5)]$ (**2** R=Ph) (**3** R=Me).

A proposed mechanism for the reaction is shown in figure 21. It relies on complex **1** adopting the alternative canonical form for the propargyl fragment seen as a σ,η^2–allene ligand. On reaction with carbon-monoxide the trailing end of the ligand de-co-ordinates to give the η^1–allene complex, this is followed by a carbonyl insertion reaction coupled with the incorporation of a second terminal carbonyl. The allene fragment can then reco-ordinate to the metal centre, facilitated by a switch in the bonding mode of the alkyne (4e-2e). It is also known that a 2 electron alkyne co-ordinated to a metal centre can undergo a carbon-carbon bond forming linkage reaction, this occurs so that the second alkyne is inserted into the metal-acyl bond. In the case of complex **2** there are two possible isomers that could be formed in this step, but it is known from the crystal structure that on coupling it is the methyl group which lies adjacent to the carbonyl carbon. The alternative orientation of the alkyne upon coupling would have led to three electron withdrawing groups on adjacent carbon atoms and hence the resultant product would be less stable.

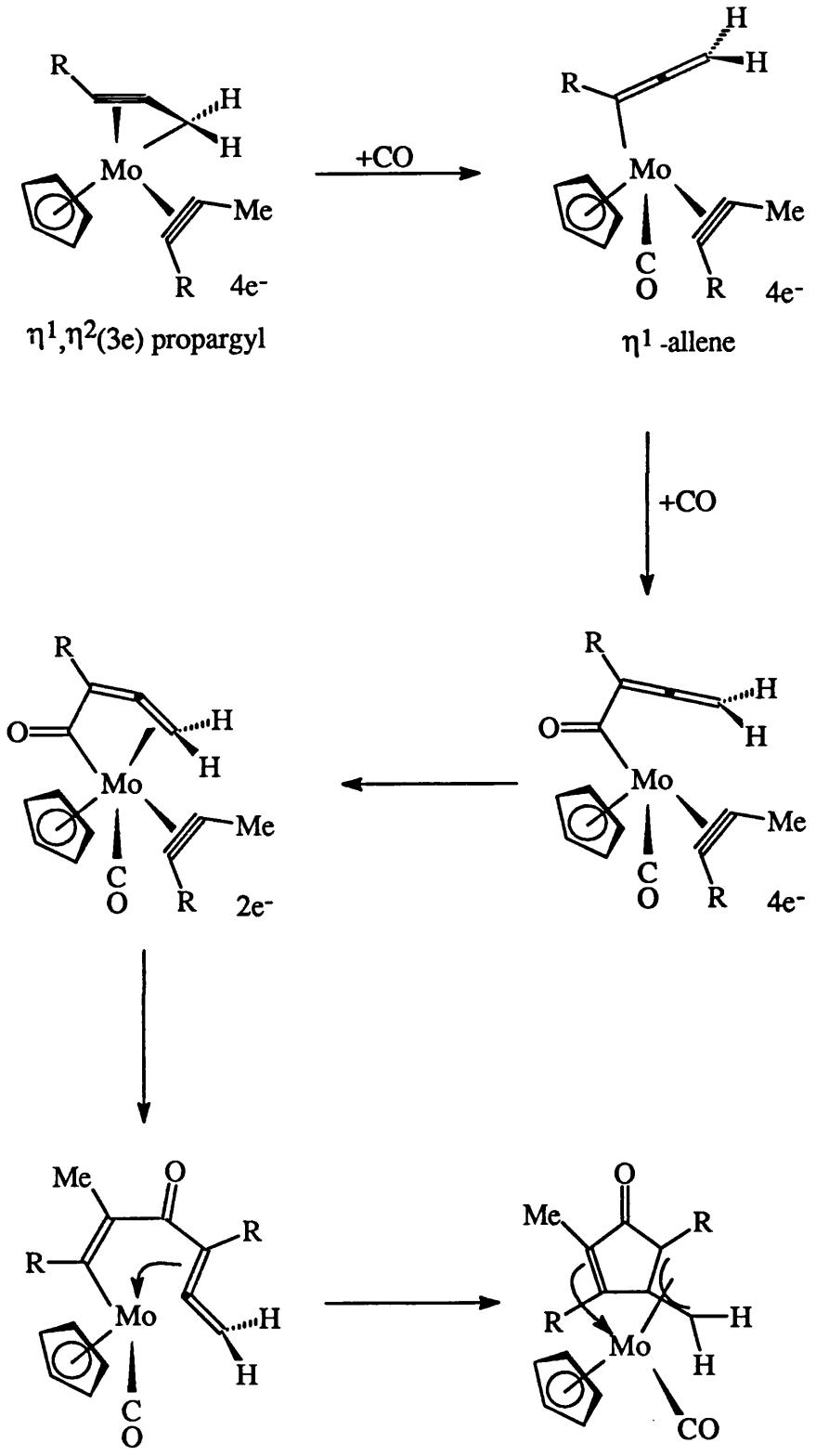
R
H
H
Mo
Me
R
4e-
+CO
H
H
R
Mo
Me
C
O
R
4e-
η1,η2(3e) propargyl
η1 -allene
+CO
R
O
H
H
Mo
Me
C
O
R
4e-
R
O
H
H
Mo
Me
C
O
R
2e-
Me
O
R
R
Mo
H
H
C
O
O
Me
R
R
Mo
H
H
CO

FIGURE 21

A ring closure reaction leads to the formation of the crystallographically identified complexes **2** and **3**. As mentioned previously the C4 fragment (C8-C9-C10-C12 for **2**, C8-C9-C10-C13 for **3**) is not as expected planar, indeed there is evidence of pyramidalisation about C9, this type of pyramidalisation has been seen previously for trimethylenemethane complexes[51]. The reasons for pyramidilisation have been well documented[52] and can be quantified by the angle ϕ which is defined in the case of complex **2** as the angle between the plane defined by C8-C9-C10 and the carbon-carbon bond C9-C12 (C9- C13 for **3**). In contrast to the trimethylenemethane system C8-C9-C10 are restrained by the cyclisation reaction and so the degree of pyramidalisation is restricted to only one branch of the C4 fragment, the values for ϕ are 36.7° for complex **2** and 34.9° for complex **3**. In comparison, the value of ϕ for the trimethylenemethane complex $[Mo\{\eta^4\text{–}C(CH_2)_3\}(CO)_2(\eta\text{–}C_5Me_5)]$ is of the order of 25°.[51] The pyramidalisation in complexes **2** and **3** is greater than that seen in the trimethylenemethane systems, this is probably due to the fact that within **2** and **3** a fifth carbon atom is also attached to the metal centre (C11) as a result the central carbon atom C9 is forced to become pyramidalised to a greater extent, (although it is still closest to the metal as seen in the trimethylenemethane case) allowing the five carbon atoms in the cyclic fragment to fall within co-ordinating distance of the metal centre.

<u>1.13 The reaction of $[Mo\{\eta^2\eta^3(5e)\text{-}C(Me)C(O)C(Me)C(Me)C\text{-}CH_2\}(CO)(\eta\text{–}C_5H_5)]$ **3** with $HBF_4.Et_2O$.</u>

As previously stated complex **3** can be seen as being related to $[Mo(CO)(\eta\text{–}C_5H_5)_2]$ and was expected to be reactive towards electrophilic reagents. This was confirmed when a dichloromethane solution of **3** was reacted in the presence of $HBF_4.Et_2O$ (-78°C), the reaction was followed by IR spectroscopy and it was noted that the two starting material peaks slowly disappeared and a single strong peak at

1980cm^{-1} appeared. This was attributed to the regioselective protonation of the acyl oxygen, nmr spectroscopy confirmed this hypothesis. The ^{1}H nmr spectrum showed two doublets attributable to the methylene protons {δ3.62, d, J(H^aH^b) 2.57Hz; δ3.32, d, J(H^aH^b) 2.57Hz} and singlets for the cyclopentadienyl and methyl groups. Also a new peak at δ7.24 which was attributed to the -OH group of the anticipated product (fig22).

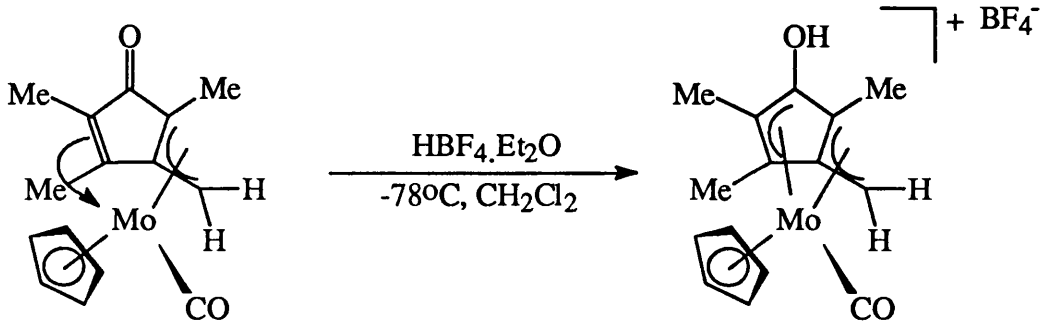

3 **4**

FIGURE 22

The precise structure of complex **4** was confirmed by a single crystal X-ray structure determination which revealed the formation of the unusual bis-η^3–allylic substituted cation.

1.14 The X-ray structure of [Mo{η^{3}η^3(6e)-C(Me)C(OH)C(Me)C(Me)C-CH_2}(CO)(η–C_5H_5)][BF_4] **4.**

Crystals of complex **4** were found to be monoclinic belonging to the space group $P2_1/c$. The unit cell parameters are a=8.376(1), b=8.454(1), c=22.898(4)Å and Z=4. Equivalent reflections were merged to give 1902 data and the structure was solved by Patterson methods using the SHELX[29] suite of programs.

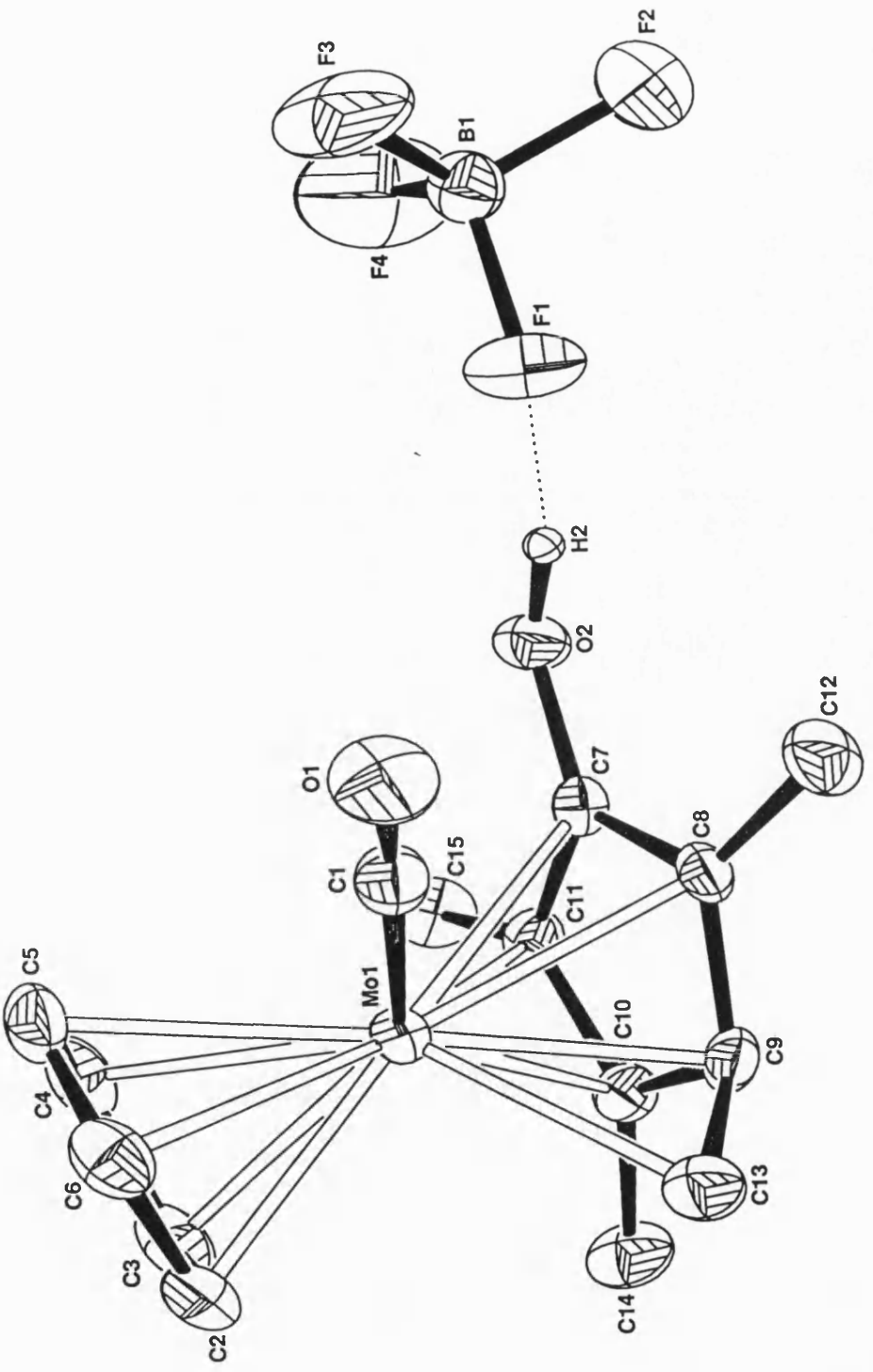

FIGURE 23

The X-ray structure of [Mo{$\eta^3\eta^3$(6e)-C(Me)C(OH)C(Me)C(Me)C-CH_2}(CO)(η-C_5H_5)](**4**) methyl and cyclopentadienyl hydrogens atoms omitted for clarity.

Hydrogen atoms were included at calculated positions on the cyclopentadienyl ring, but located in the remainder of cases and refined at a fixed distance from the relevant parent atoms. Final residuals after 8 cycles of least squares were R=0.0363, Rw=0.0413, full tables of the X-ray data can be found in the appendix. Figure 23 shows the geometry of complex **4** and the atomic numbering scheme used, table 5 contains selected bond lengths and angles.

Bond Lengths/Å				Bond Angles/°	
Mo-C8	2.300	C8-C9	1.450	C8-C9-C13	118.0
Mo-C9	2.176	C9-C13	1.423	C10-C11-C7	108.4
Mo-C13	2.328	C7-C11	1.400	C7-C11-C15	124.8
Mo-C7	2.414	C10-C11	1.427	C7-C8-C12	125.3
Mo-C10	2.271	C7-O2	1.345	C11-C10-C14	126.7
Mo-C11	2.389				

TABLE 5

The bond lengths shown in table 5 are consistent with those expected for an η^3–allyl fragment, with the central atom being closer to the metal than the other two, the allylic bond angles are consistent for those expected for exo- and endo-cyclic allyls.[53] The bond length between C7-O2 (1.345Å) is of the magnitude expected for a carbon-oxygen single bond. The X-ray structure also shows that there is a hydrogen bond (1.699Å) between H2 and one of the fluorine's of the BF_4 counterion (fig 23).

CHAPTER 2:

Synthesis of a novel rhenium η^4(5e) butadienyl complex: Evidence for the formation of a bent rhenium-carbon bond.

2.1 Development of metal η^2–vinyl chemistry.

Metal alkyne species within which the alkyne behaves as a four electron donor,[20,23,54] are known to react with nucleophilic reagents, resulting in both η^1–(σ) vinyl and η^2–vinyl complexes. Reaction of $[Mo\{P(OMe)_3\}_2(\eta^2\text{–}RC_2R')(\eta\text{–}C_5H_5)]^+$ with the hydride sources $NaBH_4$/$[KBHBu^s_3]$ is seen to produce both types of vinyl ligand (fig24).[55]

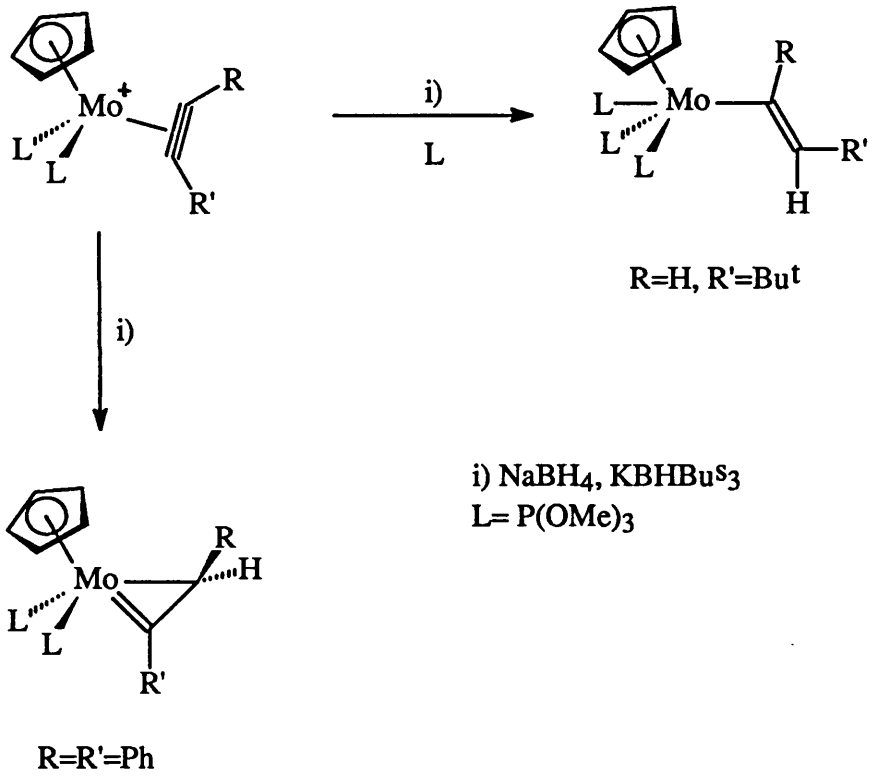

FIGURE 24

The class of complexes containing the η^2–vinyl ligand was firmly established during the 1980's. Isolation and characterisation of η^2–vinyl (or metallocyclopropanes), has had important mechanistic implications since their formation from η^1–species clearly help to stabilise unsaturated intermediates. The research groups of M. Green and J. Davidson have dominated this area of chemistry

for many years. M. Green has mainly capitalised on the positively charged family of cationic mono-alkyne molybdenum (II) complexes to effect addition of H^-, R^- or Ar^- to alkynes.[26]

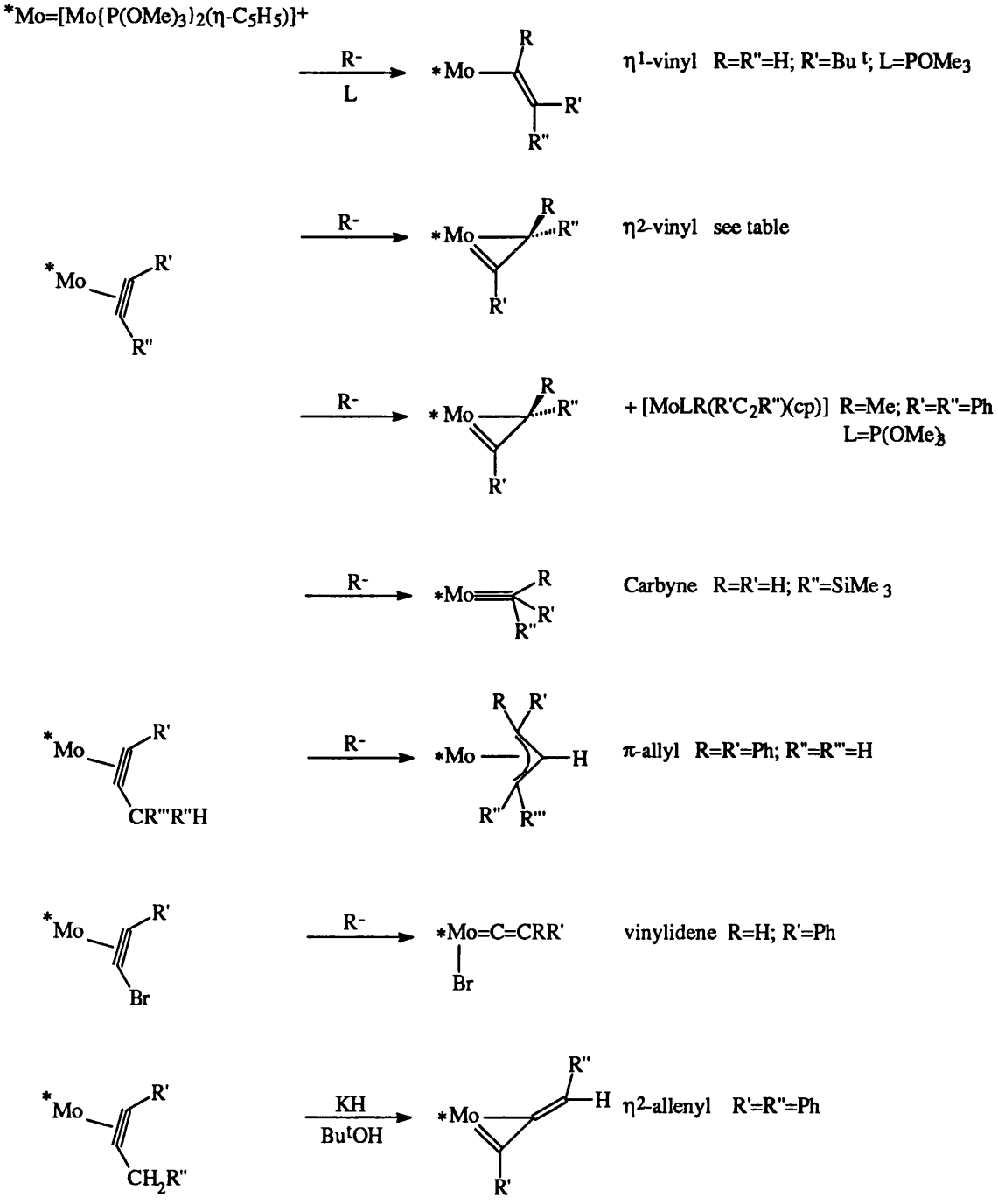

FIGURE 25

Davidson, however, has focused on the use of alkynes containing electron withdrawing substituents to promote nucleophilic attack on the alkyne carbon, (this is affected by the increased electrophilicity of alkyne carbons when bonded to electron withdrawing species) using phosphines, isonitrile and thiolate reagents.[56,57]

Development of this area of chemistry with variation of alkyne and nucleophilic reagents showed a wide ranging effect on the reactivity of these species. It has become clear that the η^2–vinyl ligand was not only a unique unit, but proved to be an intermediate in various classes of reactions where the final product is quite markedly different. The classes of reaction seen are summarised in figure 25.[15,25,26,58-60] Reactions which were seen to result in η^2–vinyls as the sole products are shown in table 6, along with some of the spectroscopic and X-ray data.

Characteristic structural features which allow identification for complexes of the type $[ML_2(\eta^2\text{–}CRCR_2)(\eta\text{–}C_5H_5)]$ include:

i) The orientation of the two C_β substituents which lie approximately orthogonal to the $MC_\alpha C_\beta$ plane, (in direct comparison to η^1–vinyl ligands where the substituents lie in the $MC_\alpha C_\beta$ plane).

ii) Short M-C_α distances (1.94-1.96Å) appropriate for a metal-carbon double bond.[61]

iii) M-C_β distances (2.25-2.30Å) within the single bond range and also C_α-C_β bond lengths (1.43-1.46Å) indicative of some double bond character within the fragment.

Identification of an η^2–vinyl species can also be based upon the $^{13}C\text{-}\{^1H\}$ nmr data, the carbenoid character of C_α is reflected in the low field chemical shifts of 230-290ppm, whereas, the metal -carbon single bond appears at much higher field shifts (20-30ppm).[5]

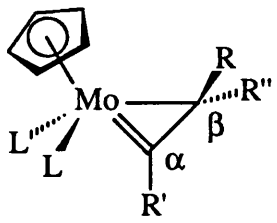

L=P(OMe)$_3$				$^{13}C-\{^1H\}$ nmr, ppm		X-ray, Å		
R'	R"	R	colour	C_α	C_β	M-C_α	M-C_β	$C_\alpha C_b$
Ph	Ph	H-a	green	255.5	26.8	1.95	2.30	1.43
Ph	Ph	Ph-b	green	230				
t-Bu	H	Ph-b	red	286.5	29.9	1.94	2.29	1.44
t-Bu	H	p-Tol-c	red	286.6	29.3			
i-Pr	H	p-Tol-c	yellow	276.2	26.1			
Me	Ph	Ph-b	red	237.4	35.7	1.96	2.25	1.46
CH_2Ph	Ph	H-a	orange	260.4	24.6			

a-from $KBHBu^s_3$; b-from Ph_2CuLi; c-from $(p\text{-Tol})_2CuLi$

TABLE 6

2.2 The bonding of an η^2–vinyl to a metal centre.

Studies have revealed that the principal molecular orbitals utilised by an η^2–vinyl fragment indicate that they are in fact isolobal with those used in alkyne-metal bonding on combination with an $[ML_2(\eta\text{–}C_5H_5)]^+$, d^4 metal fragment (figure 26).[5,62]

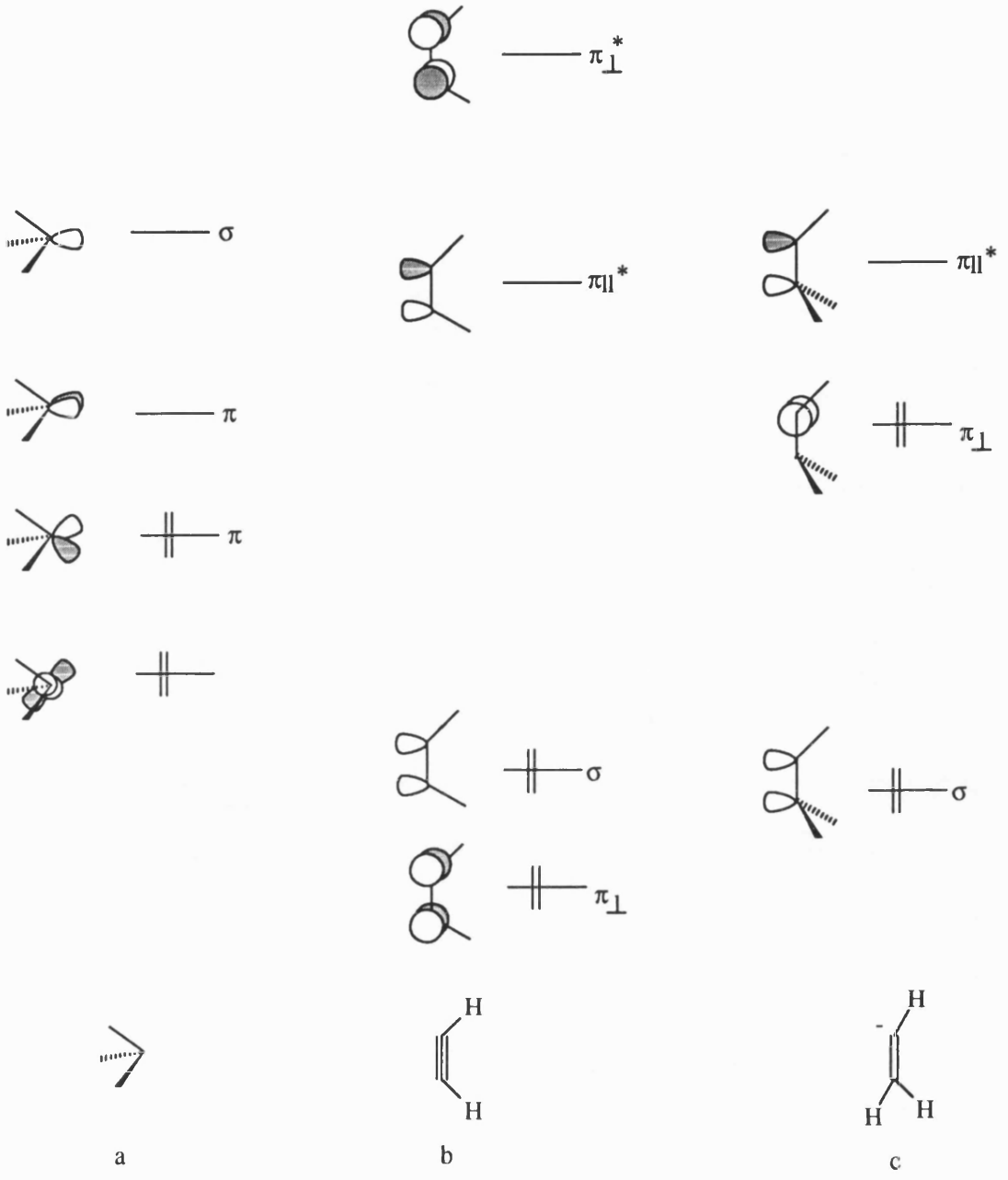

Frontier orbitals for a) $[Mo\{P(OH)_3\}_2(\eta-C_5H_5)]^+$, b) HCCH, c) $H_2C=CH^-$ fragments.

FIGURE 26

The frontier orbitals of the metal fragment[63,64] are well matched symmetrically for overlap with the incoming ligand orbitals, (one empty σ, one empty and one filled π and a filled σ orbital). The incoming ligand can donate electrons through both filled σ and π orbitals to the metal, and backbonding can occur via the empty π^* perpendicular orbital, thus reducing the bond order within the organic fragment. Using this analogy between the bonding of alkynes and η^2–vinyls, predictions of the product geometry on conversion of alkyne to η^2–vinyl can be made. However, the presence of two orthogonal π orbitals of similar energy can result in some reactions where the η^2–vinyl adopts an orientation which lies perpendicular to the alkyne bonded within the original complex.[5] For the complex $[Mo\{P(OMe)_3\}_2(\eta^2\text{–}RCCR_2)(\eta\text{–}C_5H_5)]$ only a single peak is observed in the $^{31}P\text{-}\{^1H\}$ nmr spectrum. This is accounted for by a windscreen wiper type of fluxionality, whereby on the nmr timescale both C_α and C_β lie in the mirror plane and therefore equilibrate both phosphorous ligands (figure 27).

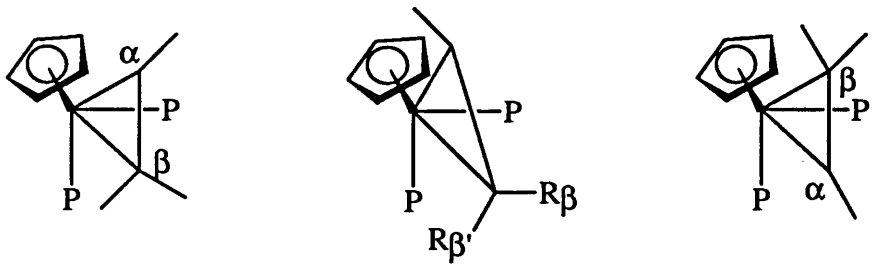

Θ = 0° Θ = 45° Θ = 180°

FIGURE 27

Application of extended Huckel molecular orbital methods to the model complex $[Mo\{P(OH)_3\}_2(\eta^2\text{–}CHCH_2)(\eta\text{–}C_5H_5)]$, predict only a small energy barrier to allow oscillation of the η^2–vinyl ligand (<5kcalmol^{-1}) which would suffice to equilibrate the

two phosphite ligands. Full rotation of the η^2–vinyl was calculated to be of a much higher energy (approx 22kcalmol^{-1}), (figure 28).

If the substituents on C_β are different then the two phosphite ligands remain inequivalent. The synthesis, reactivity and role as reaction intermediate of several rhenium η^2–vinyls is discussed in more detail in later sections.

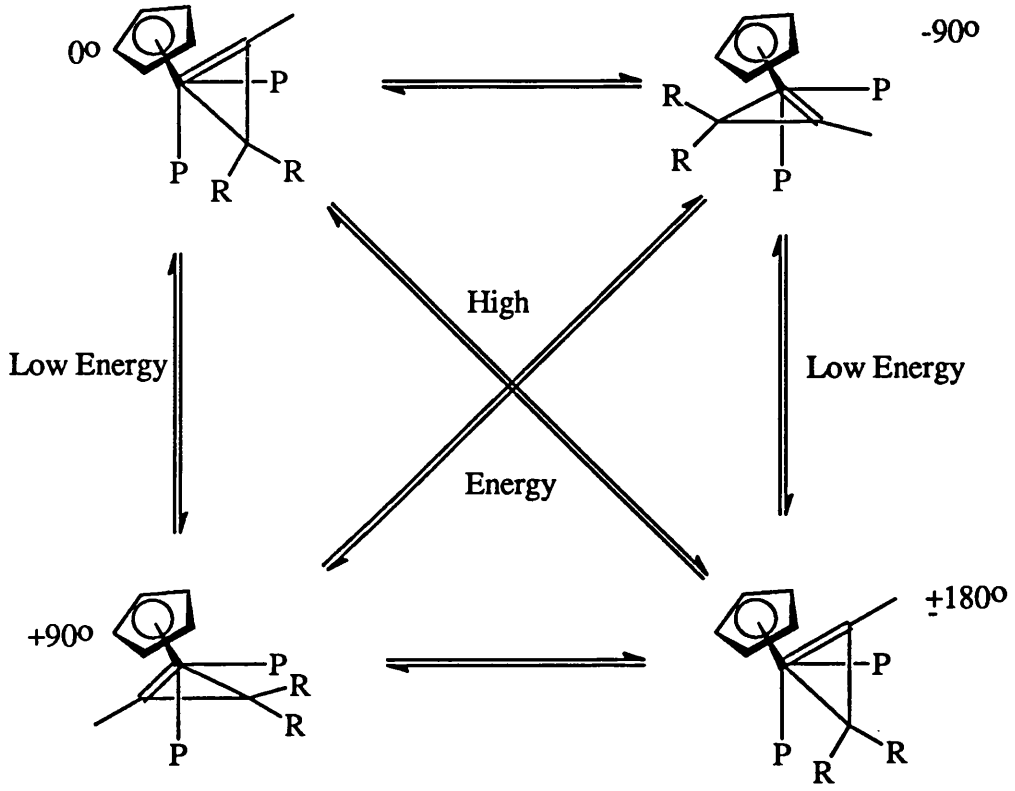

FIGURE 28

2.3 The chemistry of metal bis-alkyne complexes.

Molybdenum (II) and tungsten (II) d^4 bis-alkyne cyclopentadienyl derivatives have been studied extensively over the past decade. They are envisaged as containing a rapidly fluxional $\eta^2(4e)/\eta^2(2e)$ electron bonding system similar to that proposed for [W(CO)(hex-3-yne)$_3$] described in section 1.1. These systems can be accessed from

the complexes $[CpM(CO)_3X]$ (M=Mo,W; X=halide) (fig29) in the presence of an alkyne on reflux in hexane.[65,66,67] The removal of CO from this system is important and prevents the formation of unwanted cyclopentadienone or duroquinone complexes.[65]

$$[MX(CO)_3(\eta\text{-}C_5H_5)] + 2RC_2R' \xrightarrow[\text{hexane}]{\Delta} [MX(\eta^2\text{-}RC_2R')_2(\eta\text{-}C_5H_5)] + 3CO$$

X= Cl, Br, I

R=R'=Me, CF_3, Ph; R=Ph, R'=Me

FIGURE 29

Cyclopentadienyl bis alkyne complexes are quite reactive readily undergoing ligand substitution. Their reaction with nucleophilic reagents forming η^2–vinyl complexes and coupling reactions forming allyl carbene complexes.[68] Cationic bis-alkyne molybdenum derivatives can be accessed by oxidative cleavage of the $[CpMo(CO)_3]_2$ dimer in the presence of free alkyne or in the case of indenyl complexes from the bis-acetonitrile complex, $[Mo(CO)_2(MeCN)_2(\eta^5\text{–}C_9H_7)][BF_4]$ which then readily undergoes ligand replacement of the labile acetonitrile ligands (fig30). These two complexes have been utilised to great effect in the majority of recent research within the group of M. Green.

$$[Mo(MeCN)_2(CO)_2(\eta^5\text{-}C_9H_7)]^+ + 2RC_2R \longrightarrow [Mo(CO)(RC_2R)_2(\eta^5\text{-}C_9H_7)]^+ + 2MeCN + CO$$

RC_2R=Bu^tC_2H, MeC_2Me, PhC_2Ph, HC_2H, MeC_2H

FIGURE 30

The crystal structure of the tungsten complex $[WCl(CF_3C_2CF_3)_2(\eta-C_5H_5)]$[65] shows that the two alkynes lie parallel with the tungsten-chlorine bond and this is an important feature of most within the systems of this type.

In the case of rhenium chemistry bis-alkyne complexes have only been synthesised recently. In 1987 Hermann et al [69] outlined a route for the synthesis of a range of cationic rhenium pentamethylcyclopentadienyl bis-alkyne complexes, $[Re(CO)_3(\eta-C_5Me_5)]$ is oxidised (hv (<300nm), O_2/thf) to give the organorhenium oxide $[ReO_3(\eta-C_5Me_5)]$, reductive halogenation leads to the formation of the organorhenium halides $[ReX_4(\eta-C_5Me_5)]$ (X= Cl, Br), these halide complexes can be reduced with HgX_2-activated aluminium powder in the presence of alkynes to produce complexes of the type $[ReX_2(\eta^2-RC_2R)(\eta-C_5Me_5)]$, reaction of these complexes with $Ag[SbF_6]$ in the presence of an alkyne leads to the formation of a rhenium bis-alkyne complex (fig31).

$$[ReX_2(\eta^2\text{-}RC_2R)(\eta\text{-}C_5Me_5)] + R'C_2R' \xrightarrow{Ag[SbF_6]} [ReX(\eta^2\text{-}RC_2R)(\eta^2\text{-}R'C_2R')(\eta\text{-}C_5Me_5)]^+$$

X	Cl	Br	Br	Br
R	Et	Me	Me	Me
R'	Et	Me	Et	Ph

FIGURE 31

Also Mayer et al[70,71] have outlined the synthesis of some low valent rhenium-oxo complexes, which were prepared by displacement of co-ordinated phosphine or arsine ligands L from $[ReO(X)_3(L)_2]$ using a variety of alkyne ligands (fig32).

$[ReOX_3(PPh_3)_2]$ + $2MeC_2Me$ ⟶

$[ReOX(\eta^2\text{-}MeC_2Me)_2]$ + PPh_3 + X_2PPh_3 X=Br, Cl

$[ReOI_3(AsPh_3)_2]$ + $2RC_2R'$ ⟶ $[ReOI(\eta^2\text{-}RC_2R')_2]$

R =	Et	Me	CMe_3	C_6H_6
R' =	Et	H	H	Me

FIGURE 32

The unusual stability of these complexes is accounted for by the pseudotetrahedral geometry the molecule adopts, in contrast to the usual octahedral geometry found for these oxo complexes. This configuration allows the metal electrons to be accommodated without causing any destabilisation of the Re-O bond.

More recently C. Vaughan[109] has synthesised a rhenium bis-diphenylacetylene complex by reaction of the mono-alkyne complex $[ReBr_2(PhC_2Ph)(\eta\text{–}C_5H_5)]$ with thallium hexafluorophosphate in the presence of excess diphenylacetylene (48 hours, dichloromethane), (fig33).

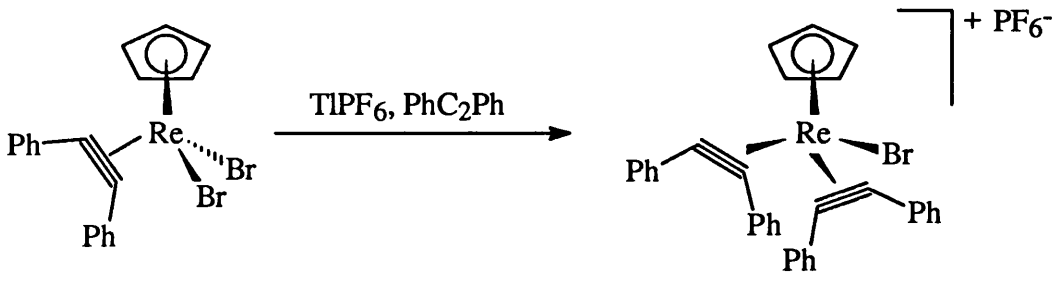

FIGURE 33

2.4 The Development of η^4(5e) Butadienyl complexes.

The butadienyl ligand has been known to act as a three electron donor for some time, Nesmeyanov[72] prepared the first 1-3-η^3–*trans*-butadienyl and in 1971 Stone successfully synthesised a η^3–*cis*-butadienyl complex (fig34).[73,74,75]

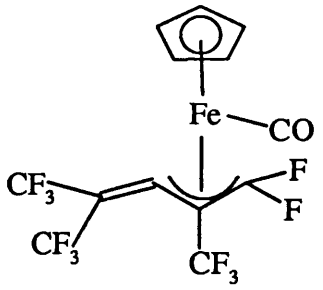

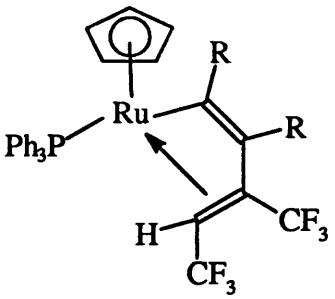

R= CF_3, CO_2Me

1-3-η^3–*trans*-butadienyl

η^3–*cis*-butadienyl

FIGURE 34

The first report of a butadienyl ligand acting as a 5 electron donor was published in 1984 (fig35).[76,77] Reaction of $LiBH(C_2H_5)_3$ with the cationic cyclobutadiene complex (a) led to the formation of an η^4(5e)-butadienyl (d), and the reaction mechanism was postulated to proceed via a 16e η^3(3e)-butadienyl species (c) which then undergoes an electronic and geometric rearrangement to form the 18 electron η^4(5e)-butadienyl complex (d). The X-ray structure of (d) showed that the hydrogen was occupying a pseudo-syn environment, for this to occur the hydride would have to attack the endo-face of the cyclobutadiene ring in preference to the expected exo-face. The η^4(5e)-butadienyl moiety is virtually co-planar and in contrast to the previously documented butadienyl systems all four carbon atoms within the ligand are bonded to the metal centre.

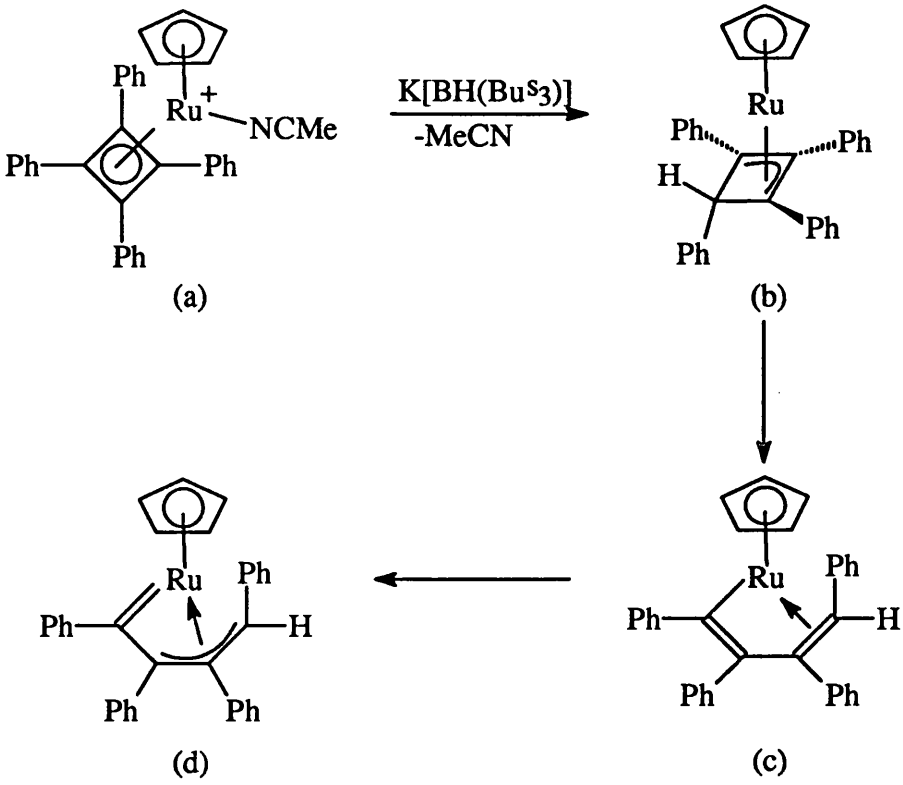

FIGURE 35

As discussed previously in section 2.2 bis-alkyne molybdenum halides are easily synthesised,[23,68] protonation of these complexes affords cationic η^2–vinyl systems (fig36).

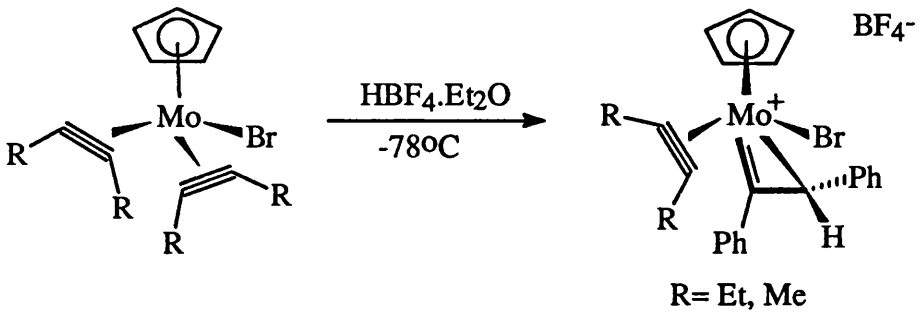

FIGURE 36

The reactivity of these cationic η^2–vinyl systems has been studied, in the case of the but-2-yne system it was found that reaction with lithium bromide led to the

formation of a bis-halo complex, within which the η^2–vinyl and alkyne ligands remain discrete (figure 37), this assumption is supported by the spectroscopic data which showed a rotating alkyne, which at low temperature could be frozen out.[28,76]

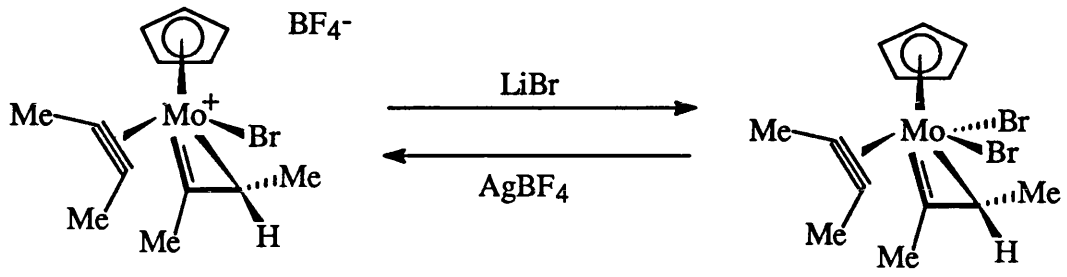

FIGURE 37

In contrast the system containing hex-3-yne proceeded to form a completely different product, the spectroscopic data confirmed the presence of a low field carbenoid resonance, showing that the metal-carbon double bond had remained intact.[77] However, the proton-nmr data was ambiguous and suggested that a new reaction had occurred. X-ray crystallography confirmed that the formation of a η^4–(5e)-butadienyl complex had occurred. The coupling of the η^2–vinyl and alkyne ligands (previously donating 7e) leads to electronic deficiency at the metal centre, this is satisfied by the incorporation of the second halide (fig38).

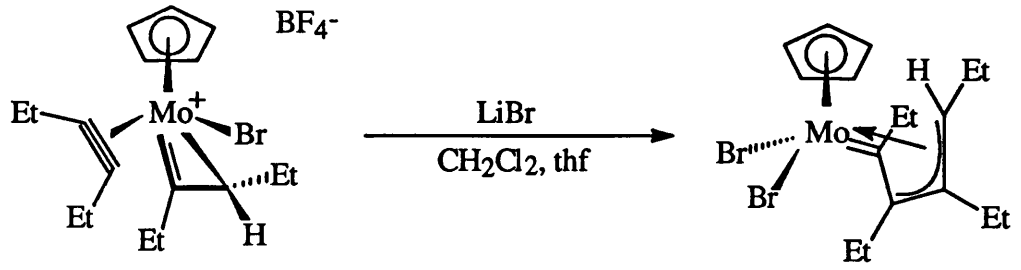

FIGURE 38

The X-ray structure shows some delocalisation across the butadienyl fragment and figure 39 shows the three canonical forms that the ligand can possibly adopt. Canonical form B has a small contribution to the structure as indicated by the shortening of the carbon-carbon bond, its effect is probably seen as the structure switches between the two major forms A and C, which contain the double bond carbene character seen in the spectroscopic data.[76]

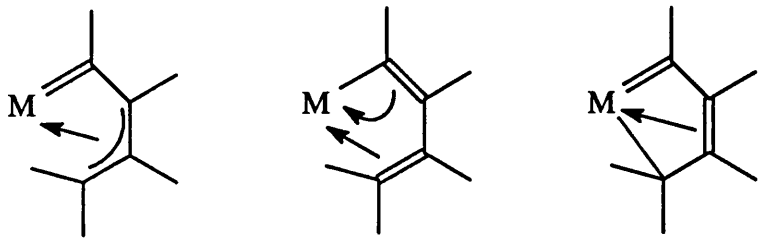

A B C

FIGURE 39

The alkyne and η^2–vinyl ligands contained within the starting material are believed to be perpendicular to each other, this is mechanistically important and is discussed in more detail in section 2.10.

2.5 The X-ray structure of $[ReBr(PhC_2Ph)_2(\eta\text{–}C_5H_5)][PF_6]$(5).

Crystals of complex **5** were found to be triclinic belonging to the space group P_1. The unit cell parameters are a=10.731(2), b=11.283(3), c=13.587(4)Å and Z=2. Equivalent reflections were collected and merged to give 3789 data and the structure was solved using Patterson methods and refined using the SHELX[29] suite of programs. In the final least squares cycles all atoms were allowed to vibrate anisotropically. Hydrogen atoms were included at calculated positions where appropriate. Final residuals after 15 cycles of blocked-matrix least squares (1 block for

each the cation and anion) were R=0.0372, Rw=0.0366, full tables of the X-ray data can be found in the appendix. Figure 40 shows the geometry of the molecule and the atomic numbering scheme used, selected bond lengths and angles appear in table 7.

Bond lengths/Å				Bond angles/°	
Re-Br	2.545	C6-C7	1.290	C7-C6-C10	139.6
Re-C6	2.073	C8-C9	1.296	C8-C9-C28	144.2
Re-C7	2.074	C6-C10	1.442	Torsion angle C6-C7-C8-C9	28.91
Re-C8	2.041	C7-C16	1.451		
Re-C9	2.031	C8-C22	1.473		
		C9-C28	1.473		

TABLE 7

The X-ray data shows that the two diphenylacetylene ligands are η^2-bonded to the rhenium centre, the previously sp hybridised quaternary carbon atoms are distorted such that the angles C7-C6-C10 and C8-C8-C28 are 139.6° and 144.2° respectively this is a common feature of metal alkyne complexes.[13,14] The two alkyne triple bonds (C6-C7, C8-C9) and the rhenium-bromine bond were expected to be parallel, but the crystal structure shows that C6 and C9 (2.069Å, 2.0113Å) are *ca.* 0.2Å further from the rhenium bromine vector than C7 and C8 (1.802Å, 1.794Å), also there is a small torsion angle of 28.91° between C6-C7-C8-C9 such that the two alkyne ligands are partially staggered.

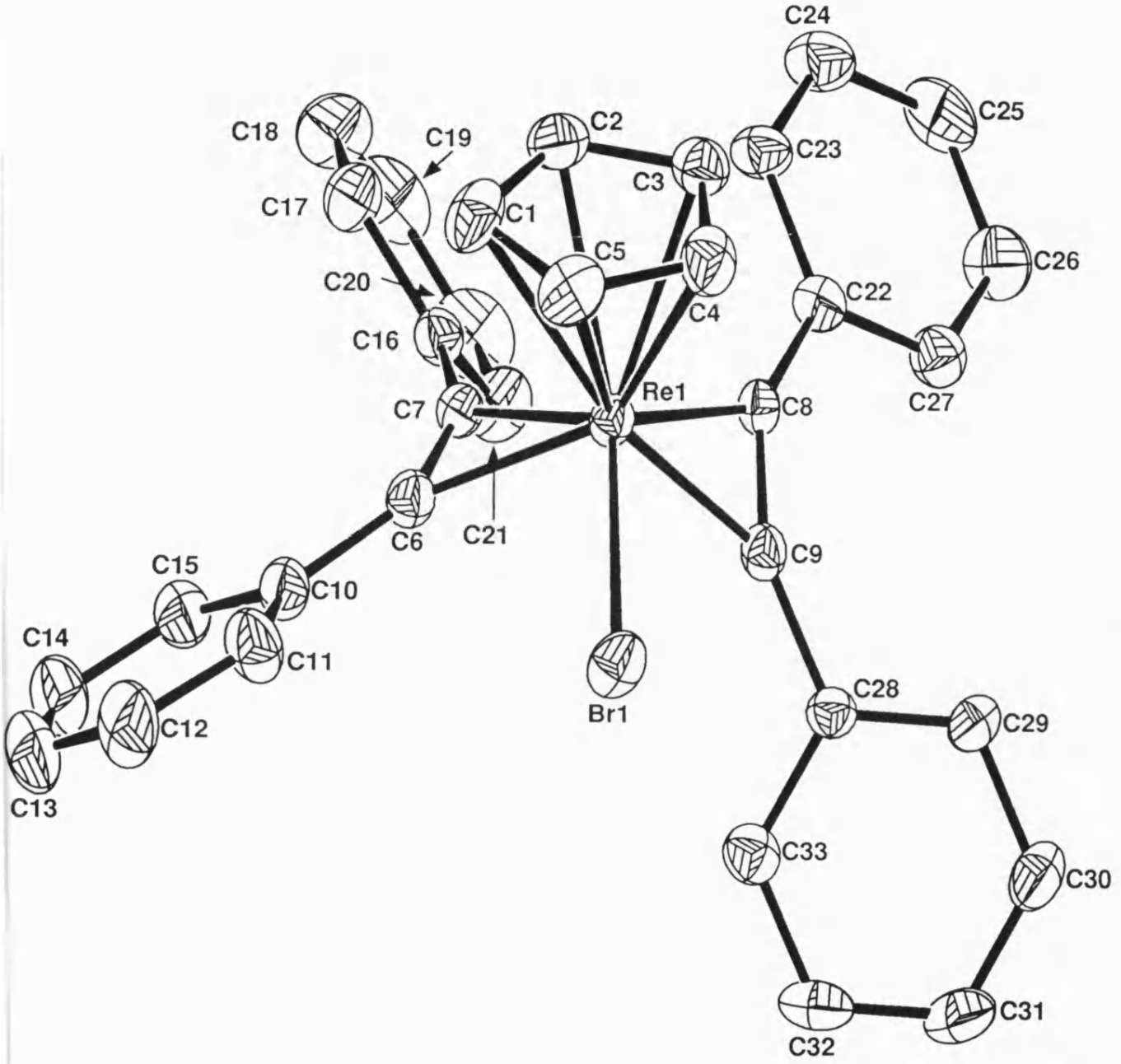

FIGURE 40

The X-ray structure of $[ReBr(\eta^2\text{-}PhC_2Ph)_2(\eta\text{–}C_5H_5)][PF_6]$ **5** hydrogen atoms omitted for clarity.

2.6 Reaction of $[ReBr(PhC_2Ph)_2(\eta\text{-}C_5H_5)][PF_6]$(5) with $LiBH(C_2H_5)_3$.

The reaction of the cationic complex **5** with a source of 'H$^-$' such as $LiBH(C_2H_5)_3$ was expected to afford a neutral η^2–vinyl complex. This product however, would also contain an alkyne ligand, and as discussed previously in section 2.4 examples where the η^2–vinyl and alkyne can either remain discrete or couple to give a η^4(5e)-butadienyl have been seen (fig 41). The latter was thought to be more likely as the alkyne within the η^2–vinyl complex would be functioning as a two electron donor and therefore a coupling reaction to form a butadienyl would not lead to an electronic deficiency at the metal centre (both coupled and uncoupled systems donate 5 electrons), this is in contrast to the molybdenum system where a loss of two electrons upon coupling is seen.

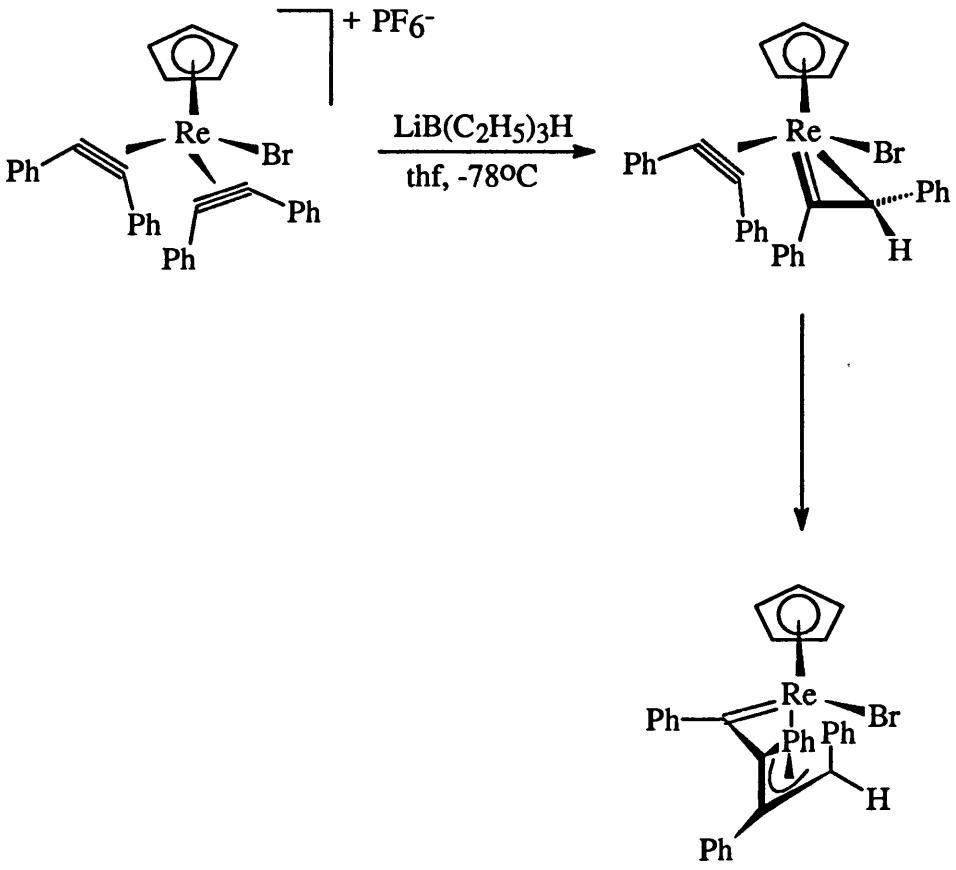

FIGURE 41

Complex **5** was reacted with $LiBH(C_2H_5)_3$ in a thf solution (-78°C), over a period of four hours a colour change from red to green was observed. On removal of the solvent *in vacuo* the resultant green solid was extracted into toluene and columned on silica gel using toluene as the eluant. Two bands were observed on the column the first was an orange band and the second the major green band, the two bands did not fully separate so two fractions were obtained from the column. The first fraction contained both the orange and green complexes, ^1H nmr spectroscopy revealed the presence of two complexes, believed to be the intermediate in the reaction and the major product. The evidence for the presence of an intermediate is discussed later in section 2.9.

The second fraction which contained only the major green product showed resonances in the ^1H and $^{13}C-\{^1H\}$ nmr spectra which were consistent with the formation of an η^4(5e)-butadienyl complex.

The $^{13}C-\{^1H\}$ nmr spectra showed the presence of a low field rhenium carbene (δ235.3) and three resonances at δ76.08, δ64.6 and δ59.01 assigned to the remaining three carbons in the chain, the latter carbon resonance was confirmed as having a single hydrogen atom attached by a ^{90}Dept experiment. The ^1H nmr spectrum showed peaks for the phenyls (δ7.9-6.9) and cyclopentadienyl (δ5.31) hydrogens with the integration ratio 4:1 as expected. However, a peak for the hydrogen on the terminus of the butadienyl fragment was thought to be masked by either the phenyl hydrogens or the solvent peak, as no other peaks were present in the spectrum. A CH correlation experiment revealed that the peak at δ59.01 in the $^{13}C-\{^1H\}$ nmr spectra was associated with a peak appearing at δ5.42 in the ^1H nmr. Due to the proximity of the solvent peaks in both spectra (deuterodichloromethane shows peaks at δ52 and δ5.33), it was suggested that the synthesis of the corresponding deuterium complex would confirm the assignment of the hydrogen peak.

The reaction of complex **5** with $LiBD(C_2H_5)_3$ (thf, -78°C) led to the formation of both an orange and green complex as seen previously in the original reaction. The ^2D nmr of the green complex showed the presence of deuterium in two environments. A peak at δ5.25 was assigned to the deuterium on the terminus of the butadienyl moiety, the second peak at δ7.33 was assigned to a C_6H_5D moiety due to deuterium exchange with the adjacent phenyl ring.

This data was consistent with the formation of the η^4(5e)-butadienyl complex $[BrRe\{\eta^1,\eta^1,\eta^2(5e)=C(Ph)C(Ph)C(Ph)=CHPh\}(\eta-C_5H_5)]$ (**7**). Crystallisation from a toluene/hexane layered mixture led to the formation of X-ray quality crystals of complex **7**. The X-ray structure, however, although confirming the formation of a five electron butadienyl showed that the fragment had adopted an unusual bonding mode (fig 42).

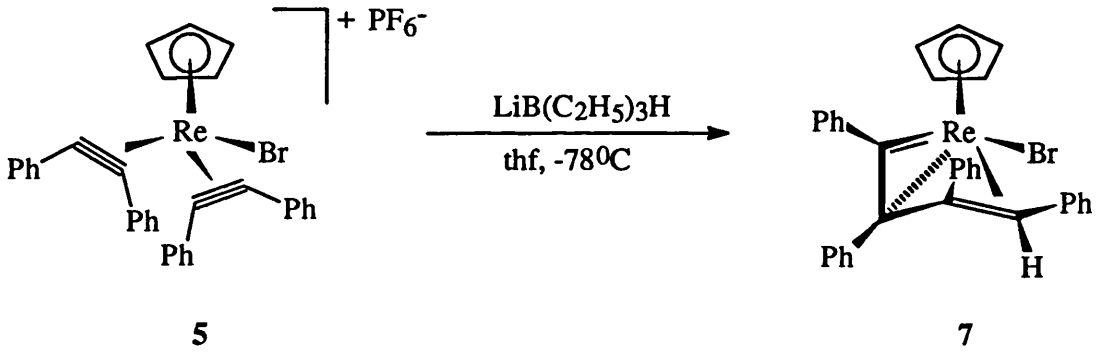

5 **7**

FIGURE 42

2.7 The X-ray crystal structure for $[BrRe\{\eta^1,\eta^1,\eta^2(5e)=C(Ph)C(Ph)C(Ph)=CHPh\}(\eta-C_5H_5)]$ (7).

Crystals of complex **7** were found to be monoclinic belonging to the space group $P2_1/n$. The unit cell parameters are a=10.24440(8), b=16.084(2), c=15.790(1)Å and Z=4. Equivalent reflections were collected and merged to give 2916 data and the structure was solved using Patterson methods and refined using the SHELX suite of programs.[29] In the final least squares cycles all atoms were allowed to vibrate

anisotropically. Hydrogen atoms were included at calculated positions except for the hydrogen attached to C9 which was located in the penultimate difference Fourier map and refined at a fixed distance of 0.96Å from the parent atom. Final residuals after 10 cycles of least squares were R=0.0266, Rw=0.0225, full tables of the X-ray data can be found in the appendix. Figure 43 shows the geometry of the molecule and the atomic numbering scheme used, selected bond lengths and angles appear in table 8.

Bond lengths/Å				Bond angles/°		
Re-C6	1.931	C6-C7	1.424	C6-C7-C8	109.8	
Re-C7	2.188	C7-C8	1.499	C7-C8-C9	109.0	
Re-C8	2.147	C8-C9	1.458	Torsion angle C6-C7-C8-C9		110.8
Re-C9	2.260					

TABLE 8

As illustrated in figure 43 the CpReBr fragment is bonded to a butadienyl fragment [C6-C7-C8-C9], which has instead of adopting the more usual and expected planar U- (or *cisoid*) geometry, has assumed a much more open and effectively twisted *transoid* configuration. This is supported by the torsion angle between C6-C7-C8-C9 of 110.8°. The fragment is seen as containing a rhenium carbon double bond (Re-C6 1.931Å) and an alkene between C8-C9 which is η^2–bonded to the metal centre. The crystal data also shows that C7 is in an essentially planar geometry [deviation of C7 from the least squares plane subtended by C6-C7-C8-C16 is 0.038Å] and shows an unusual type of bonding to the rhenium metal centre discussed in greater detail in the next section.

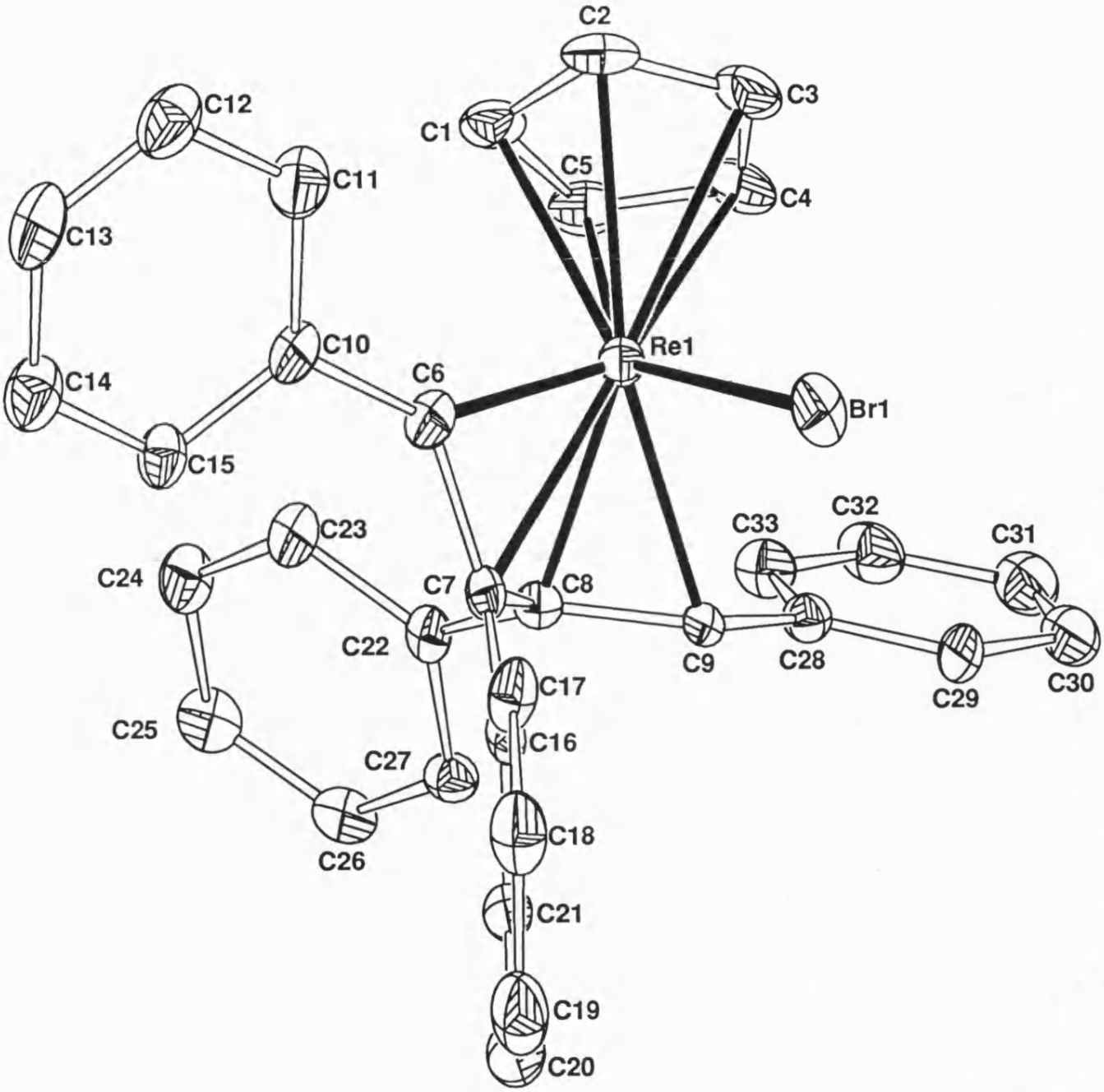

FIGURE 43

The X-ray structure of [BrRe{η^1,η^1,η^2(5e)=C(Ph)C(Ph)C(Ph)=CHPh}(η–C_5H_5)]

(7), hydrogen atoms omitted for clarity.

2.8 The nature of the unusual Rhenium-carbon (Re-C7) interaction within complex 7.

As seen from the crystal data C7 lies in a planar geometry, to adopt the normal four co-ordinate bonding mode for a carbon atom, an unusual type of interaction with the metal centre is observed. It is well known that tetraco-ordinate carbons in organic compounds favours a tetrahedral co-ordination geometry.[78,79] Few examples of stable and isolable complexes containing planar tetraco-ordinate carbon centres have been reported. Chisholm *et al* reported the formation of a (μ–allene) ditungsten complex[80] (fig 44) containing such a carbon which shows electronic features similar to those calculated for the unsubstituted 1,1,dimetallamethane systems.[81]

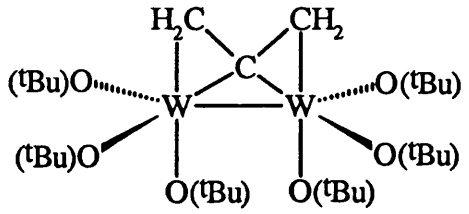

FIGURE 44

G. Erker has recently published papers describing the synthesis of dimetallic zirconium/aluminium complexes containing planar tetraco-ordinate carbons.[82,83]

In a more recent example he has predicted the existence of a through space metal-carbon interaction within a hypothetical bimetallic Zr/Al complex (fig 45).[84]

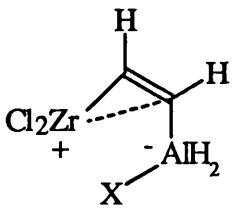

X= H, Cl

FIGURE 45

The precise nature of the bonding between the Re and butadienyl fragment of complex **7** was studied using Extended Huckel Molecular Orbital theory as implemented in Mealli and Proserpios CACAO2 program.[85] The crystallographic co-ordinates were used with the simplification of hydrogen atoms in place of the phenyl substituents on C6, C7, C8, C9 and all C-H distances were idealised to 1.10Å. The highly unusual and distorted geometry of the ligand leads to complex orbital interactions spread over many MO's. Plots of the highest fifteen or so MO's did however reveal an underlying pattern. There was evidence for a variety of interactions indicating both σ and π symmetry bonding between C6 and suitable Re d orbitals as well as a strong interaction between the C8-C9 π bond and metal based d functions. In addition and surprisingly the p orbitals of C7 are available to σ overlap with Re d orbitals, but in a decidedly non-linear fashion. Plots of selected orbital interactions are shown in figure 46A-D.

Figure 46-A shows the metal-d and C6-p orbitals involved in the rhenium-carbon double bond. Figure 46-B shows the C8-C9 double bond orbitals and 46-C shows the interaction of the double bond with the metal-d orbitals. Figure 46-D shows the C7-p and metal-d orbital interactions leading to the bent rhenium-carbon bond.

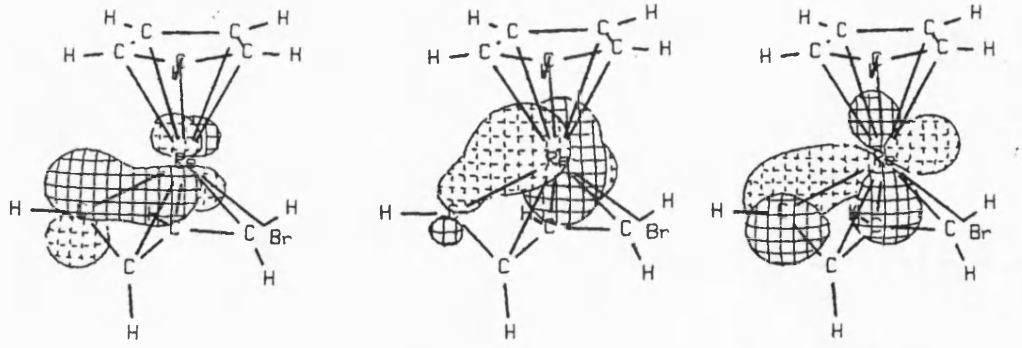

A Orbitals involved in the rhenium-carbon double bond.

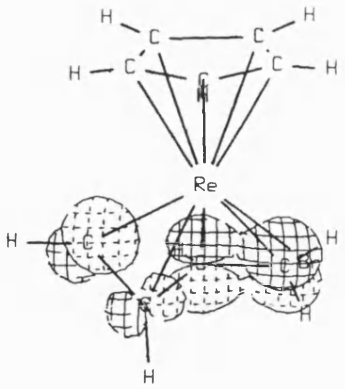

B Orbitals involved in the C8-C9 double bond.

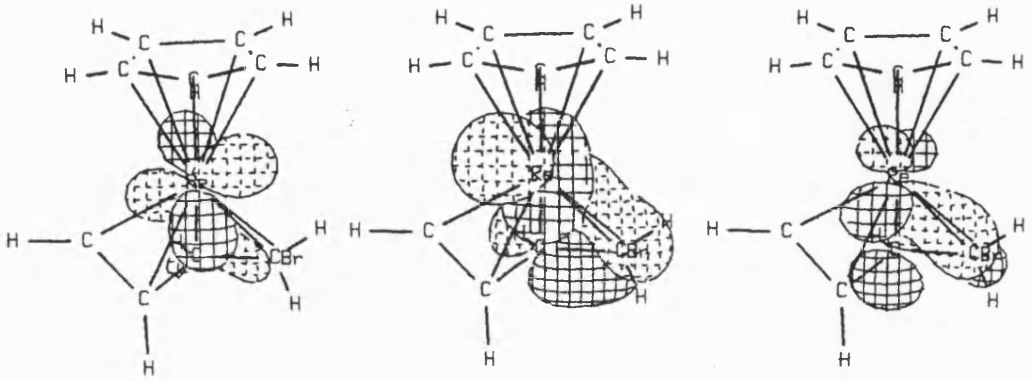

C Orbitals involved in the C8-C9 to rhenium interaction.

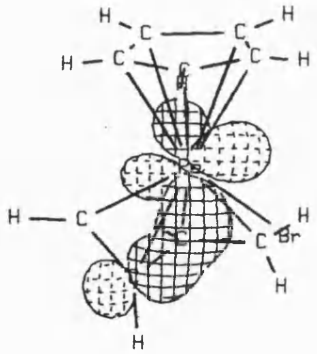

D Orbitals involved in the bent rhenium to C7 bond.

FIGURE 46

The bonding can essentially be rationalised in terms of the two ends of the C4 fragment being anchored to the metal (fig 47) which imposes the highly strained geometry at C7.

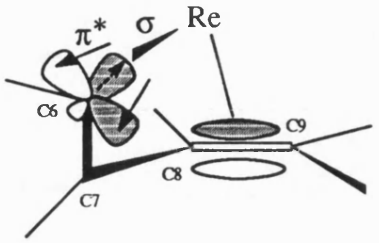

FIGURE 47

The latter is still sufficiently close as to attempt interaction with the metal but the twisted nature of the C4 fragment and essentially planar geometry at C7, leads to a bent rhenium-carbon σ bond (fig 48).

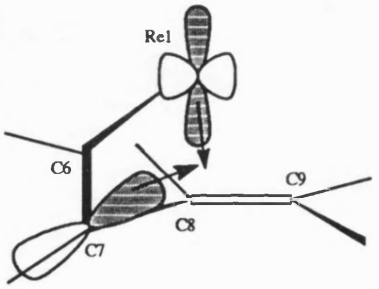

FIGURE 48

The atomic overlap populations support this view of the molecule. The metal carbon overlaps for C6, C7, C8, C9 are 0.68, 0.10, 0.22 and 0.28 respectively. Taking C8-C9 together as a π bonded pair leads to large overlaps of 0.68 and 0.50 at each end of the C4 chain and a much smaller overlap for the central carbon atom. Nevertheless it was interesting to note that this smaller overlap does not translate into a radically different

atomic charge on C7, on the contrary the largest charge is on C9 (-0.19) while the remaining carbons all have a small positive charge of about 0.02.

Thus these calculations would predict that any electrophilic reagents would attack at C9. Indeed preliminary studies have shown that reaction of complex **7** with $HBF_4.Et_2O$ leads to the formation of an as yet uncharacterised red cationic solid.

The unusual bonding of complex **7** is hypothesised as arising from the geometrical requirements of the reaction pathway for its formation. The proposed reaction mechanism for the formation of complex **7** is discussed in section 2.10.

2.9 Evidence for the formation of an η^2–vinyl intermediate in the synthesis of **7.**

As discussed in section 2.5 a second band was seen on the silica column which contained the crystallographically identified complex **7** and an unknown orange complex. The $^{13}C-\{^1H\}$ nmr spectrum for this mixture showed the presence of two complexes, upon accounting for the resonances previously assigned to complex **7** the remaining peaks were fully consistent with the presence of an η^2–vinyl complex. A low field rhenium carbene at δ215.45 was observed. Also a resonance due to the quaternary carbon of the remaining alkyne ligand (δ173.38), the cyclopentadienyl (δ85.12) and the high field resonance (δ21.81) assigned to the carbon-hydrogen single bond of the η^2–vinyl fragment. To confirm the presence of this intermediate a ^2D nmr of the mixture was also run, showing the two peaks seen for **7** and also two more peaks at δ2.77 and δ7.06 corresponding to the presence of an η^2–vinyl and C_6H_5D moiety due to deuterium exchange with the adjacent phenyl ring. Attempts at isolation and crystallisation of this complex were unsuccessful. The role of this intermediate in the reaction pathway is discussed in the next section.

2.10 A proposed mechanism for the formation of the novel η^4(5e)-butadienyl complex [BrRe{η^1,η^1,η^2(5e)=C(Ph)C(Ph)C(Ph)=CHPh}(η-C_5H_5)] 7.

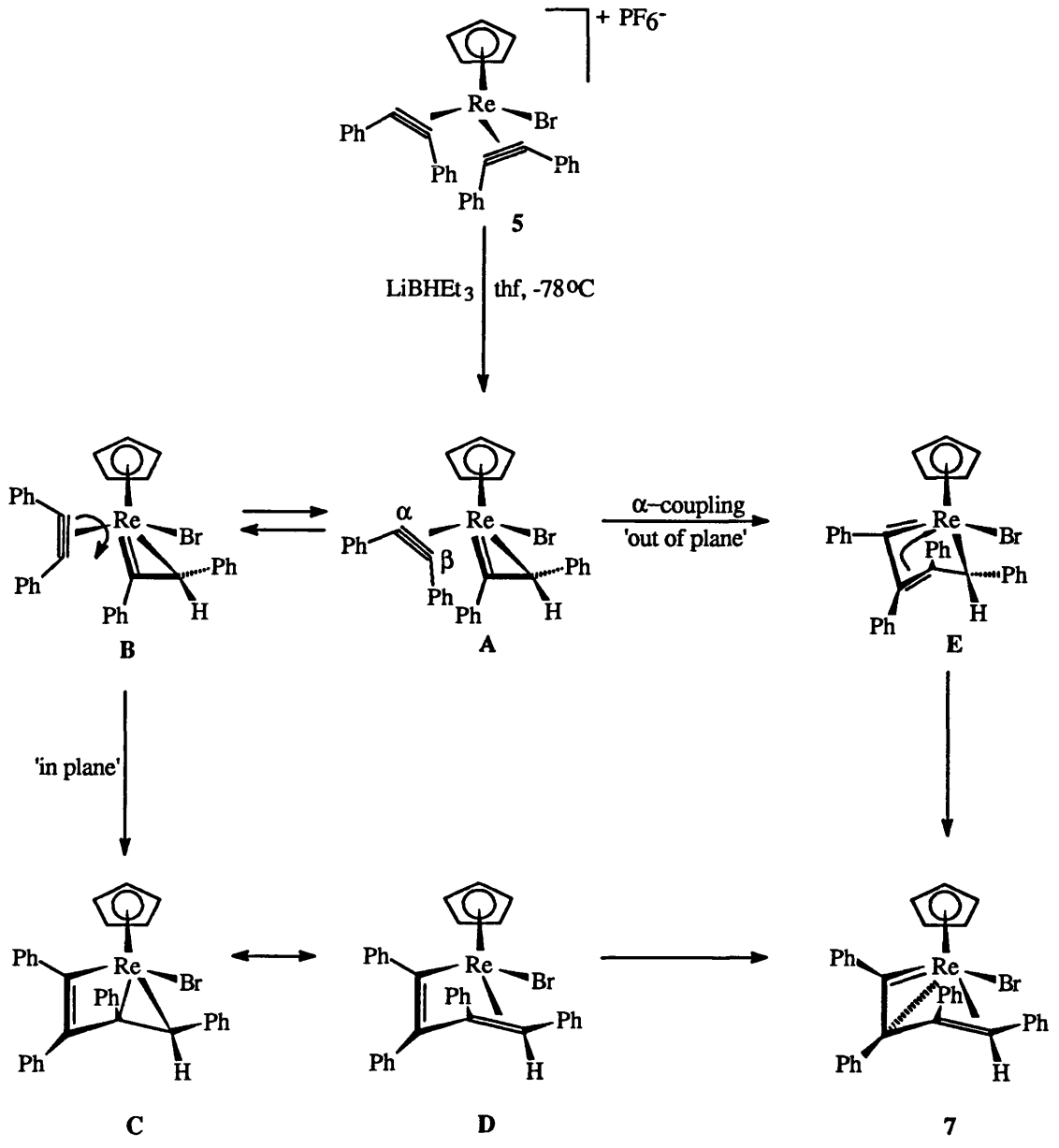

FIGURE 49

The proposed mechanism for the formation of complex **7** is shown in figure 49. The novel bonding mode is thought to arise from the geometrical requirements of an

alkylidene/alkyne coupling reaction, which as such might be expected to undergo a coupling reaction similar to that postulated in the Dotz reaction[86] which involves the coupling of a carbene with an alkyne to form a metallacyclobutene complex (fig 50).

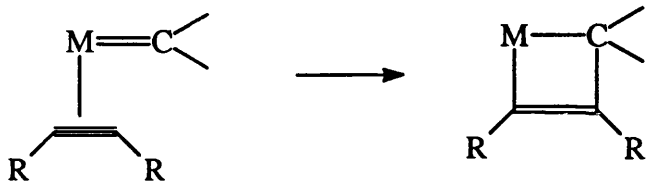

FIGURE 50

A recent paper discusses the mechanism of the Dotz coupling reaction with respect to a chromium carbene system.[87] Within this publication a calculation involving a theoretical chromium tetra-carbonyl complex containing a C_3H_4 ligand, shows that the idea that the reaction forms a planar metallacyclobutene complex is unrealistic, (although several examples containing the planar cyclic fragment have been characterised [88,89,90,91]). The calculations show that an out of plane distortion (or 2nd order Jahn-Teller stabilisation[92]) of the metallacyclobutene results in a more stable structure (fig 51). Analogous structures to the calculated system which contain this out of plane distortion have been experimentally established.[93,94]

FIGURE 51

The first step in the reaction pathway is the formation of the η^2–vinyl intermediate **A** (see section 2.8). It is not known whether the original point of attack for the incoming hydride is the alkyne carbon forming the η^2–vinyl directly, or whether the hydride attacks the metal first and then attacks the alkyne, in both cases however it is assumed that to produce the η^2(3e) vinyl/η^2(2e)-alkyne intermediate **A** the $LiBHEt_3$ delivers the hydride via an 'inside' trajectory to one of the co-ordinated diphenylacetylene ligands of complex **5**. From the known geometry of the final product it is believed that the hydride is delivered to the 'inside' of the alkyne carbon adjacent (*cis*) to the Re-Br bond, indeed the alternative possible directions of attack for the hydride lead to products with an alternate geometry to the known product. The intermediate **A** can be seen as containing an η^2–vinyl, (the η^2–CH_2=CH^- moiety being isolobal with the 4 electron alkyne present in the starting material as shown in figure 26) and a two electron donor alkyne. It is known that two electron donor alkynes are very reactive and can easily undergo a coupling reaction with many available ligands. The orientation of the η^2–vinyl and alkyne fragment in **A** has a profound effect on the proposed pathway for the formation of complex **7**. As discussed in section 2.1 reactions are known where the η^2–vinyl fragment formed in a reaction acts as an intermediate to the formation of coupled products. Examples are known where the η^2–vinyl fragment can either retain its geometry (i.e lies parallel to the Re-Br vector) or can rotate through 90^o and lie perpendicular to the geometry of the alkyne contained within the starting material. Also the diphenylacetylene ligand contained within **A** can rotate to such an orientation as to allow coupling to take place. With these assumptions of the geometry of the two fragments there are two possible pathways from **5** to **7**. The first pathway involves rotation of the η^2-(2e) diphenylacetylene to form intermediate **B**, followed by an 'in plane' coupling of the alkyne and rhenium carbon double bond to form **C**, a valence bond representation of the *transoid*-η^3(3e)-butadienyl substituted species **D**, which transforms into **7** *via* an

electronic rearrangement. Alternatively, the vinylcarbene **E**, a possible precursor of **7**, can be formed directly by the 'out of plane' coupling of the alkyne α-carbon to the rhenium centre, an electronic rearrangement leads directly to **7**, it is important to note that the calculations discussed previously for the chromiun system show that 'out of plane' coupling is preferred. Unlike the symmetrical chromium system, however, the alkyne contact carbons of **A** are inequivalent, and therefore there is an alternative 'out of plane' coupling which proceeds *via* the β-carbon to produce the *cisoid*-η^4(5e)-butadienyl geometry (fig52), seen in molybdenum and tungsten chemistry.[76, 95-98]

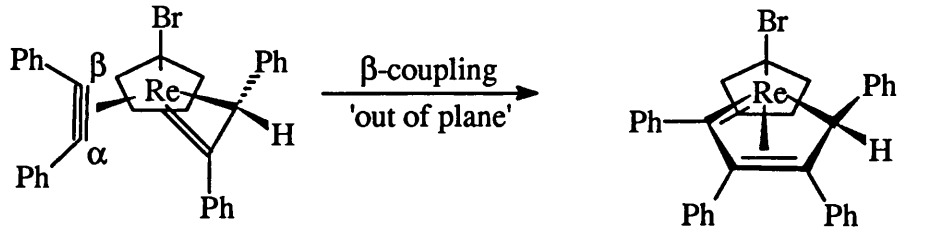

A cisoid-η^4(5e)-butadienyl

FIGURE 52

The formation of complex **7** is the first example of a new reaction pathway to η^4(5e)-butadienyls, it is particularly important to recognise that the butadienyl adopts a hitherto unrecognised twisted or *transoid* bonding mode which involves the formation of a novel bent rhenium carbon bond.

2.11 The synthesis of $[ReBr(PhC_2Me)_2(\eta-C_5H_5)][PF_6]$(6).

The addition of one equivalent of thallium hexafluorophosphate to a solution of $[ReBr_2(PhC_2Me)(\eta-C_5H_5)]$ and excess phenyl-1-propyne over a period of 24 hours leads to the precipitation of TlBr and the formation of the orange crystalline solid $[ReBr(PhC_2Me)_2(\eta-C_5H_5)][PF_6]$ **6** (figure 53).

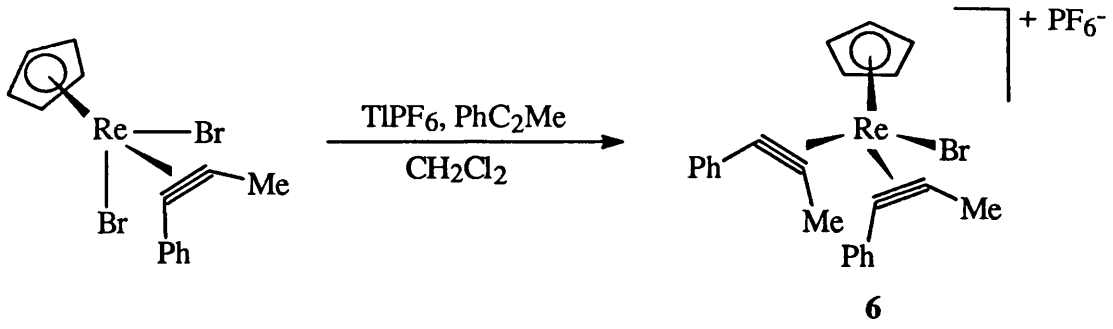

6

FIGURE 53

The ^{1}H and $^{13}C\text{-}\{^{1}H\}$ nmr spectra reveal that both the alkynes are rotating as the two methyls are equivalent and only two quaternary peaks are seen. Complex **6** was expected to react with super-hydride to form a neutral complex similar to complex **7**, preliminary studies showed that the reaction did indeed form a red, neutral, air sensitive product. Attempts to purify the product by chromatography however failed due to the sensitivity of the product.

CHAPTER 3:

The synthesis of rhenium alkene complexes: Evidence for η^2–stabilisation from a phenyl ring.

3.1 Transition metal-alkene chemistry.

The first example of a metal alkene complex was Zeise's salt first synthesised in 1827 by boiling $PtCl_4$ in ethanol[99], the first preparation of this complex from ethylene was described by Birnbaum (fig54).[100]

$$K_2[PtCl_4] + C_2H_4 \xrightarrow[60\ bar]{\text{dilute HCl}} K[C_2H_4PtCl_3].H_2O + KCl$$

FIGURE 54

Olefin complexes are widespread among the series of transition metals and play an important role in catalytic reactions, such as hydrogenation, oligomerization, polymerisation and hydroformylation.

Recent examples of metal-alkene complexes include the synthesis of several rhenium-alkene complexes. Casey reported the synthesis of rhenium-alkene complexes from the reaction of a heterobimetallic dihydride with an alkyne source. Such metal complexes show great promise as catalysts due to the co-operation of two metal centres, however due to the problem of needing to optimise conditions for both metals few examples have been seen.[101-104] Casey reports that the bimetallic complex $[Cp(CO)_2HRePtH(PPh_3)_2]$ acts as a catalyst for ethylene hydrogenation and reacts stoichiometrically with alkynes to produce rhenium-alkene complexes.[105] Reaction of $[Cp(CO)_2HRe\text{-}PtH(PPh_3)_2]$ with propyne led to the formation of the rhenium-propene complex $[Cp(CO)_2Re(CH_2{=}CHCH_3)]$ and the corresponding platinum-propyne complex. This reaction constitutes the first example of a stoichiometric hydrogenation of an alkyne to metal-alkene complex.[106]

The reaction of the bimetallic complex with diphenylacetylene proved to be unusual because it led to the formation of both *cis* and *trans* stilbene complexes (fig 55). The stereochemistry of the two products assigned due to the difference in the $^{13}C\text{-}\{^1H\}$

carbonyl shifts, (two resonances for the *trans* complex whereas only one carbonyl resonance is seen for the *cis* complex). A possible mechanism to account for the formation of *trans* stilbene in this reaction involves reversible hydride transfer from rhenium to give an intermediate vinyl-platinum moiety to produce a platinum-carbene complex.

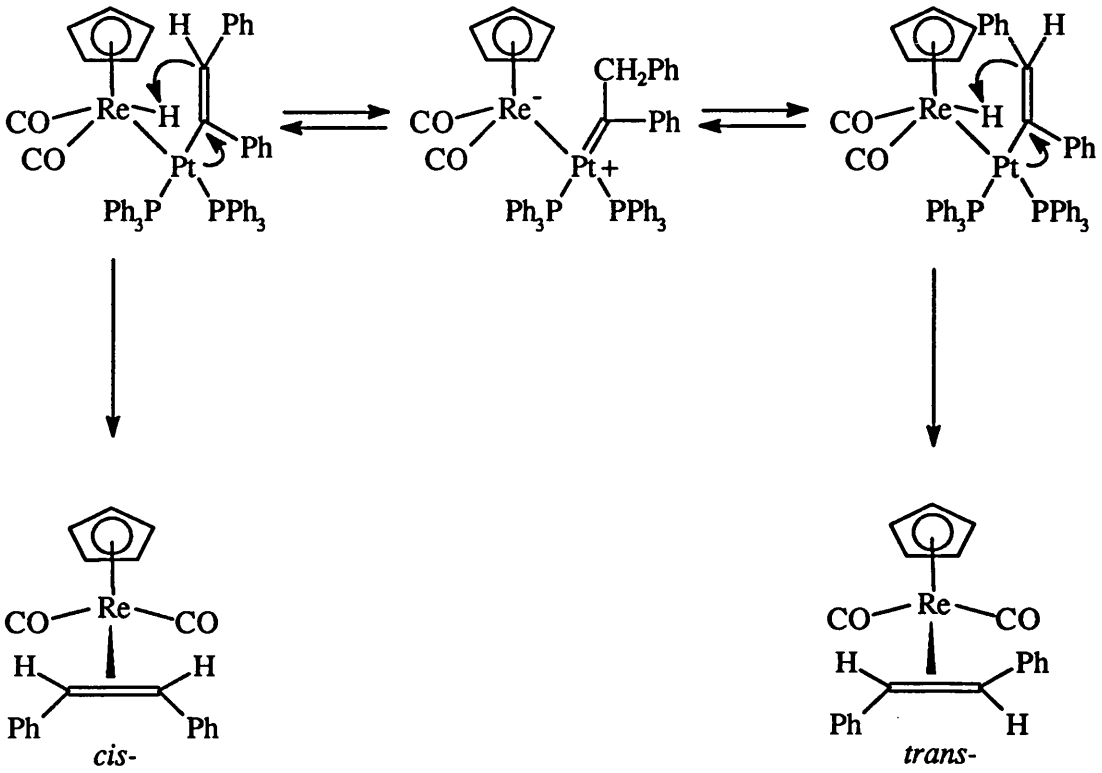

FIGURE 55

Trans hydrogenation of alkynes is rare but has been seen previously by Muetterties[107] and McQuillen.[108] As seen previously cationic η^2–vinyls can be synthesised and would be expected to be reactive towards nucleophilic reagents. The complex $[Re(Ph_2PCH_2CH_2PPh_2)(\eta^2\text{–}PhC_2Ph)(\eta\text{–}C_5H_5)][BF_4]_2$ is easily synthesised from $[ReBr_2(\eta^2\text{–}PhC_2Ph)(\eta\text{–}C_5H_5)]$ by reaction with two equivalents of $AgBF_4$ and dppe in a dichloromethane solution.[109]

This complex can then be reacted with one molar equivalent of $KBHBu^s_3$ in a thf solution (-78°C) to give the cationic η^2–vinyl complex $[Re{=}C(Ph)CH(Ph)(Ph_2PCH_2CH_2PPh_2)(\eta\text{–}C_5H_5)][BF_4]$, this complex was shown to contain a hydrogen atom within the η^2–vinyl fragment which lies in a pseudo-axial site, parallel to the rhenium-carbon double bond. Reaction of the η^2–vinyl complex with a second molar equivalent of $KBHBu^s_3$, (thf, 25°C) led to the formation of a *cis*-stilbene complex (fig 56).[110] A EHMO calculation[111] showed that the expected site for attack was the rhenium-carbon double bond of the η^2-vinyl complex, however, the selectivity of this reaction is proposed to arise due to an interaction of the Lewis acid BBu^s_3, which is liberated on 'H⁻' transfer, with the π-cloud of the dppe ligand.[110]

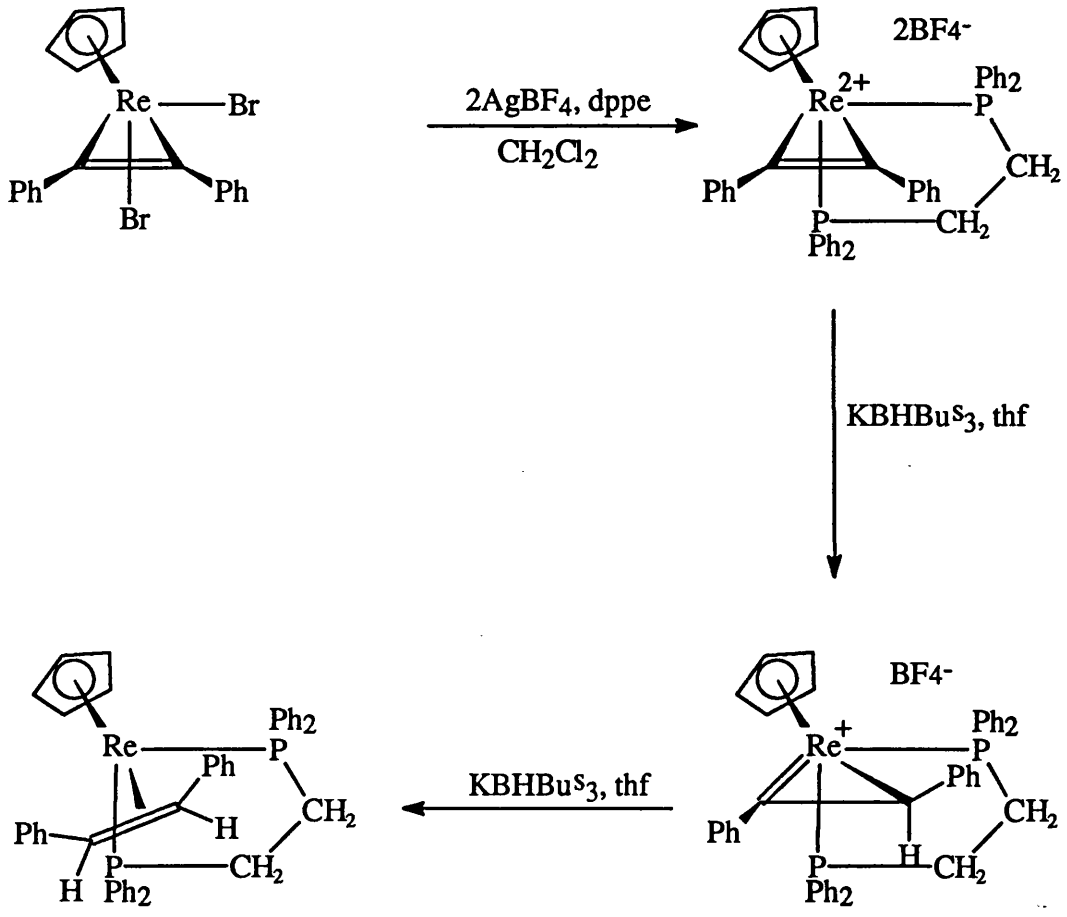

FIGURE 56

This chapter discusses the synthesis of two cationic rhenium-alkene complexes by reaction of the corresponding neutral η^2–vinyl complex with electrophilic reagents, (trityl tetrafluoroborate and tetrafluoroboric acid were used as the electrophilic reagents). The reaction with $[Ph_3C][BF_4]$ was of particular interest, as the original aim of the experiment was an attempt to reverse the η^2–vinyl synthesis by hydride abstraction.

3.2 The reaction of $[BrRe{=}C(Ph)CH(Ph)(Ph_2MeP)(\eta{-}C_5H_5)]$ (9) with $[Ph_3C][BF_4]$.

The complex $[BrRe{=}C(Ph)CH(Ph)(Ph_2MeP)(\eta{-}C_5H_5)]$ (**9**) was prepared by reaction of $[ReBr(Ph_2MeP)(\eta^2\text{-}PhC_2Ph)(\eta{-}C_5H_5)][PF_6]$ with $KBHBu^s_3$ (thf, -78°C)[109], it was thought that the reaction of trityl tetrafluoroborate (as a source of the trityl cation Ph_3C^+) with a solution of the η^2–vinyl would lead to hydride abstraction and the formation of the original rhenium-alkyne complex (fig 57).

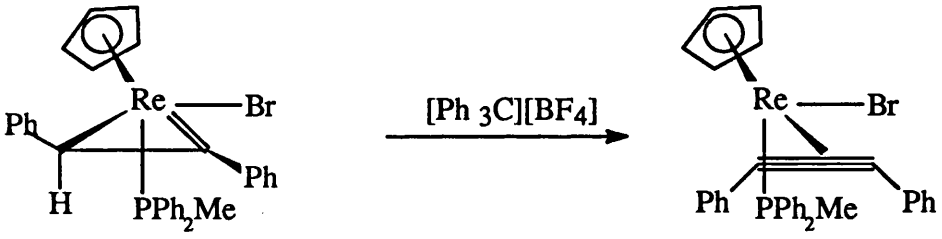

FIGURE 57

However, when the reaction was attempted in dichloromethane (-78°C) a colour change on warming over 2 hours from green to red was observed. This suggested that the sought after reaction had not occurred, as it is known that the colour of the expected product is green.[109] After Celite filtration and recrystallisation from dichloromethane and diethyl-ether, a purple, air and moisture sensitive crystalline solid was isolated. The complex (**10**) was found to be extremely unstable and an accurate

elemental analysis could not be obtained. The ^{1}H nmr spectrum suggested that the trityl cation had become incorporated into the complex, the integration of cyclopentadienyl (δ6.17ppm) and phenyl (δ7.96-7.15ppm) hydrogens showing a ratio of 1:7. The spectrum also showed a singlet at δ4.72 which would be attributable to the hydrogen which had not been abstracted from the complex as expected. This signal showed no coupling to the phosphorous, (the original η^2–vinyl hydrogen shows coupling to the phosphorous $J(^{1}H^{31}P)$ 14Hz). The chemical shift of the hydrogen suggests the formation of an alkene complex as it is in the region expected for this type of complex.[110] This was confirmed by $^{13}C-\{^{1}H\}$ nmr which showed the presence of two resonances (δ101.13 and δ69.49) typical for a sp^2 hybridised alkene carbon,[112] also the presence of a peak at δ18.33 (typical for an sp^3 hybridised carbon[112]), confirmed the incorporation of the trityl fragment.

The carbon resonance at δ101.13 was confirmed by a ^{90}Dept experiment as having one hydrogen atom attached (the second alkene resonance was not present in the ^{90}Dept spectrum). Both the $^{13}C-\{^{1}H\}$ and ^{90}Dept spectra showed a broad peak at δ95.0, which was attributed to the arene carbons of an η^2–bonded phenyl ring. This type of interaction has been seen previously for Rh[113], Os[114,115], Mo[116] and Co[117]. The $^{31}P-\{^{1}H\}$ nmr showed a single resonance at -δ10.15ppm suggesting that only one isomer has been formed. It would have been expected that there would be some coupling of the phosphorous to the hydrogen, but the absence of such coupling is probably due to the shielding from the two phenyl rings, which are thought to lie either side of the rhenium centre in a *cisoid* configuration (fig 58).

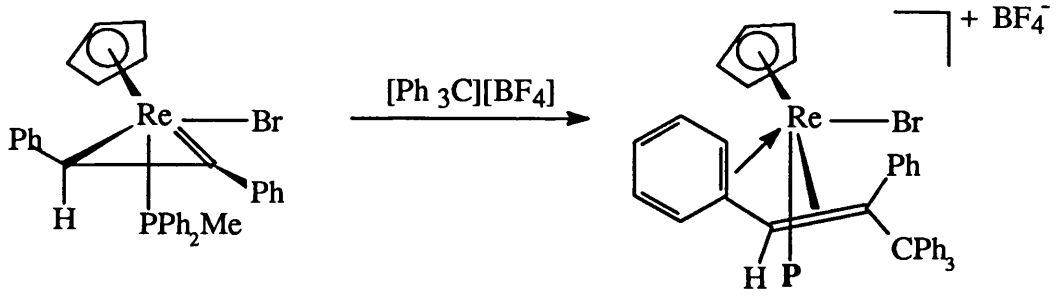

9 **10** **P** = PPh_2Me

FIGURE 58

The η^2–interaction from the phenyl ring within this complex helps to stabilise the otherwise electron deficient 16 electron species. The interaction of the ring is thought to arise such that the alkene fragment is bonded as an η^4(4e)-buta-1,3-diene (fig58), although co-ordination involving a different arene carbon-carbon bond cannot be ruled out. A proposal for the mechanism of formation and stereochemistry of complex **10** can be found in section 3.5.

3.3 The reaction of [BrRe=C(Ph)CH(Ph)(Ph_2MeP)(η–C_5H_5)] (9) with $HBF_4.Et_2O$.

As discussed in section 3.1 it has been shown that the reaction of a cationic η^2–vinyl complex with a source of 'H$^-$' led to the formation of a neutral rhenium-alkene complex, in this case identified as *cis*-stilbene. In the light of the reaction of [BrRe=C(Ph)CH(Ph)(Ph_2MeP)(η–C_5H_5)] (**9**) with the trityl cation it seemed plausible that reaction of **9** with a source of 'H$^+$' might lead to the formation of a co-ordinately unsaturated cationic stilbene complex. This unsaturation may be stabilised by either an agostic interaction from one of the hydrogens or by an η^2-interaction from a phenyl ring to form an η^4(4e)-buta-1,3-diene as seen for complex **10**.

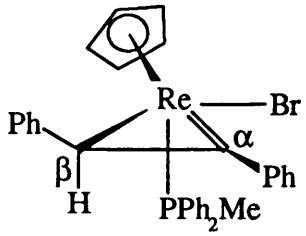

FIGURE 59

There are however two possible sites of attack on the η^2–vinyl moiety for the incoming electrophile (fig59), attack on the α carbon of the η^2–vinyl would lead to the formation of the anticipated unsaturated stilbene complex.

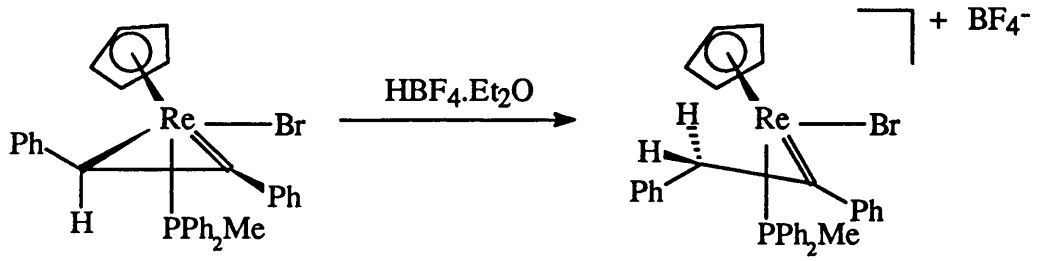

FIGURE 60

Attack on the β carbon on the other hand would lead to the formation of a sixteen electron rhenium carbene complex (fig60). This type of reaction has been observed previously by J. L. Templeton[118] for the reaction of a (hydrotris(3,5-dimethylpyrazolyl)borato) tungsten η^2–vinyl complex with tetrafluoroboric acid (fig61), in this example the resultant cation is also a sixteen electron species and is stabilised by an agostic interaction from one of the hydrogens on the β carbon, but within this paper he also suggests that the complex might have been stabilised by an η^2–interaction from the phenyl ring forming a η^4(4e)-buta-1,3-diene complex.

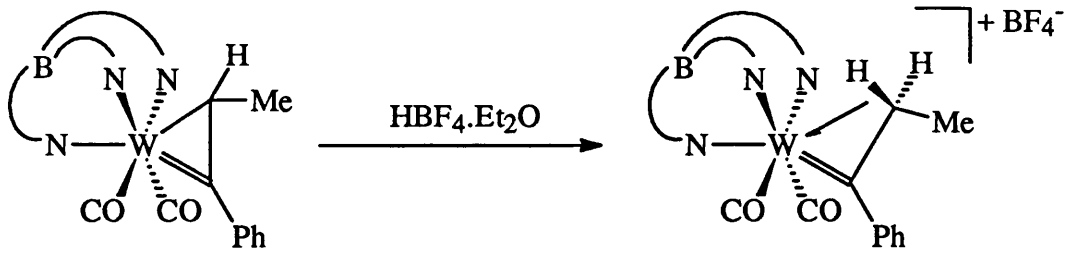

FIGURE 61

The reaction of **9** with tetrafluoroboric acid was carried out in a dichloromethane solution (-78°C) and over a period of two hours a colour change from green to red was observed. After Celite filtration and recrystallisation from dichloromethane and diethyl-ether, a purple, air and moisture sensitive crystalline solid was isolated. The complex was found to be extremely unstable and an accurate elemental analysis could not be obtained. The ^{1}H nmr spectrum seemed to confirm that the expected product had indeed been formed. The expected cyclopentadienyl and phosphine methyl peaks were seen at almost identical chemical shifts to those seen for complex **10** (δ6.17, η–C_5H_5; δ2.72, methyl). Two doublets at δ6.48 and δ4.74 attributable to the alkene hydrogens were seen, but as for complex **10** no coupling to the phosphorous was seen, however, a small coupling between the two hydrogens was observed (1.47Hz and 3.66Hz). The magnitude of this coupling is very small and *cis*- and *trans*-couplings are usually larger. However, the $^{31}P-\{^{1}H\}$ nmr spectrum showed only one peak at -δ10.15ppm and this suggests that one isomer only is formed in the reaction. The $^{13}C-\{^{1}H\}$ nmr and ^{90}Dept experiments confirmed the presence of the alkene moiety, also present is a broad peak at δ94.55 attributable to the η^2–interaction from one of the phenyl rings (fig 62).

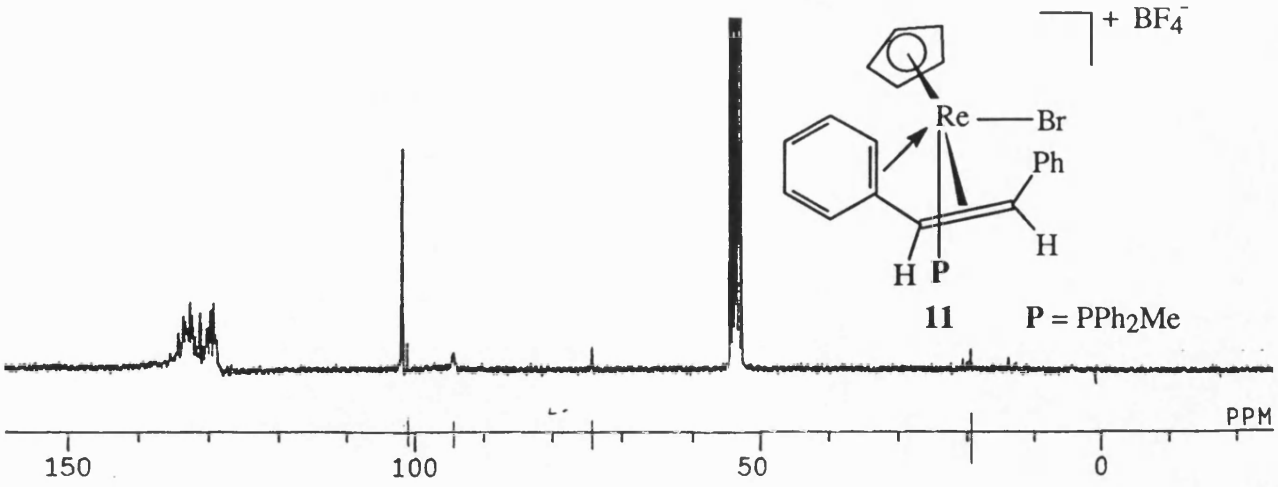

FIGURE 62

The inequivalence of the two hydrogens suggests that the stilbene fragment is static on the spectroscopic timescale (i.e there is only η^2–bonding seen from one of the phenyl rings). The similarity of the data for this complex and the previously discussed complex **10** suggests that the stilbene fragment is formed with the *cisoid* conformation, whereby the two hydrogens are shielded by the two rings and no coupling is seen to the phosphorous (fig 63).

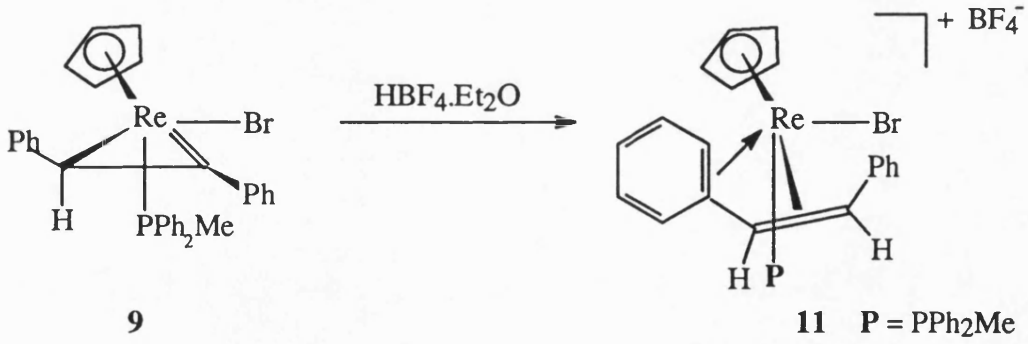

9 **11** **P** = PPh_2Me

FIGURE 63

As seen previously the η^2–interaction from the phenyl ring satisfies the electronic unsaturation at the rhenium centre to give an eighteen electron η^4(4e)-buta-1,3-diene complex. A proposed mechanism for the formation and stereochemistry of this complex can be found in section 3.6. Both these complexes have very similar spectroscopic properties summarised below.

i) The ^1H and ^{13}C-{^1H} nmr data shows that the cyclopentadienyl and methyls of the two are equivalent.

ii) Both complexes have a CH fragment within the alkene, which are equivalent, (^1H δ4.72 and δ4.74, ^{13}C-{^1H} δ101.13 and δ101.12ppm).

iii) The ^{31}P–{^1H} nmr chemical shifts for both are identical (-δ10.15ppm).

iv) Neither complex shows any coupling to phosphorous, supporting the *cisoid* geometry whereby the hydrogens are shielded by the two phenyl rings.

v) Both complexes show an η^2–bonding interaction from a phenyl ring to the metal centre, thought to be within a static system.

In the light of these similarities an EHMO study was performed to identify the likely site for electrophilic attack, and therefore a possible mechanism for the formation of the two cationic rhenium-alkene complexes **10** and **11**.[119]

3.4 A Theoretical study on [BrRe=C(H)CH$_2$(PH$_3$)(η–C$_5$H$_5$)].

To help clarify the mechanism of the two reactions discussed in sections 3.2 and 3.3 an EHMO study was carried out for the theoretical η^2–vinyl complex [BrRe=C(H)CH$_2$(PH$_3$)(η–C$_5$H$_5$)] which is equivalent to complex **9** with hydrogens in place of the phenyl rings and phosphine methyl groups. The X-ray structure and bond parameters for complex **9** were used to set up the calculation, all hydrogens were set at a distance of 1.10Å from the parent atoms. The calculated electronic charges for the rhenium atom and the two carbons of the η^2–vinyl moiety are shown in table 9.

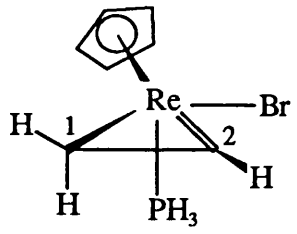

Re	-0.465	C1	0.010	C2	-0.22

TABLE 9

The calculations show that the most likely site for electrophilic attack was not one of the η^2-vinyl carbons as expected but the metal centre. There are two possible types of reaction that could occur with the electrophile, in the case of the reaction with $[Ph_3C][BF_4]$ it is believed to proceed via a frontier orbital controlled reaction. In contrast the reaction with 'H^+' would be expected to be charge controlled and as shown by the calculation would attack the metal centre. In the case of the frontier orbital controlled reaction the trityl cation would attack the highest occupied molecular orbital (HOMO) of the molecule. Figure 64 shows that the calculated HOMO for the molecule is one of the metal d-orbitals, the direction of the attack on the metal centre was predicted to be from behind, bisecting the Br-Re-C2 angle. Interestingly these calculations show that both the frontier orbital and charge controlled reactions would in this case attack at the same site within the complex. With the results of the calculation and the nmr data collected, proposed mechanisms for the formation of complexes **10** and **11** are discussed in sections 3.5 and 3.6.

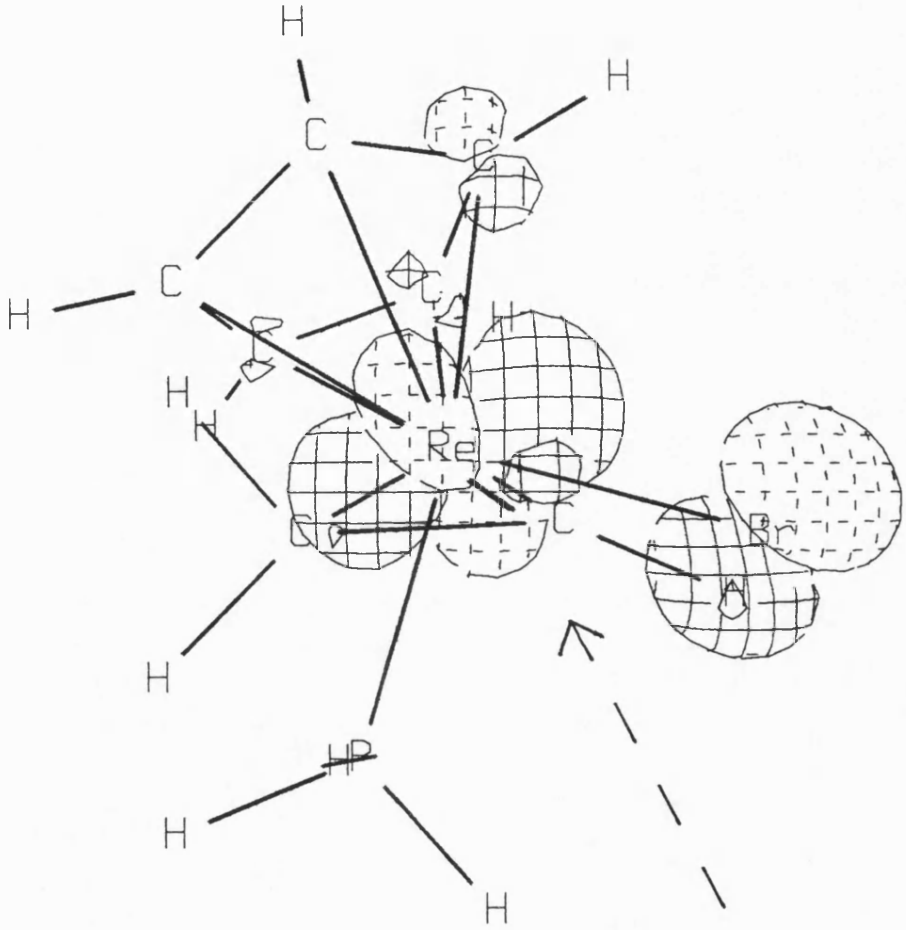

FIGURE 64

A plot of the HOMO for the theoretical complex [BrRe=C(H)CH$_2$(PH$_3$)(η–C$_5$H$_5$)]

the arrow denotes the predicted direction for electrophilic attack.

3.5 A proposed mechanism for the formation of the rhenium alkene complex [ReBr(Ph_2MeP){CH(Ph)=CPh(CPh_3)}(η-C_5H_5)] (10).

The original aim of the experiment was to attempt to use trityl tetrafluoroborate to abstract the hydrogen from complex **9** and form the original starting complex containing an alkyne (fig 55). The trityl cation has been widely used in this manner[120-124] but examples are known where during the reaction the trityl cation has added to a metal bound organic fragment, resulting in carbon-carbon bond formation (fig 65).[125-128]

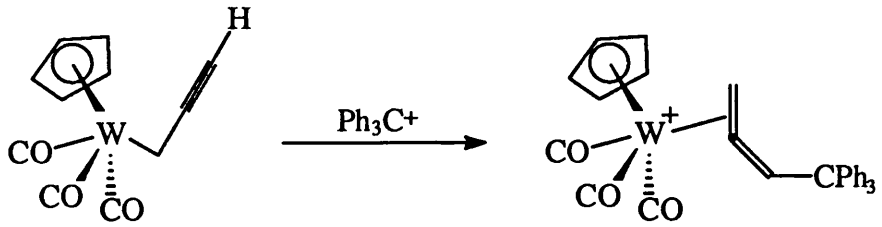

FIGURE 65

There is, however, a third method by which the trityl cation has been seen to react with an organometallic complex, that is namely as a one electron oxidant leading to the production of a radical-cation complex.[129-132] These radical cations then usually undergo hydride abstraction by the remaining trityl radical [$Ph_3C^{\bullet}$] leading to the formation of Ph_3CH (fig66).

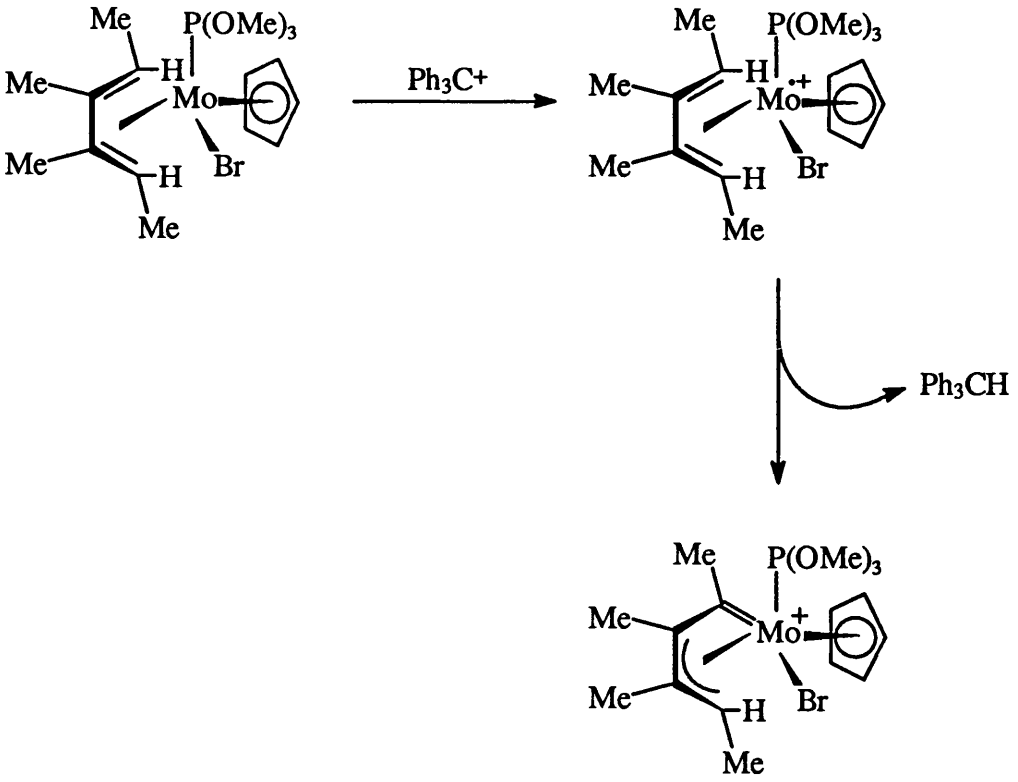

FIGURE 66

The proposed reaction mechanism for the formation of **10** is shown in figure 67. It is predicted from the theoretical calculation that a frontier orbital controlled electrophilic attack would take place via the HOMO, located on the rhenium atom and that the direction of attack would be from behind and below the rhenium carbon double bond, as this is the least sterically hindered part of the complex (fig64). On comparison with the examples seen in the literature it is likely that in this situation the trityl cation acts as a one electron oxidant and leads to the formation of the radical-cation **A**. However, instead of the more usual hydride abstraction the radical-cation rearranges to the more stable intermediate **B** where the radical is situated on the carbon atom of the organic fragment, this radical can be stabilised by delocalisation of the odd electron into the phenyl ring. There is then thought to be an instantaneous coupling reaction between **B** and the free trityl radical leading to the formation of the

rhenium-alkene complex **10** where the two phenyl rings have a *cisoid*-orientation. The electron deficiency of this complex can be satisfied by an η^2–interaction with a phenyl ring , it is not known, however, whether this interaction takes place upon the formation of intermediate **B** (which as shown would be a sixteen electron species) or on formation of complex **10**. Due to the necessity for the radical in **B** to be planar it is thought that the phenyl ring that is involved in the η^2–interaction is most likely to be the ring situated on the β carbon atom of the original η^2–vinyl complex, this would also be the least sterically hindered of the two rings in complex **10**.

P = PPh_2Me

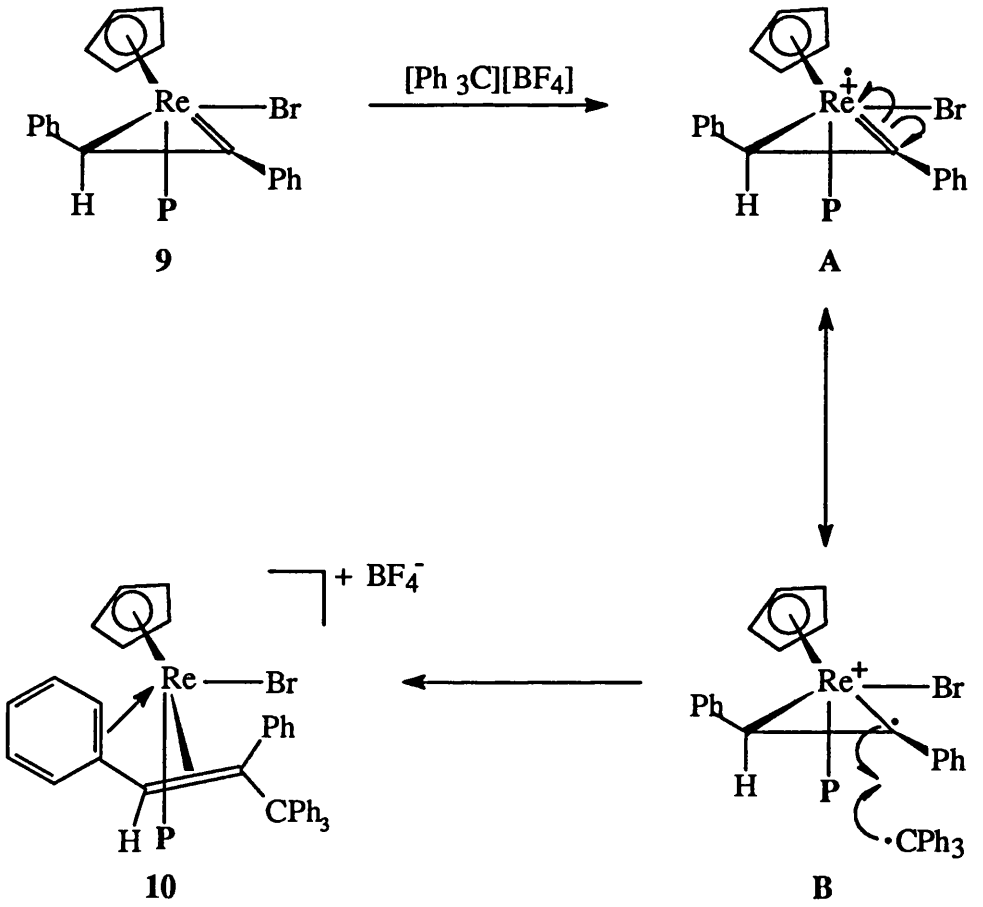

FIGURE 67

3.6 A proposed mechanism for the formation of the rhenium-alkene [ReBr(Ph$_2$MeP){CH(Ph)=CH(Ph)}(η–C$_5$H$_5$)] (**11**).

The proposed mechanism for the formation of the cationic rhenium-alkene complex [ReBr(Ph$_2$MeP){CH(Ph)=CH(Ph)}(η–C$_5$H$_5$)] (**11**) is shown in figure 68. The theoretical study predicts that the electrophile (in this case H^+) would attack from behind the molecule (fig64) and would lead to the formation of intermediate **C**. As shown in the diagram the metal-hydride is situated beneath the rhenium-carbon double bond and hydrogen migration onto the double bond would lead to the

P = PPh$_2$Me

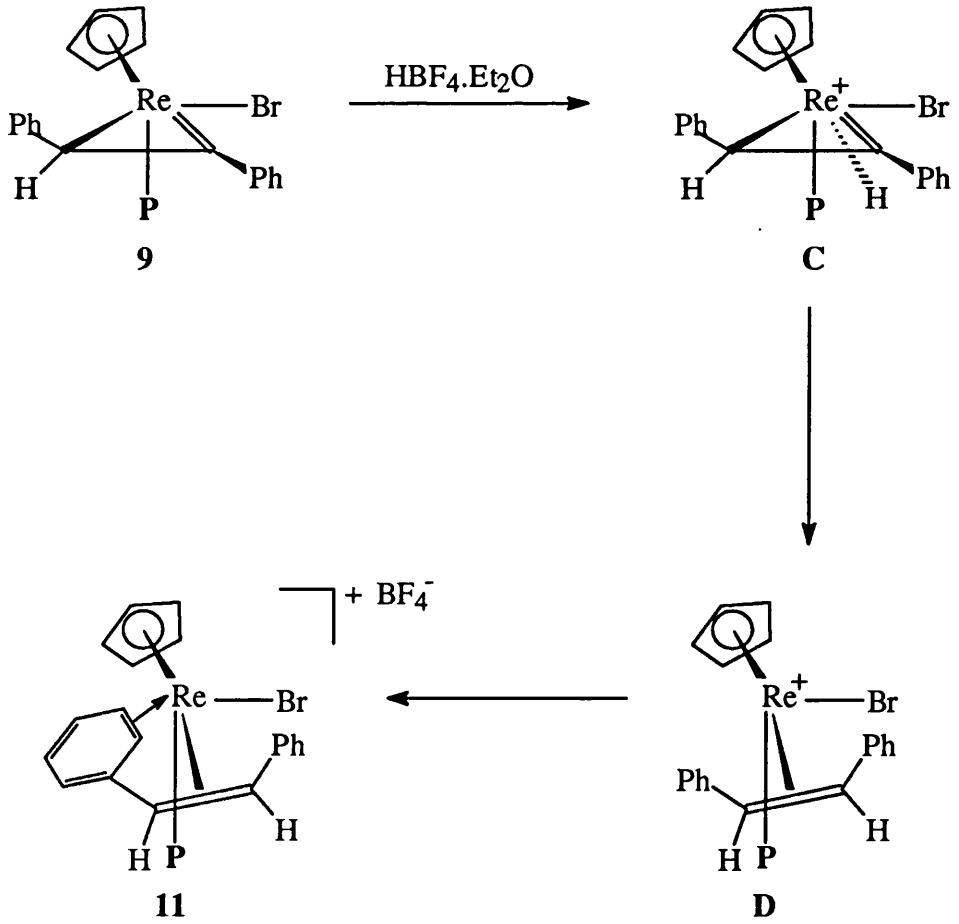

FIGURE 68

formation of intermediate **D**, where the alkene formed would have the *cisoid*-configuration as predicted from the nmr data. This species is an electron deficient sixteen electron system and is stabilised by an η^2-interaction from one of the phenyl rings forming the formal η^4(4e)-buta-1,3-diene complex **11** which now satisfies the eighteen electron rule. Again it is not known which of the two rings fulfils the complexes electronic requirements but it is known from the nmr data that the system is static at ambient temperature.

3.7 Closing comments.

There is scope for development within this area of chemistry as many examples of neutral η^2–vinyls are known, further theoretical and experimental studies may help to clarify the proposed mechanisms for the synthesis of **10** and **11**.

The aim for further research would be to find a system which is stable enough as to allow the growth of crystals, therefore confirming the precise nature of the bonding between the two phenyls of the alkene moiety and the rhenium metal centre, this could be accomplished by either changing the phosphine ligand or source of H^+, and therefore the counterion.

CHAPTER 4

The reactions of $[ReBr_2(\eta^2\text{-}PhC_2R)(\eta\text{–}C_5H_5)]$ (R=Ph, Me) towards phosphorous containing ligands.

4.1 The reactivity of $[ReBr_2(\eta^2\text{-}PhC_2Me)(\eta\text{–}C_5H_5)]$ towards phosphorous ligands.

The reactivity of the rhenium alkyne complex $[ReBr_2(\eta^2\text{-}PhC_2Ph)(\eta\text{–}C_5H_5)]$ towards phosphorous containing ligands has been previously studied by C. Vaughan.[109]

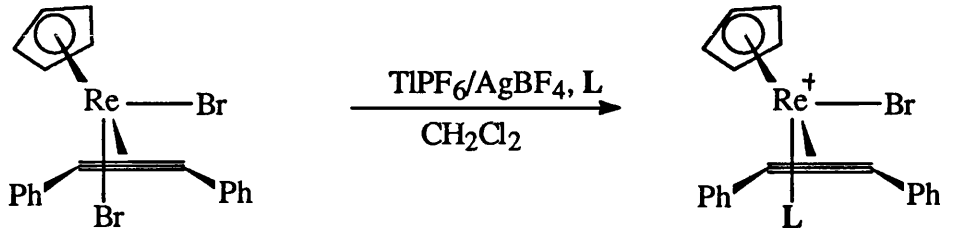

L = PMe_3, PPh_3, Ph_2PMe, $P(OMe)_3$

FIGURE 69

It was found that the reaction of $[ReBr_2(\eta^2\text{-}PhC_2Ph)(\eta\text{–}C_5H_5)]$ in a dichloromethane solution, with one equivalent of silver tetrafluoroborate or thallium hexafluorophosphate, (as in some systems the use of silver salts led to poor yields or decomposition products only) and an excess of the appropriate phosphorous ligand, led to the deposition of the relevant metal bromide and the formation of the cationic rhenium complexes $[ReBrL(\eta^2\text{-}PhC_2Ph)(\eta\text{–}C_5H_5)]^+$, [L = PMe_3, PPh_3, Ph_2MeP, $P(OMe)_3$] (fig69). A preliminary reaction by C. Vaughan with the phenyl-1-propyne complex $[ReBr_2(\eta^2\text{-}PhC_2Me)(\eta\text{–}C_5H_5)]$, triphenylphosphine and thallium hexafluorophosphate led to the formation of $[ReBr(PPh_3)(\eta^2\text{-}PhC_2Me)(\eta\text{–}C_5H_5)][PF_6]$ (**12**) and suggested that this type of reaction could be generalised. This was confirmed when it was shown that the corresponding diphenylmethylphosphine (**13**) and trimethylphosphite (**14**) complexes could be synthesised by the reaction of a dichloromethane solution of $[ReBr_2(\eta^2\text{-}PhC_2Me)(\eta\text{–}C_5H_5)]$ with $TlPF_6$ and an excess of the phosphorous ligand (fig 70).

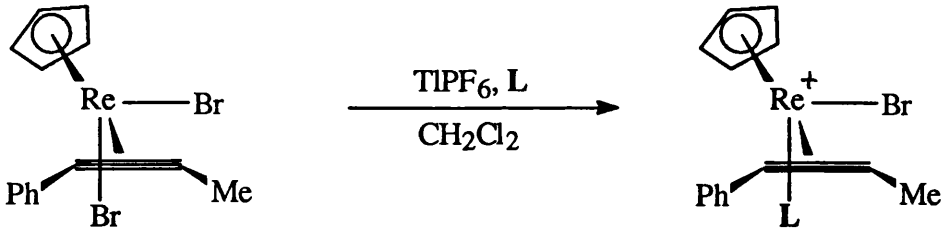

13, L = Ph_2MeP

14, L = $P(OMe)_3$

FIGURE 70

The ^1H and ^{13}C-{^1H} nmr spectra for complexes **13** and **14** are directly comparable with those observed for the corresponding diphenylacetylene systems. The ^1H nmr of complex **13** shows a cyclopentadienyl peak at δ5.79, also present were alkyne (δ3.23) and phosphine (δ2.58) methyl peaks. The ^{13}C-{^1H} nmr showed a cyclopentadienyl signal at δ95.8 and alkyne (δ15.3) and phosphine (δ88.6) methyl signals, also present were signals for the two quaternary contact carbons (δ227.3, δ212.4). The ^{31}P-{^1H} nmr spectra showed one singlet (-δ13.49), suggesting that only one isomer was formed in the reaction. Interestingly there was no coupling from the phosphorous to either the alkyne methyl or contact carbons. This could be due either to the coupling being too small to observe or that the rhenium-phosphorous bond is particularly long. The ^1H nmr spectra for complex **14** showed a cyclopentadienyl peak at δ5.93, also doublets for the phosphite (δ4.04, J=11.26Hz) and alkyne (δ3.72, J=3.38Hz) methyls. The ^{13}C-{^1H} nmr showed a cyclopentadienyl signal at δ95.8 and two doublets for the phosphite (δ56.3, J=8.1Hz) and alkyne (δ23.6, J=9.5Hz) methyls, the two quaternary carbons appeared at δ212 (methyl quaternary split into a doublet J=27Hz) and δ207. As seen for complex **13** the ^{31}P-{^1H} nmr showed one resonance (δ92.5) indicating that only one isomer had been formed. The substitution of a bromine atom by a phosphine or phosphite ligand in these types of systems leads to a loss of symmetry for the molecule and the formation of a chiral rhenium centre.

An X-ray study carried out for the complex [ReBr(Ph_2MeP)(η^2-PhC_2Ph)(η-C_5H_5)][PF_6][109], revealed the exact stereochemistry around the metal centre, the assignment of the absolute configuration was determined using the suggestions of Stanley and Baird[133] which extends previous conventions for determining configuration[134-136] and employs a pseudo-atom convention to assign configuration of chiral complexes. Application of these suggestions show that the absolute configuration for these complexes is S, (fig71).

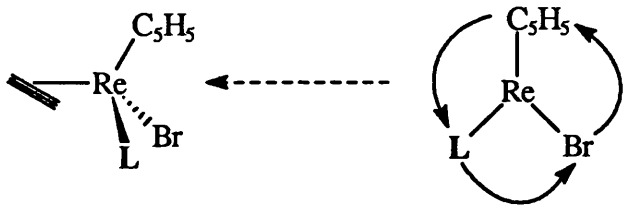

S

FIGURE 71

4.2 The synthesis of rhenium alkyne dications by reaction of [$ReBr_2$(η^2-PhC_2R)(η-C_5H_5)] (R=Ph, Me) with various bidentate phosphorous ligands.

Reaction of [$ReBr_2$(η^2-PhC_2Me)(η-C_5H_5)] with two equivalents of silver tetrafluoroborate and dppe in a dichloromethane solution, led to the deposition of silver bromide and a solution of the dicationic complex [Re(dppe)(η^2-PhC_2Me)(η-C_5H_5)][BF_4]$_2$ **15** (fig72). The ^{1}H nmr spectrum showed resonances fully consistent with the presence of cyclopentadienyl (δ5.93) and dppe (δ3.8-3.68) ligands, also present was a resonance for the methyl (δ1.73) of the alkyne. The ^{13}C-{^{1}H} showed resonances for the cyclopentadienyl (δ99.7) and dppe (δ29.3, J=37Hz) ligands and the methyl of the alkyne (δ24.7), the resonances for the two quaternary contact carbons appeared at δ222.5 and δ212.9ppm.

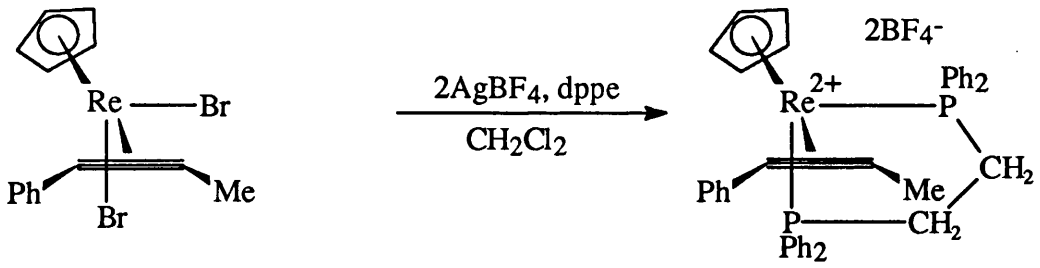

15

FIGURE 72

The $^{31}P-\{^{1}H\}$ nmr showed one resonance at δ26.55 suggesting that the alkyne ligand is freely rotating at ambient temperature.

Previously it has been shown that the reaction of $[ReBr_2(\eta^2\text{-}PhC_2Ph)(\eta\text{–}C_5H_5)]$ with two equivalents of silver tetrafluoroborate and dppe in a dichloromethane solution led to the formation of the dicationic complex $[Re(dppe)(\eta^2\text{-}PhC_2Ph)(\eta\text{–}C_5H_5)][BF_4]_2$, subsequent reaction with one molar equivalent of $KBHBu^s{}_3$ led to the formation of an η^2-vinyl complex, and reaction with a further equivalent of $KBHBu^s{}_3$ was thought to give a neutral stilbene complex. Attempts to grow crystals of this stilbene complex had proved unsuccessful, and therefore the precise nature of the stilbene ligand was unknown (*i.e* it was unknown whether *cis* or *trans* stilbene was formed). It was thought that the reaction with bulkier or asymmetric ligands would allow identification of the stilbene conformation by either spectroscopic or crystallographic methods. The two ligands used were 1-diphenylphosphino, 2-diphenylarsino ethane (arphos) an asymmetric ligand, and 1,1`-bis (diphenylphosphino)ferrocene (dppf). The synthesis of the dicationic rhenium-alkyne pre-cursors for the stilbene complex is discussed below.

The reaction of $[ReBr_2(\eta^2\text{-}PhC_2Ph)(\eta\text{–}C_5H_5)]$ with two equivalents of silver tetrafluoroborate and the mixed bidentate complex arphos, led to the formation of the dicationic complex $[Re(arphos)(\eta^2\text{-}PhC_2Ph)(\eta\text{–}C_5H_5)][BF_4]_2$ **16** (fig73).

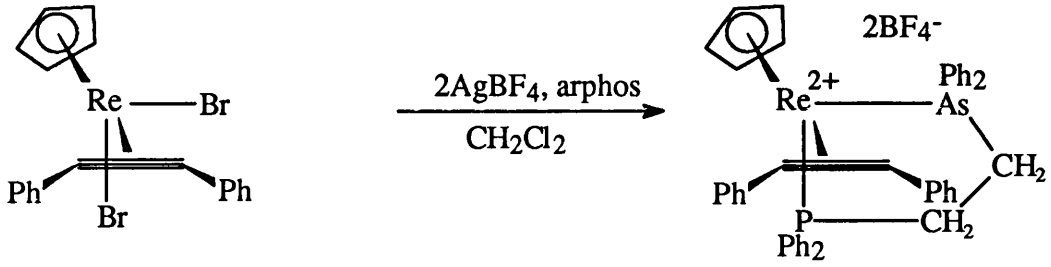

16

FIGURE 73

The ^1H nmr spectrum for complex **16** showed cyclopentadienyl (δ5.82) and arphos (δ3.4-2.76) peaks. The $^{13}C\text{-}\{^1H\}$ nmr showed both cyclopentadienyl (δ97.6) and arphos (δ30, δ25.4) resonances as well as the quaternary contact carbons (δ223.9) of the alkyne, which are seen to be equivalent suggesting that the diphenylacetylene ligand is freely rotating at ambient temperature. The $^{31}P\text{-}\{^1H\}$ nmr showed one resonance at δ37.85. Attempts to grow crystals of this system proved unsuccessful so the reaction was extended to the incorporation of a dppf ligand, which is much bulkier and was thought to be more likely to yield crystals. The reaction of $[ReBr_2(\eta^2\text{-}PhC_2Ph)(\eta\text{–}C_5H_5)]$ with two equivalents of thallium hexafluorophosphate and dppf in a dichloromethane solution, led to the formation of the green dicationic complex $[Re(dppf)(\eta^2\text{-}PhC_2Ph)(\eta\text{–}C_5H_5)][PF_6]_2$ **17** (fig74). The ^1H nmr spectra for complex **17** showed cyclopentadienyl (δ5.64, J=5.31Hz) and dppf cyclopentadienyl (δ4.19-3.48) peaks. The $^{13}C\text{-}\{^1H\}$ nmr showed resonances for the cyclopentadienyl (δ96.9) and dppf cyclopentadienyls (δ76.3-73.4), also the presence of a peak assigned to the quaternary carbons (δ226.1) of the alkyne. The $^{31}P\text{-}\{^1H\}$ nmr showed one resonance

at -δ4.02 . Again, however, attempts to grow crystals of this system proved unsuccessful.

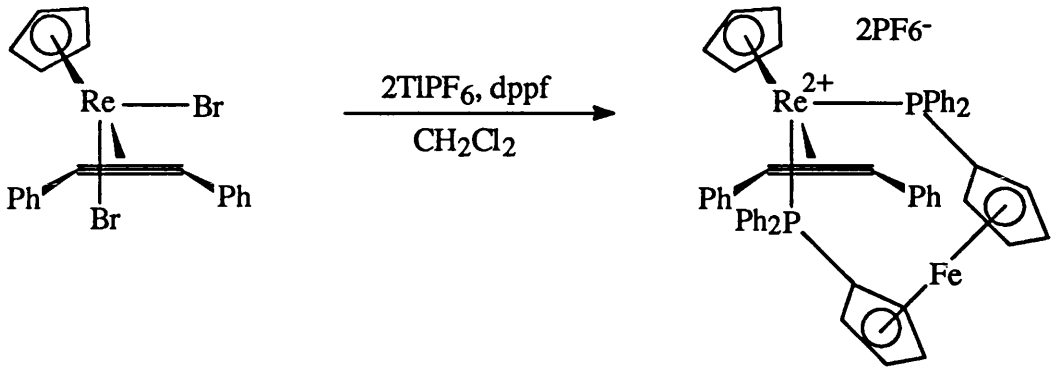

17

FIGURE 74

4.3 The formation of the neutral η^2-vinyl complex [BrRe=C(Me)CH(Ph)(PPh$_3$)(η-C$_5$H$_5$)].

The availability of the cationic complexes [ReBr(η^2-PhC$_2$Me)L(η–C$_5$H$_5$)][PF$_6$] (L = PPh$_3$, Ph$_2$MeP, P(OMe)$_3$), provide an opportunity to explore their reactivity towards nucleophilic reagents such as 'H$^-$'. This would allow a comparison with the diphenylacetylene systems previously studied.[109] A solution of [ReBr(PPh$_3$)(η^2-PhC$_2$Me)(η–C$_5$H$_5$)][PF$_6$] **12** (thf, -78°C) was treated with one molar equivalent of 'H$^-$', delivered by KBHBu$^s_3$, a rapid colour change from orange to red was observed and this colour remained on warming to room temperature (in contrast the diphenylacetylene system which became green in colour upon warming). The resultant neutral red product was stable towards alumina and purification by column chromatography and recrystallisation afforded a red crystalline solid, identified as [BrRe=C(Me)CH(Ph)(PPh$_3$)(η–C$_5$H$_5$)] **18** (fig75).

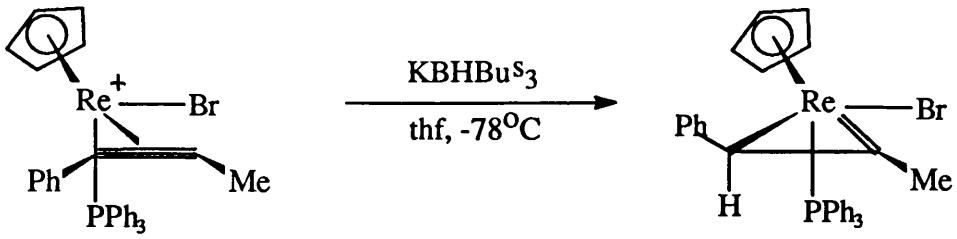

FIGURE 75

Examination of the analytical data confirmed the molecular formula for **18.** The ^{13}C-{^{1}H} nmr spectrum showed the expected low field alkylidene carbon signal (δ240.6), in addition a high field C-H carbon signal (δ32.7) was observed and verified by a ^{90}Dept experiment, also present were methyl and cyclopentadienyl peaks (δ16.4 and δ90.7 respectively). The ^{31}P-{^{1}H} nmr spectrum showed the presence of a singlet at δ16.9ppm. The ^{1}H nmr spectrum showed the expected cyclopentadienyl peak (δ4.65), also present was a doublet attributable to the alkyne methyl (δ2.9, J=1.83Hz) and a broad multiplet (δ2.51) attributable to the CH of the η^2-vinyl and confirmed by a CH correlation experiment. The multiplicity of this signal suggests a coupling to the methyl and a small unresolved coupling to the phosphorous. The magnitude of the coupling for the methyl doublet suggests a 4 bond coupling, such that it is the methyl which is situated on the carbene carbon, (the alternative structure would show a larger 3 bond coupling). Attempts to confirm the precise structure of complex **18** by X-ray crystallography proved unsuccessful as suitable crystals could not be grown.

These reactions to form η^2-vinyls obviously lead to the introduction of a chiral carbon atom as well as the chiral rhenium metal centre. The possible configurations for these complexes is shown in figure 76. Using the methods of Stanley and Baird[133], the following priorities for assigning R/S configurations to the rhenium centre are used: Br> η–C_5H_5> L> η^2-RC_2R. These ligands may be considered as pseudo-atoms of

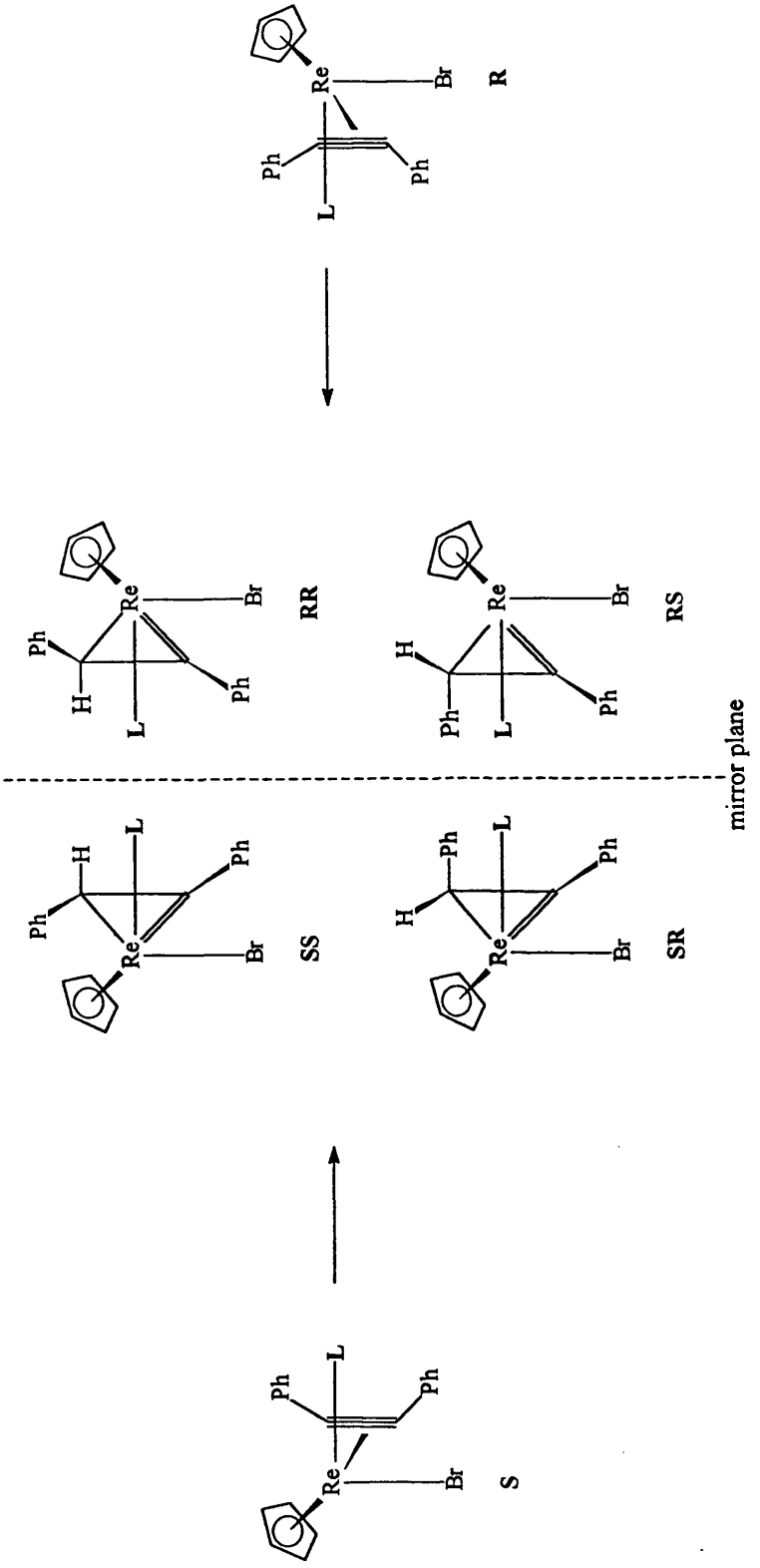

FIGURE 76

atomic numbers 80, 60, 31 and 24 respectively, consideration of the groups attached to the chiral η^2-vinyl carbon produces a priority sequence Re> CR> R> H. The absolute configuration for complex **18** cannot be assigned without crystallographic evidence, however, the RS and SR configurations (the metal configuration is quoted first following the suggestion of Reich-Rohrwig and Wojcicki[137]) can be discounted on steric grounds, because they place the most demanding substituent, attached to Cβ, in close proximity to the phenyls of the triphenylphosphine ligand. A prediction of the structure of **18** can be made from the spectroscopic data. The ^{1}H nmr spectrum shows that there is a coupling seen between the η^2-vinyl CH and the phosphorous, suggesting that the sp^3 hybridised carbon is in closer proximity to the phosphorous than the carbenoid carbon (as no coupling to the phosphorous is seen), with the hydrogen atom in a pseudo-axial site. The preferred orientation for the η^2-vinyl from molecular orbital considerations places the η^2-vinyl unit parallel to the rhenium-bromine bond and orthogonal to the phosphorous, this evidence suggests that complex **18** has the structure shown in figure 77. The absolute configuration for complex **18** would probably be a mixture of the RR and SS configurations.

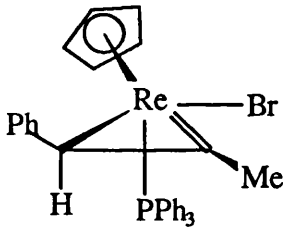

FIGURE 77

4.4 The synthesis of [BrRe=C(Ph)CH(Ph){P(OMe)$_3$}(η-C_5H_5)] **19** and a spin-saturation transfer experiment.

The neutral η^2-vinyl complex **19** was prepared using the method of Vaughan.[109] Reaction of [$ReBr_2(PhC_2Ph)(C_5H_5)$] with trimethylphosphite and thallium hexafluorophosphate and subsequent reaction of the phosphite cation with one molar equivalent of $LiBH(C_2H_5)_3$ led to the formation of two η^2-vinyl isomers in an approximate ratio of 2:1. The proposed mechanism for the formation of these two isomers is that the 'H$^-$' is delivered to both ends of the alkyne, leading to the two isomers shown in figure 78, whereby the hydrogen occupies the pseudo-axial site and the η^2-vinyl unit lies parallel to the rhenium-bromine bond, (as seen in the previous examples).

FIGURE 78

These two isomers could in principal be formed either under kinetic or thermodynamic control. A variable temperature study suggested that the two isomers were interconvertible, as it was observed that there was a variation of the integral ratio for the two phosphorous signals in the ^{31}P -{^1H} spectra with varying temperature. However, these integrals are measured with only 4-5 data points and were therefore deemed too inaccurate for proof of interconversion. A more accurate experiment to show whether the two isomers are interconvertible is a spin-saturation

transfer experiment.[138,139] This experiment involves the irradiation of the sample at a given frequency over varying lengths of time. The sample of complex **19** was prepared in deutero-toluene and was irradiated for times varying from 0.2 to 20 seconds, the spectra were referenced to the methyl signals for the two isomers as this would remain constant irrespective of any interconversion. The peak chosen for irradiation was the cyclopentadienyl of the minor isomer (δ4.96), the effect of irradiation is that the nuclei of the minor isomer are promoted into a higher energy state and any molecules of complex **19** in this spin saturated state will not appear in the ^1H nmr spectrum. Any interconversion of the two isomers will lead to a drop in intensity of the cyclopentadienyl of the major isomer, as any of the major isomer on conversion to the minor isomer will become excited and will not appear in the spectra. Conversely any of the excited minor isomer that is converted into the major isomer will remain in the excited state, (there may be a small amount of relaxation but this should be approximately constant throughout) and would also not show up on the nmr spectra. If the two isomers of **19** are indeed interconverting then the ratio of M/Mo (where Mo is the integral of the major cyclopentadienyl peak before irradiation and M the same integral after irradiation), should decrease and a plot of M/Mo versus irradiation time should be exponential. Figure 79 shows that such a plot is exponential and confirms that there is interconversion of the two isomers. However, to eliminate the possibility that the observed effect was due to stray irradiation rather than interconversion a second experiment was required. In this second experiment the sample was irradiated at an equivalent distance upfield of the major cyclopentadienyl peak, no change in peak size was observed confirming that the two isomers do indeed interconvert.

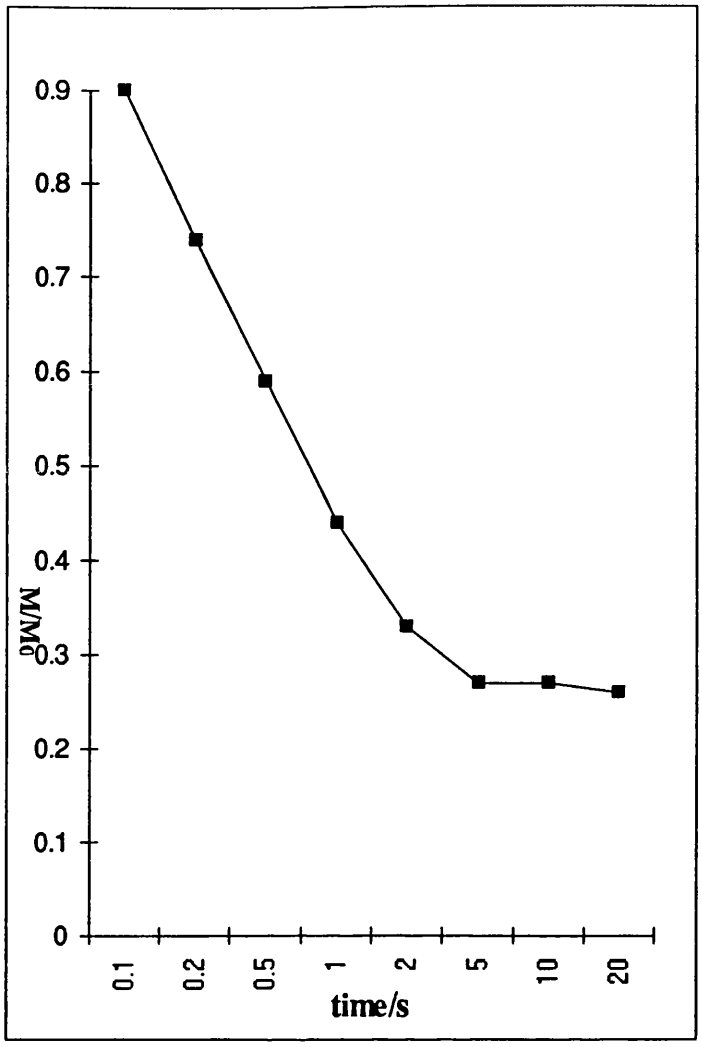

FIGURE 79

Two possible explanations could account for this interconversion, the first is simply rotation of the η^2-vinyl through 180°, but as discussed in section 2.2 the energy barrier for this type of rotation is of the order of 20 kcal/mol, as no thermal energy is being put into the system during the spin-saturation experiment this is unlikely to be the source of the interconversion.

The second possibility involves the opening of the η^2-vinyl to form an electronically unsaturated 16 electron η^1-vinyl, followed by a rotation and ring closure reaction leading to the η^2-vinyl being in the alternative orientation (fig80).

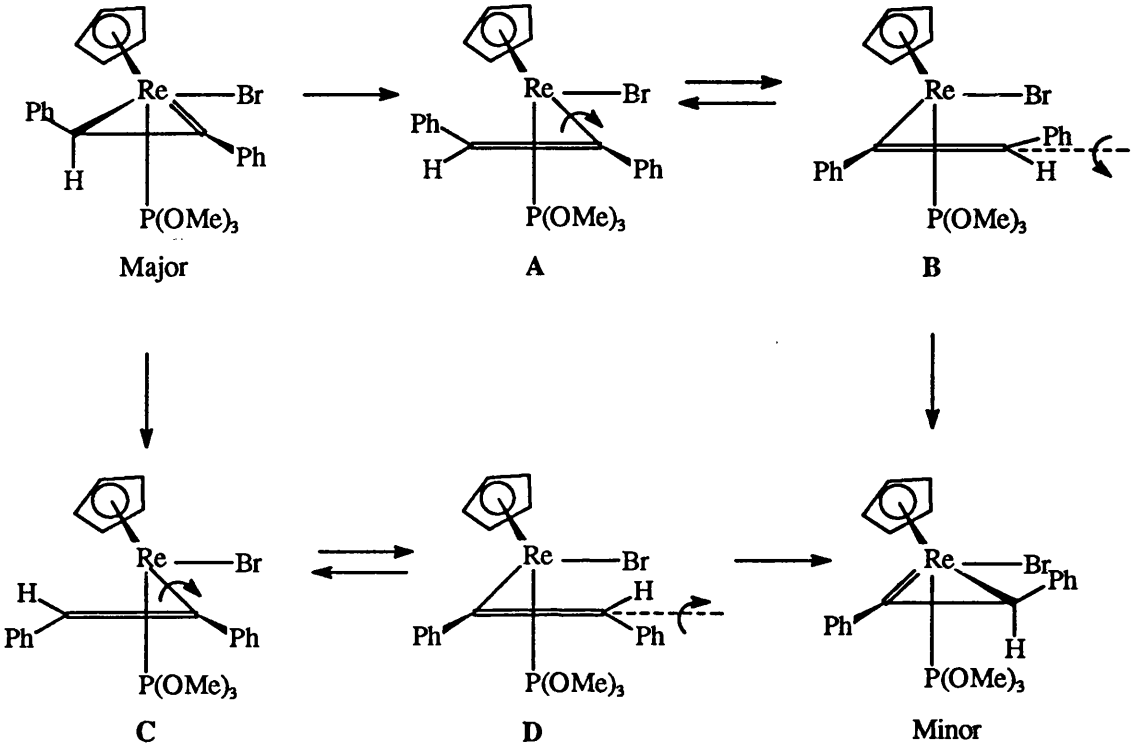

FIGURE 80

The first step in the conversion of the two isomers is the opening of the η^2-vinyl to a sixteen electron η^1-vinyl, this can occur in two ways to give either intermediate **A** or **C** differing in the orientation of the phenyl and hydrogen groups on C_β. A rotation of the η^1-vinyls **A** or **C** lead to the alternative η^1-vinyls **B** and **D**, the ring closure of these two intermediates to form the minor isomer involves the rotation around C_α-C_β such that the hydrogen lies in the pseudo-axial site. The alternative ring closure leads to the formation of an isomer whereby the phenyl ring lies in the pseudo-axial site

which is known not to occur on steric grounds. In view of the above findings it is likely that the two isomers result from a thermodynamically controlled reaction. Following the rules for the assignment of absolute configurations it is thought that the configuration for the major and minor isomers of **19** is either RR or SS, as the re-orientation of the η^2-vinyl on conversion of the two isomers does not alter the configuration of either the chiral rhenium or carbon atoms.

CHAPTER 5

EXPERIMENTAL SECTION

5.1 General Practical Details

All experiments were performed in an atmosphere of dry, oxygen free nitrogen using standard schlenk line techniques. Solvents were freshly distilled in a nitrogen atmosphere from potassium/sodium alloy and benzophenone (hexane, pentane and diethyl ether), potassium metal (tetrahydrofuran, toluene) and calcium hydride (dichloromethane and acetonitrile).

Chromatography columns were packed with BDH aluminium oxide, Brockman activity II, florosil or silica gel.

Unless otherwise stated, all chemicals were reagent grade and were used as received.

Deuterated solvents for n.m.r were degassed and dried as necessary before use.

5.2 Characterisations

(i) Microanalyses for C, H and N, were carried out by Mr A. Carver in the micro analytical laboratory of the School of Chemistry, University of Bath.

(ii) Infra-red spectra were recorded using NaCl cells on a Nicolet 510P FT-IR spectrophotometer.

(iii) Mass spectra were recorded on a VG analytical 7070E mass spectrometer at the University of Bath.

(iv) ^{1}H nmr, ^{31}P nmr and $^{13}C-\{^{1}H\}$ nmr spectra were recorded on the following machines, Jeol GX270 and EX400 spectrometers. Spectra were recorded at ambient temperature unless otherwise stated, and were referenced internally to the protic impurity in the deuterated solvents.

v) All X-ray crystal determinations were carried out by Dr M. Mahon on a CAD4 automatic four-circle diffractometer in the chemistry department University of Bath.

5.3 Synthesis of starting materials.

The following complexes were used as starting materials to the reactions contained in this chapter. They were prepared from the parent carbonyls, $Mo(CO)_6$ was used as obtained from Fluka Chemical Company and $Re_2(CO)_{10}$ as obtained from the Strem Chemical Company.

$[Mo(CO)_3(\eta\text{-}C_5H_5)]_2$ was prepared using the method of Birdwhistell, Hackett and Manning.[140]

$[Mo(CO)(\eta^2\text{–}RC_2R')_2(\eta\text{-}C_5H_5)][BF_4]$; (R=R'=Me; R=Ph, R'=Me) was prepared using the method of Bottrill and Green.[16]

$[Mo(MeCN)(\eta^2\text{–}RC_2R')_2(\eta\text{-}C_5H_5)][BF_4]$; (R=R'=Me; R=Ph, R'=Me) was prepared using the methods of Allen, Baker, Barnes, Green, Trollope, Manojlovic-Muir and Muir.[23]

$[MoBr(\eta^2\text{–}RC_2R')_2(\eta\text{-}C_5H_5)]$; (R=R'=Me; R=Ph, R'=Me) was prepared using the methods of Conole, Green, McPartlin, Reeve and Woolhouse.[66]

$[ReBr_2(CO)_2(\eta\text{-}C_5H_5)]$ was prepared using the methods of King and Reimann briefly outlined below.[141]

Commercial $Re_2(CO)_{10}$ was converted to $[ReBr(CO)_5]$ by direct bromination in a dichloromethane solution at 0°C, this was then converted to $[Re(CO)_3(\eta\text{-}C_5H_5)]$ after 17 hours reflux in a thf in the presence of a 1.5 excess of thalliumcyclopentadienide in suspension. Pure $[Re(CO)_3(\eta\text{-}C_5H_5)]$ was obtained after an alumina column, eluted with hexane. This is then reacted with bromine in a solution of trifluoroacetic acid to produce after work up a mixture of the diagonal and lateral isomers of $[Re(CO)_2Br_2(\eta\text{-}C_5H_5)]$.

$[ReBr_2(\eta^2\text{–}RC_2R')(\eta\text{-}C_5H_5)]$; (R=R'=Ph; R=Me, R'=Ph) were prepared using the method of Vaughan.[109]

K-Selectride is the trade name of potassium tri-sec-butylborohydride.

Super-hydride is the trade name for lithium triethylborohydride.

5.4 Preparation of [Mo(σ,η^2–CH_2C_2Ph)(η^2–MeC_2Ph)(η–C_5H_5)](**1**).

The synthesis of complex **1** was effected by the reaction of [MoBr(η^2–MeC_2Ph)$_2$(η–C_5H_5)] (300mg, 0.634mmol) with one molar equivalent of the base Li[N($SiMe_3$)$_2$] in a solution of thf at -78°C. The reaction mixture was allowed to warm to room temperature over a period of 1-1$^1/_2$ hours resulting in a colour change from yellow to dark red. The solvent was removed *in vacuo* and the resultant purple solid was extracted into hexane and filtered through Celite. Crystallisation from toluene-hexane yielded a purple crystalline solid (**1**), (161mg ,65%). X-ray quality crystals were grown from a toluene-hexane layer crystallisation and were obtained as 20% of the original product.

^{1}H nmr: (C_6D_6) δ8.03-6.99 (m, 10H, phenyls), δ5.01 [d, 1H, H^a, J(H^aH^b) 10.8Hz], δ4.88 (s, 5H, C_5H_5), δ3.90 [d, 1H, H^b, J(H^aH^b) 10.81Hz], δ2.42ppm (s, 3H, MeC_2Ph).

^{13}C-{^{1}H} nmr: (C_6D_6) δ207.38 (MeC_2Ph), δ197.04 (MeC_2Ph), δ142.3 ($PhCCCH_2$), δ140.82-126.78 (phenyls), δ124.86 ($PhCCCH_2$), δ93.62 (C_5H_5), δ41.62 ($PhCCCH_2$) [^{1}H coupled ^{13}C, dd, CH^aH^b, J(CH^a) 158.6Hz, J(CH^b) 165.3Hz], δ18.95ppm (MeC_2Ph).

Elemental analysis: Found C-70.25%, H-5.09%; $C_{23}H_{20}Mo$ requires C-70.41%, H-5.14%.

The crystallographic data for this complex can be found in the appendix.

5.5 The reaction of [Mo(σ,η^2–CH_2C_2Ph)(η^2–MeC_2Ph)(η–C_5H_5)](**1**) with carbon-monoxide.

To a solution of **1** (218mg, 0.556mmol) in thf was bubbled carbon-monoxide for a period of $^1/_2$ hour this resulted in a colour change from red to yellow and a small amount of precipitate was observed. The solvent was reduced to *ca* 5cm^3 *in vacuo* and hexane was added, resulting in the precipitation of a yellow crystalline solid, this was recrystallised from dichloromethane/hexane to yield a small quantity of X-ray quality crystals of [Mo{η^2,η^3–C(Ph)C(O)C(Me)C(Ph)CCH_2}(CO)(η–C_5H_5)](**2**), (50mg, 20%).

I.r.: ν_{co} 1925cm^{-1}, 1603cm^{-1}.

^{1}H nmr: (CD_2Cl_2) δ8.086-7.33 (m, 10H, phenyls), δ4.88 (s, 5H, C_5H_5), δ3.91 [d, 1H, H^a, J(H^aH^b) 1.83Hz], δ3.34 [d, 1H, H^b, J(H^aH^b) 2.02Hz], δ2.29ppm (s, 3H, Me).

^{13}C nmr: (CD_2Cl_2) δ243.99 (**C**O), δ133.5 {C(Ph)**C**(O)}, δ112.45, δ111.86 {C(Ph)C(O)C(Me)}, δ90.81 (**C**$_5$H$_5$), δ92.33, δ90.29 {**C**(Ph)**C**CH_2}, δ56.51 (CCH_2), δ11.95ppm (**Me**).

Elemental analysis: Found C-63.2%, H-4.15%; $C_{25}H_{20}O_2Mo$ requires C-66.97%, H-4.50%.

The crystallographic data for this complex can be found in the appendix.

5.6 The reaction of [Mo(σ,η^2–CH_2C_2Me)(η^2–MeC_2Me)(η–C_5H_5)] with carbon-monoxide.

This reaction is a repeat of that attempted by C. Woolhouse.[28] The resultant yellow solid was recrystallised from dichloromethane-hexane and crystals of X-ray quality were grown, [Mo{η^2,η^3–C(Me)C(O)C(Me)C(Me)CCH_2}(CO)(η–C_5H_5)](**3**), (50.5mg, 82%).

I.r: ν_{co} 1916cm^{-1}, 1595cm^{-1}

^{1}H nmr: (CD_2Cl_2) δ4.96 (s, C_5H_5) δ3.27 [d, 1H, H^a, J(H^aH^b) 2.2Hz], δ2.94 [d, 1H, H^b, J(H^aH^b) 2.2Hz], δ1.88 [s, 3H, C(**Me**)C(O)C(Me)], δ1.74 [s, 3H, C(**Me**)C(Me)C(O)], δ1.64ppm [3H, C(Me)C(O)C(**Me**)].

^{13}C-{^{1}H} nmr: (CD_2Cl_2) δ241.2 (**C**O), δ170.4 (**C**=O), δ107.67 [**C**(Me)C(Me)C(O)], δ100.4 [C(Me)**C**(Me)C(O)], δ99.9 [C(Me)**C**CH_2], δ96.57 [C(Me)C(O)**C**(Me)], δ89.2 (C_5H_5), δ49.96 (CCH_2) [^{1}H coupled ^{13}C, dd, CH^aH^b, J(CH^a) 156.4Hz, J(CH^b) 163.0Hz], δ12.99 [C(Me)C(O)C(**Me**)], δ10.5 [C(**Me**)C(Me)C(O)], δ9.15ppm [C(Me)C(O)C(**Me**)].

Elemental analysis: Found C-55.6%, H-4.9%; $C_{15}H_{16}MoO_2$ requires C-55.7%, H-5.1%.

The crystallographic data for this complex can be found in the appendix.

5.7 The reaction of [Mo{η^2,η^3–C(Me)C(O)C(Me)C(Me)CCH$_2$}(CO)(η–C_5H_5)](3) with $HBF_4.Et_2O$.

This reaction is a repeat of that previously attempted by C. Woolhouse[28]. The resultant yellow solid was recrystallised from dichloromethane-diethyl ether and crystals of X-ray quality were grown, the complex was identified as [Mo{η^3,η^3–C(Me)C(OH)C(Me)C(Me)CCH$_2$}(CO)(η–C_5H_5)][BF_4](4).

I.r.: ν_{co} 1980cm^{-1}

^{1}H nmr: (CD_2Cl_2) δ7.24ppm (s, 1H, OH), δ5.28 (s, 5H, C_5H_5), δ3.62 [d, 1H, H^a, J(H^aH^b) 2.57Hz], δ3.32 [d, 1H, H^b, J(H^aH^b) 2.57Hz], δ2.25 (s, 3H, Me), δ2.02 (s, 3H, Me), δ1.71 (s, 3H, Me).

^{13}C-{^{1}H} nmr: (CD_3NO_2) δ233.4 (CO), δ141.8 (COH), δ108.2 [C(Me)C(Me)CCH$_2$], δ106.3[C(Me)C(Me)CCH$_2$], δ103.9 [C(Me)C(Me)CCH$_2$], δ100.3 [C(Me)C(OH)C(Me)], δ93.5 (C_5H_5), δ52.8 (CCH$_2$), δ12.2 (Me), δ10.3 (Me), δ10.2ppm (Me).

Elemental analysis: Found C-44.1%, H-4.34%; $C_{15}H_{17}MoO_2BF_4$ requires C-43.72%, H-4.16%.

The crystallographic data for this complex can be found in the appendix.

5.8 Synthesis of the complexes $[ReBr(\eta^2\text{-}RC_2R')_2(\eta\text{-}C_5H_5)][PF_6]$; R=R'=Ph; R=Ph, R'=Me.

i) The synthesis of $[ReBr(PhC_2Ph)_2(\eta\text{-}C_5H_5)][PF_6]$(**5**) was a repeat of a reaction of that attempted by C. Vaughan[109], crystals of X-ray quality were grown from a solution of dichloromethane and diethyl-ether.

The crystallographic data for this complex can be found in the appendix.

ii) To a solution of $[ReBr_2(\eta^2\text{-}PhC_2Me)(\eta\text{-}C_5H_5)]$ (135mg, 0.256mmol) in dichloromethane was added phenyl-1-propyne (96µl, 0.75mmol) and thallium hexafluorophosphate (89.5mg, 0.256mmol). The reaction mixture was allowed to stir for 24 hours and resulted in a colour change from deep red to bright orange. The reaction mixture was filtered through Celite and the solvent removed *in vacuo*, recrystallisation from dichloromethane and diethyl-ether resulted in an orange crystalline solid $[ReBr(\eta^2\text{-}PhC_2Me)_2(\eta\text{-}C_5H_5)][PF_6]$ (**6**), (170mg, 94%).

^{1}H nmr: (CD_2Cl_2) δ7.9-7.49 (m, 10H, phenyls), δ6.39 (s, 5H, C_5H_5), δ3.5ppm (s, 6H, methyls).

^{13}C-{^{1}H} nmr: (CD_2Cl_2) δ173.8 (Ph-CC-CH_3), δ163.1 (Ph-CC-CH_3), δ133.4-129.7 (phenyls), δ104.5 (C_5H_5), δ20.3ppm (Ph-CC-CH_3).

Elemental analysis: Found C-39.2%, H-2.99%; $C_{23}H_{21}ReBrPF_6$ requires C-38.99%, H-2.99%.

Mass Spectrum: 563 (M^+), 447 (M^+, -PhC_2Me), 368 (M^+, -PhC_2Me, -Br).

5.9 The reaction of $[ReBr(\eta^2\text{–}PhC_2Ph)_2(\eta\text{–}C_5H_5)][PF_6]$ (5) with Super-hydride.

To a solution of $[ReBr(\eta^2\text{–}PhC_2Ph)_2(\eta\text{–}C_5H_5)][PF_6]$ (5) (272mg, 0.327mmol) in thf (-78°C) was added Super-hydride, the reaction mixture was allowed to warm to room temperature and left to stir for 4 hours. A colour change from red to green was observed, the solvent was removed *in vacuo* and the resultant solid was extracted into toluene and columned on a silica column using toluene as an eluant. The first band on the column was orange, this was thought to be the η^2–vinyl intermediate which seemed to decompose on the column, the second green band was collected and on removal of the solvent *in vacuo* gave a green solid identified as $[BrRe\{\eta^1,\eta^1,\eta^2(5e)=C(Ph)C(Ph)C(Ph)=CHPh\}(\eta\text{–}C_5H_5)]$(7), (55mg, 24.5%). Crystals of X-ray quality were grown from a toluene-hexane mixture.

^{1}H nmr: (CD_2Cl_2) δ7.92-6.87 (m, 20H, Ph), δ5.42 (s, 1H, CHPh), δ5.31ppm (s, 5H, C_5H_5).

^{13}C-{^{1}H} nmr: δ235.31 (Re=C), δ151.5-143.7 (ipso carbons of phenyls), δ134.6-125.6 (phenyls), δ94.31 (C_5H_5), δ76.08 [(C(Ph)C(Ph)CHPh], δ64.6 [(C(Ph)C(Ph)CHPh], δ59.01ppm [(C(Ph)C(Ph)CHPh] (identified by ^{90}Dept experiment).

CH correlation experiment: ^{13}C δ59.01ppm corresponds to ^{1}H δ5.42ppm.

Elemental analysis: Found C-57.1%, H-3.62%; $C_{33}H_{26}ReBr$ requires C-57.55%, H-3.81%.

Mass Spectrum: 688 (M^+)

The crystallographic data for this complex can be found in the appendix.

Evidence for η^2–vinyl intermediate.

^{1}H nmr: (CD_2Cl_2) δ7.93-6.58 (m, phenyls), δ4.77ppm (s, C_5H_5).

^{13}C-{^{1}H} nmr: (CD_2Cl_2) δ215.45 (Re=**C**), δ173.38 (Ph**C**$_2$Ph), δ143.7-124.4 (phenyls), δ85.12 (**C**$_5$H$_5$), δ21.81ppm (**C**HPh).

5.10 The reaction of [ReBr(η^2–PhC$_2$Ph)$_2$(η–C$_5$H$_5$)][PF$_6$] with Super-deuteride.

The reaction was repeated as above but using Super-deuteride as a source of D^-, leading to the formation of [BrRe{η^1,η^1,η^2(5e)=C(Ph)C(Ph)C(Ph)=CDPh}(η–C_5H_5)] (**8**) allowing the chemical shift location of the deuterium in complex **8** by deuterium spectroscopy. Therefore assisting the assignment for the hydrogen contained within complex **7**, which was found to be located under the solvent peak in the ^{1}H nmr spectrum.

^{2}D nmr: (CD_2Cl_2) δ7.33 (s, 1D C_6H_5D), δ5.25ppm (s, 1D, CDPh).

Evidence for η^2–vinyl intermediate.

^{2}D nmr: (CD_2Cl_2) δ7.06 (s, 1D C_6H_5D), δ2.77ppm (s, 1D, CDPh).

5.11 The reaction of [BrRe=C(Ph)CH(Ph)(Ph$_2$MeP)(η–C$_5$H$_5$)] (**9**) with [Ph$_3$C][BF$_4$].

The starting material [BrRe=C(Ph)CH(Ph)(Ph$_2$MeP)(η–C$_5$H$_5$)] (**9**) was prepared using the method of Vaughan.[109]

To a solution of (**9**), (177mg, 0.249mmol) in dichloromethane (-78°C) was added trityl tetrafluoroborate (84mg, 0.254mmol). The solution was allowed to warm to room temperature and stirred for 2 hours, a colour change from green to red was observed. The solvent was removed *in vacuo* and after recrystallisation from dichloromethane and diethyl-ether afforded a deep purple, air sensitive, crystalline

solid identified by nmr spectroscopy as [ReBr(Ph_2MeP){(Ph)HC=CPh(Ph_3C)}(η–C_5H_5)][BF_4] (**10**), (143mg, 55%). Despite several attempts to grow crystals of **10** only decomposition occurred due to the extreme sensitivity of this compound to solvents. No satisfactory elemental analysis could be obtained.

^{1}H nmr: δ7.96-7.15 (m, 35H, phenyls), δ6.17 (s, 5H, C_5H_5), δ4.72 [s, 1H, (Ph)CH], δ2.72ppm [d, 3H, CH_3 J($^1H^{31}P$) 11.73Hz].

^{31}P nmr: -δ10.15ppm (Ph_2MeP).

^{13}C-{^{1}H} nmr: (CD_2Cl_2) δ135.54-129.73 (phenyls), δ101.88 (C_5H_5), δ101.13 [(Ph)CH], δ95.10 (η^2–phenyl), δ69.49 [(Ph_3C)(Ph)C], δ18.88 (CH_3), δ18.33ppm (Ph_3C).

^{90}Dept: (CD_2Cl_2) δ135.2-129.8 (phenyls), δ101.91 (C_5H_5), δ101.18 [(Ph)CH], δ95.08ppm (η^2–phenyl).

5.12 The reaction of [BrRe=C(Ph)CH(Ph)(Ph_2MeP)(η–C_5H_5)] (**9**) with $HBF_4.Et_2O$.

The starting material [BrRe=C(Ph)CH(Ph)(Ph_2MeP)(η–C_5H_5)] (**9**) was prepared using the method of Vaughan.[109]

To a solution of (**9**), (136mg, 0.191mmol) in dichloromethane (-78°C) was added $HBF_4.Et_2O$ (28μl, 0,191mmol). The solution was allowed to warm to room temperature and stirred for 2 hours, a colour change from green to red was observed. The solvent was removed *in vacuo* and after recrystallisation from dichloromethane and diethyl-ether afforded a deep purple, air sensitive, crystalline solid identified by nmr spectroscopy as [ReBr(Ph_2MeP){(Ph)HC=CH(Ph)}(η–C_5H_5)][BF_4] (**11**), (97mg, 64%). Despite several attempts to grow crystals of **11** only decomposition

occurred due to the extreme sensitivity of this compound to solvents. No satisfactory elemental analysis could be obtained.

^{1}H nmr: (CD_2Cl_2) δ7.83-7.48 (m, 20H, phenyls), δ6.48 [d, 1H, J(H^aH^b) 1.47Hz], δ6.17 (s, 5H, C_5H_5), δ4.74 [d, 1H, J(H^aH^b) 3.66Hz], δ2.72ppm [d, 3H, CH_3, J($^{1}H^{31}P$) 11.72Hz].

^{31}P nmr: (CD_2Cl_2) -δ10.15ppm (Ph_2MeP).

^{13}C-{^{1}H} nmr: (CD_2Cl_2) δ134.4-129.5 (phenyls), δ101.86 (C_5H_5), δ101.12 [(Ph)HC], δ94.55 (η^2–phenyl), δ74.04 [CH(Ph)], δ19.09ppm (CH_3).

^{90}Dept: (CD_2Cl_2) δ134-128.9 (phenyls), δ101.86 (C_5H_5), δ101.11 [(Ph)HC], δ94.55 (η^2–phenyl), δ74.40ppm [CH(Ph)].

5.13 Synthesis of [$ReBr(Ph_2MeP)(\eta^2$-$PhC_2Me)(\eta$–$C_5H_5)$][PF_6](**13**).

To a solution of [$ReBr_2(\eta^2$-$PhC_2Me)(\eta$–$C_5H_5)$] (200mg, 0.379mmol) in dichloromethane was added diphenylmethylphosphine (85μl, 0.415mmol) which resulted in an immediate colour change from red to green. The addition of one molar equivalent of thallium hexafluorophosphate (132.5mg, 0.379mmol) resulted in the precipitation of thallium bromide over a period of 1 hour. After filtration through Celite the solvent was reduced *in vacuo* to ca. 5cm^3, the addition of diethyl-ether resulted in the precipitation of a bright green crystalline solid, identified after recrystallisation from dichloromethane and diethyl-ether as [$ReBr(Ph_2MeP)(\eta^2$-$PhC_2Me)(\eta$–$C_5H_5)$][PF_6] (**13**), (218mg, 73%).

^{1}H nmr: (CD_2Cl_2) δ7.95-7.43 (m, 15H, phenyls), δ5.79 (s, 5H, C_5H_5), δ3.23 (s, 3H, Me), δ2.58ppm (br, 3H, Ph_2MeP).

^{31}P nmr: (CD_2Cl_2) -δ13.49ppm (Ph_2Me**P**).

^{13}C-{^{1}H} nmr: (CD_2Cl_2) δ227.3 (Ph-**C**), δ212.4 (**C**-Me), δ136.3-128.9(phenyls), δ96.6 (C_5H_5), δ88.6 (Ph_2C**Me**), δ15.3ppm (PhC_2**Me**).

Elemental analysis: Found C-43.9%, H-3.64%; $C_{27}H_{26}ReBrP_2F_6$ requires C-40.9%, H-3.31%.

Mass Spectrum: 647 (M^+), 447 (M^+-Ph_2MeP), 531 (M^+-PhC_2Me).

5.14 Synthesis of [ReBr{P(OMe)$_3$}(η^2-PhC$_2$Me)(η–C$_5$H$_5$)][PF$_6$](**14**).

To a solution of [$ReBr_2$(η^2-PhC$_2$Me)(η–C_5H_5)] (168mg, 0.319mmol) in dichloromethane was added trimethylphosphite (45μl, 0.398mmol) which resulted in an immediate colour change from red to dark green. The addition of one molar equivalent of thallium hexafluorophosphate (111.3mg, 0.319mmol) resulted in the precipitation of thallium bromide over a period of 1 hour. After filtration through Celite the solvent was reduced *in vacuo* to ca. 5cm^3, the addition of diethyl-ether resulted in the precipitation of a dark green oily solid, after recrystallisation from dichloromethane and diethyl-ether the resultant dark green solid was identified as [ReBr{P(OMe)$_3$}(η^2-PhC$_2$Me)(η–C_5H_5)][PF_6] (**14**), (150mg, 65.7%).

^{1}H nmr: (CD_2Cl_2) δ7.96-7.69 (m, 5H, phenyl), δ5.93 (s, 5H, C_5H_5), δ4.04 [d, 9H, P(OCH_3)$_3$, J(^{1}H^{31}P) 11.26Hz], δ3.719ppm [d, 3H, Me, J(^{1}H^{31}P) 3.38Hz].

^{31}P nmr: (CD_2Cl_2) δ92.51ppm **P**(OMe)$_3$.

^{13}C-{^{1}H} nmr: (CD_2Cl_2) δ212.1 [d, MeC, J($^{13}C^{31}P$) 27.1Hz], δ207.0 (CPh), δ136.6-120.1 (phenyls), δ95.8 (C_5H_5), δ56.3 [d, $P(OMe)_3$, J($^{13}C^{31}P$) 8.1Hz], δ23.6ppm [d, PhC_2Me, J($^{13}C^{31}P$) 9.5Hz].

Elemental analysis: Satisfactory analysis could not be obtained.

5.15 Reaction of [$ReBr_2(\eta^2$-$PhC_2Me)(\eta$-$C_5H_5)$] with silver tetrafluoroborate and dppe.

To a solution of [$ReBr_2(\eta^2$-$PhC_2Me)(\eta$-$C_5H_5)$] (140mg, 0.266mmol) and diphenylphosphinoethane (dppe), (105.8mg, 0.266mmol) in dichloromethane was added two equivalents of silver tetrafluoroborate (103.4mg, 0.531mmol). The reaction mixture was stirred for 1 hour at room temperature and the resulting solution was filtered through Celite to remove the precipitated silver bromide. Reduction of the solvent *in vacuo* to ca $5cm^3$ and the subsequent addition of diethyl-ether led to the precipitation of a red-brown crystalline solid. Repeated washing with hexane (5 x $20cm^3$) to remove any unreacted dppe and recrystallisation from dichloromethane and diethyl-ether afforded [$Re(dppe)(\eta^2$-$PhC_2Me)(\eta$-$C_5H_5)][BF_4]_2$ (**15**), (160mg, 64%).

^{1}H nmr: (CD_3CN) δ8.08-7.35 (m, 25H, phenyls), δ5.93 (s, 5H, C_5H_5), δ3.81-3.68 (m, 4H, PCH_2CH_2P), δ1.73ppm (s, 3H, Me).

^{31}P nmr: (CD_3CN) δ26.55ppm (PCH_2CH_2P).

^{13}C-{^{1}H} nmr: (CD_3CN) δ222.5 [t, MeC, J($^{13}C^{31}P$) 11Hz], δ212.9 (CPh), δ136.8-130.4 (phenyls), δ99.7 (C_5H_5), δ29.3 [d, PCH_2CH_2P, J($^{13}C^{31}P$) 37Hz], δ24.7ppm (CH3).

Elemental analysis: Found C-51.2%, H-4.00%; $C_{40}H_{37}ReP_2B_2F_8$ require C-51.14%, H-3.97%.

5.16 Reaction of [$ReBr_2(\eta^2$-$PhC_2Ph)(\eta$–$C_5H_5)$] with silver tetrafluoroborate and arphos.

To a solution of [$ReBr_2(\eta^2$-$PhC_2Ph)(\eta$–$C_5H_5)$] (141mg, 0.239mmol) and arphos, (106mg, 0.240mmol) in dichloromethane was added two equivalents of silver tetrafluoroborate (93mg, 0.478mmol). The reaction mixture was stirred for 2 hours at room temperature and the resulting solution was filtered through Celite to remove the precipitated silver bromide. Reduction of the solvent *in vacuo* to ca $5cm^3$ and the subsequent addition of diethyl-ether led to the precipitation of a dark purple solid. Repeated washing with hexane (4 x $20cm^3$) to remove any unreacted arphos and recrystallisation from dichloromethane and diethyl-ether afforded a red-purple crystalline solid identified as [Re(arphos)(η^2-$PhC_2Ph)(\eta$–$C_5H_5)$][PF_6]$_2$ (**16**), (124mg, 49.6%).

^{1}H nmr: (CD_2Cl_2) δ7.76-6.71 (m, 30H, phenyls), δ5.82 (s, 5H, C_5H_5), δ3.4-2.76ppm (m, 4H, PCH_2CH_2As).

^{31}P nmr: (CD_2Cl_2) 37.85ppm (PCH_2CH_2As).

^{13}C-{^{1}H} nmr: (CD_2Cl_2) δ223.9 (PhC_2Ph), δ135.6-129.7 (phenyls), δ97.6 (C_5H_5), δ30.0 (PCH_2CH_2As), δ25.37ppm (PCH_2CH_2As).

Elemental analysis: Found C-49.6%, H-3.61%; $C_{45}H_{39}RePAsB_2F_8 \cdot CH_2Cl_2$ requires C-48.87%, H-3.66%.

5.17 Reaction of [$ReBr_2(\eta^2$-$PhC_2Ph)(\eta$–$C_5H_5)$] with thallium hexafluorophosphate and dppf.

To a solution of [$ReBr_2(\eta^2$-$PhC_2Ph)(\eta$–$C_5H_5)$] (239mg, 0.406mmol) and 1,1`-bis(diphenylphosphino)ferrocene (dppf), (225mg, 0.406mmol) in dichloromethane was added two equivalents of thallium hexafluorophosphate (283mg, 0.810mmol). The reaction mixture was stirred for 2 hours at room temperature and the resulting solution was filtered through Celite to remove the precipitated thallium bromide. Reduction of the solvent *in vacuo* to ca $5cm^3$ and the subsequent addition of diethyl-ether led to the precipitation of a dark green crystalline solid. Repeated washing with hexane (4 x $20cm^3$) to remove any unreacted dppf and recrystallisation from dichloromethane and diethyl-ether afforded [Re(dppf)(η^2-$PhC_2Ph)(\eta$–$C_5H_5)$][PF_6]$_2$ (**17**), (397mg, 77%).

^{1}H nmr: (CD_2Cl_2) δ7.70-7.21 (m, 30H, phenyls), δ5.64 [d, 5H, C_5H_5 , J($^{1}H^{31}P$) 5.31Hz], δ4.19-3.48ppm [m, 8H, Fe{$C_5H_4P(Ph)_2$}$_2$].

^{31}P nmr: (CD_2Cl_2) -δ4.02ppm (PC_5H_4)Fe(C_5H_4P).

^{13}C-{^{1}H} nmr: (CD_2Cl_2) δ226.1 (PhC_2Ph), δ136.6-126.8 (phenyls), δ96.9 (C_5H_5), δ76.3-73.4ppm [Fe{$C_5H_4P(Ph)_2$}$_2$].

Elemental analysis: Found C-49.8%, H-3.56%; $C_{53}H_{43}ReFeP_4F_{12}$ requires C-49.97%, H-3.40%.

Mass Spectrum: 984 (M^+).

5.18 Synthesis of [BrRe=C(Me)CH(Ph)(PPh_3)(η–C_5H_5)] (18).

The complex [ReBr(PPh_3)(η^2-PhC_2Me)(η–C_5H_5)][PF_6] (**12**) was prepared using the method of Vaughan.[109]

The reaction of **12** (180mg, 0.211mmol) with K-selectride (211µl, 0.211mmol) in a thf solution (-78°C) led to an observable colour change from green to red. The reaction vessel was allowed to warm to room temperature over a period of 2 hours. On removal of the solvent *in vacuo*, the resultant red solid was extracted into toluene and columned on alumina using toluene as an eluent. Removal of the solvent afforded a red crystalline solid identified as [BrRe=C(Me)CH(Ph)(PPh_3)(C_5H_5)] (**18**), (86mg, 57.5%).

^{1}H nmr: (CD_2Cl_2) δ7.46-6.87 (m, 20H, phenyls), δ4.65 (s, 5H, C_5H_5), δ2.9 [d, 3H, Me, J(HP) 1.83Hz], δ2.51ppm (br, m, 1H, CHPh).

^{31}P nmr: (CD_2Cl_2) δ16.9ppm (PPh_3).

^{13}C-{^{1}H} nmr: (CD_2Cl_2) δ240.6 (Re=C), δ136.6-123.8 (phenyls), δ90.67 (C_5H_5), δ32.72 (CHPh, identified by a ^{90}Dept experiment), δ16.39ppm (CH_3).

CH correlation: (CD_2Cl_2) ^{13}C δ32ppm corresponds to ^{1}H δ2.5ppm.

Elemental analysis: Found C-56.1%, H-4.76%; $C_{32}H_{29}ReBrP.Et_2O$ requires C-55.1%, H-5.00%.

5.19 Synthesis of [BrRe=C(Ph)CH(Ph){P(OMe)$_3$}(η-C_5H_5)] (**19**) and a spin saturation transfer nmr experiment.

Complex **19** was prepared using the methods of Vaughan.[109] Attempts to separate the two isomers proved unsuccessful. The complete nmr data for this complex is shown below, ^{1}H and ^{13}C data collected by C. Vaughan.

^{1}H nmr: (CD_2Cl_2) δ8.32-6.86 (phenyls), δ4.96 (s, 5H, C_5H_5, minor), δ4.80 (s, 5H, C_5H_5, major), δ4.30 [d, 1H, ReCHPh, J(^{1}H^{31}P) 9Hz, minor], δ3.76 [d, 1H, ReCHPh, J(^{1}H^{31}P) 7.69Hz], δ3.52 [d, 3H, P(OCH_3)$_3$, J(^{1}H^{31}P) 11.35Hz, minor], δ3.43ppm [d, 3H, P(OCH_3)$_3$, J(^{1}H^{31}P) 11.17Hz, major].

^{31}P nmr: (CD_2Cl_2) δ119.65 [P(OCH_3)$_3$, major], δ118.18ppm [P(OCH_3)$_3$, minor].

^{13}C-{^{1}H} nmr: (CD_2Cl_2) δ251.8 [d, Re=C, J(^{13}C^{31}P) 5.4Hz], δ251.2 (Re=C), δ131.1-126.4 (phenyls), δ89.6 (C_5H_5, minor), δ87.8 (C5H_5, major), δ52.9 [d, P(OCH_3)$_3$, J(^{13}C^{31}P) 5.4Hz, minor], δ49.4 [d, P(OCH_3)$_3$, J(^{13}C^{31}P) 5.4Hz, major], δ29.7 [ReCH(Ph), major], δ27.4ppm [ReCH(Ph), minor].

A preliminary variable temperature nmr study showed that the two isomers may be able to interconvert, however any change was measured by the change of the ratio of the two integrals in the ^{31}P nmr spectra and due to the possible inaccuracies of these figures a further experiment was needed.

The experiment used was a spin saturation transfer experiment described in detail in chapter 4. Complex **19** was placed in an nmr tube using deuterated toluene as a solvent. All spectra were referenced to the integral for the methyl doublets of the two isomers as this would remain constant throughout the experiment. The experiment was performed at 40°C and the sample was irradiated at a frequency corresponding to

the chemical shift for the cyclopentadienyl of the minor isomer (δ4.96ppm) for times varying from 0.1 to 20 seconds. On completion of the irradiation, spectra were run and the intensity of the second cyclopentadienyl peak measured (major isomer), the comparison of its integral with that for the reference peak allows any reduction in peak intensity to be calculated. A second experiment was performed with the irradiation point an equal distance upfield of the major cyclopentadienyl peak, this would show whether any reduction in peak intensity during the first experiment was due to stray irradiation or the result of interchanging isomers.

The results can be assessed from a plot of relative change in peak intensity versus time, which if the two isomers are indeed interchangeable would show an exponential curve.

REFERENCES

References:

1. M. J. S. Dewar, *Bull. Soc. Chim. Fr.*, **18**, C79, 1951.

2. J. Chatt and L. A. Duncanson, *J. Chem. Soc.*, 2939, 1953

3. F. R. Hartley, *Angew. Chem. Int. Ed. Engl.*, **11**, 596, 1972.

4. R. Ugo, G. LaMonica, F. Carlarti, S. Cenini and F. Conti, *Inorg. Chim. Acta.*, **4**, 390, 1970.

5. J. L. Templeton, *Adv. Organomet. Chem.*, **29**, 1, 1989.

6. F. R. Hartley, *Chem. Rev.*, **69**, 799, 1969.

7. D. P. Tate and J. M. Augl, *J. Am. Chem. Soc.*, **85**, 2174, 1963.

8. D. P. Tate, J. M. Augl, W. M. Rickey, B. L. Ros and J. G. Grasselli, *J. Am. Chem. Soc.*, **86**, 3261, 1964.

9. J. Chatt, G. A. Rowe and A. A. Williams, *Proc. Chem. Soc.*, 208, 1957.

10. R. Colton, R. Levitus and G. Wilkinson, *Nature.*, **186**, 233, 1960.

11. R. B. King, *Inorg. Chem.*, **7**, 1044, 1968.

12. R. M. Laine, R. F. Moriarty and R. Bau, *J. Am. Chem. Soc.*, **94**, 1402, 1972.

13. L. F. Dahl and D. L. Smith, *J. Am. Chem. Soc.*, **84**, 2450, 1962.

14. J. O. Granville, J. M. Stewart and S. O. Grim, *J. Organometallic. Chem.*, **7**, P9, 1967.

15. M. Bottrill and M. Green, *J. Am.Chem. Soc.*, **99**, 5795, 1977.

16. M. Bottrill and M. Green, *J. Chem. Soc., Dalton. Trans.*, 2365, 1977.

17. K. Tasumi, R. Hoffmann and J. L. Templeton, *Inorg. Chem.*, **21**, 466, 1982

18. J. R. Marrow, T. L. Tanler and J. L. Templeton, *J. Am. Chem. Soc.*, **107**, 6956, 1985.

19. J. L. Templeton, P. B. Winston and B. C. Ward, *J. Am. Chem. Soc.*, **103**, 7713, 1981.

20. J. L. Templeton and B. C. Ward, *J. Am. Chem. Soc.*, **102**, 3288, 1980.

21. M. Bottrill and M. Green, *J. Am.Chem. Soc.*, **99**, 5795, 1977.

22. M. Bottrill and M. Green, *J. Chem. Soc., Dalton. Trans.*, 2365, 1977.

23. S. R. Allen, P. K. Baker, S. G. Barnes, M. Green, L. Trollope, L. Manojilovic-Muir and K. W. Muir, *J. Chem. Soc., Dalton. Trans.*, 873, 1981.

24. S. R. Allen, P. K. Baker, S. G. Barnes, M. Bottrill, M. Green, A. G. Orpen, I. D. Williams and A. J. Welch, *J. Chem. Soc., Dalton. Trans.*, 927, 1983.

25. F. J. Feher, M. Green and R. A. Rodrigues, *J. Chem. Soc., Chem. Commun.*, 1206, 1987.

26. S. R. Allen, R. G. Beevar, M. Green, N. C. Norman, A. G. Orpen and I. D. Williams, *J. Chem. Soc., Dalton. Trans.*, 435, 1985.

27. D. C. Brower, K. R. Birdwhistell and J. L. Templeton, *Organometallics.*, **5**, 94, 1986.

28. C. Woolhouse, PhD Thesis, 1989.

29. G. M. Sheldick, SHELX86, SHELX76, computer programs for crystal structure determinations.

30. L. D. Field, A. V. George and T. W. Hambley, *Inorg. Chem.*, **29**, 4565, 1990.

31. A. Hills, D. L. Hughes, M. Jimenz Tenorio, G. L. Leigh, C. A. McGeary, A. T. Rowley, M. Bravo, G. E. McKenna and M. C. McKenna, *J. Chem. Soc., Chem. Commun.*, 522, 1991.

32. A. Dobson, D. S. Moore, S. D. Robinson, M. B. Hursthouse and L. New, *Polyhedron.*, 1119, 1985.

33. G. Jia, A. L. Rheingold and D. W. Meek, *Organometallics.*, **8**, 1387, 1989.

34. C. Bianchini, M. Peruzzini, F. Zanobini, P. Frediani and A. Albineti, *J. Am. Chem. Soc.*, **113**, 5453, 1991.

35. J. Gottig, H. Otto and H. Werner, *J. Organometallic. Chem.*, **287**, 247, 1985.

36. A. K. McCullen, J. P Selegue and J. G. Wong, *Organometallics.*, **10**, 3421, 1991.

37. V. V. Krivykh, E. S. Taits, P. V. Petrovskii, V. T. Struchkov and A. I. Yanovskii, *Mendeleev. Commun.*, 103, 1991.

38. N. W. Murrall and A. J. Welch, *Acta. Crystallogr. Sect C.*, **40**, 401, 1984.

39. J. L. Davidson and G. Vasopollo, *J. Organometallic. Chem.*, **291**, 42, 1984.

40. A. DeCian, J. Colin, M. Schappacher, L. Ricard and R. Weiss, *J. Am. Chem. Soc.*, **103**, 1850, 1981.

41. K. A. Mead, H. Morgan and P. Woodward, *J. Chem. Soc., Dalton. Trans.*, 271, 1983.

42. C. P. Casey and C. S. Yi, *J. Am. Chem. Soc.*, **114**, 6597, 1992.

43. C. P. Casey and C. S. Yi, *Organometallics.*, **9**, 2413, 1990.

44. P. W. Blosser, J. C. Gallucci and W. J. Wojcicki, *J. Am. Chem. Soc.*, **115**, 2994, 1993.

45. G. H. Young, R. R. Willis, A. J. Wojcicki, M. Calligaris and P. Faleschini, *Organometallics.*, **11**, 154, 1992.

46. C. E. Shuchart, R. R. Willis and A. J. Wojcicki, *J. Organometallic. Chem.*, **185**, 424, 1992.

47. M. C. Chen, R. S. Keng, Y. C. Lin, Y. Wong, M. C. Cheng and G. H. Lee, *J. Chem. Soc., Chem. Commun.*, 1138, 1990.

48. R. S. Keng and Y. C. Lin, *Organometallics.*, **9**, 289, 1990.

49. C. Carfagna, M. Green, M. Mahon, S. Rumble and C. Woolhouse, *J. Chem. Soc., Chem. Commun.*, **10**, 879, 1993.

50. M. D. Curtis and O. Eisenstein, *Organometallics.*, **3**, 887, 1984.

51. S. R. Allen, S. G. Barnes, M. Green, G. Moran and L. Trollope, *J. Chem. Soc., Dalton. Trans.*, 1157, 1984.

52. T. Albright, P. Hofmann and R. Hoffmann, *J. Am. Chem. Soc.*, **99**, 7546, 1977.

53. M. Green, J. Z. Nyathi, C. Scott, F. G. A. Stone, A. J. Welch and P. Woodward, *J. Chem. Soc., Dalton. Trans.*, 1067, 1978.

54. B. C. Ward and J. L. Templeton, *J. Am. Chem. Soc.*, **102**, 1432, 1980.

55. M. Green, N. C. Norman and A. G. Orpen, *J. Am. Chem. Soc.*, **103**, 1267, 1981.

56. J. L. Davidson, W. F. Wilson, L. Manojlovic-Muir and K. Muir, *J. Organometallic. Chem.*, **254**, C6-C10, 1983.

57. J L. Davidson, I. E. P. Murray, P. N. Preston and M. V. Russo, *J. Chem. Soc., Dalton. Trans.*, 1783, 1983.

58. S. R. Allen, M. Green, A. G. Orpen and I. D. Williams, *J. Chem. Soc., Chem. Commun.*, 826, 1982.

59. S. R. Allen, R. G. Beevor, M. Green, A. G. Orpen, K. E. Paddick and I. D. Williams, *J. Chem. Soc., Dalton. Trans.*, 591, 1987.

60. R. G. Beevor, M. Green, A. G. Orpen and I. D. Williams, *J. Chem. Soc., Dalton. Trans.*, 1319, 1987.

61. M. R. Churchill and W. J. Youngs, *Inorg. Chem.*, **18**, 2454, 1979.

62. D. C. Brower, K. R. Birdwhistell and J. L. Templeton, *Organometallics.*, **5**, 94, 1986.

63. B. E. Schilling, R. Hoffmann and D. L. Lichtenberger, *J. Am. Chem. Soc.*, **101**, 585, 1979.

64. N. M. Kostiz and R. F. Fenske, *Organometallics.*, **1**, 974, 1982.

65. J. L. Davidson, M. Green, D. W. A. Sharp, F. G. A. Stone and A. J. Welch, *J. Chem. Soc.; Chem. Commun.*, 706, 1974.

66. J. L. Davidson, M. Green, F. G. A. Stone and A. J. Welch, *J. Chem. Soc., Dalton. Trans.*, 738, 1976.

67. J. L. Davidson and D. W. A. Sharp, *J. Chem. Soc., Dalton. Trans.*, 2531, 1975.

68. G. C. Conole, M. Green, M. McPartlin, C. Reeve and C. M. Woolhouse, *J. Chem. Soc.; Chem. Commun.*, 1310, 1988.

69. W. A. Herrmann, R. A. Fischer and E. Herdweck, *Angew. Chem. Int. Ed. Engl.*, **12**, 1263, 1987.

70. J. M. Mayer and T. H. Tulip, *J. Am. Chem. Soc.*, **106**, 3878, 1984.

71. J. M. Mayer, D. L. Thorn and T. H. Tulip, *J. Am. Chem. Soc.*, **107**, 7454, 1985.

72. A. N. Nesmeyanov, N. E. Kolobova, I. B. Zlotina, B. V. Lokshin, I. F. Leshcheva, G. K. Znobina and K. N. Anisimov, *J. Organometallic. Chem.*, **110**, 339, 1976.

73. T. Blackmore, M. I. Bruce, F. G. A. Stone, R. E. Davis and A. Garza, *J. Chem. Soc.; Chem. Commun.*, 852, 1971.

74. T. Blackmore, M. I. Bruce and F. G. A. Stone, *J. Chem. Soc., Dalton. Trans.*, 106, 1974.

75. L. E. Smart, *J. Chem. Soc., Dalton. Trans.*, 390, 1976.

76. C. Nation, PhD Thesis, 1991.

77. Ch. Elschenbroich, A.Salzer, 'Organometallics', VCH, F.R.G., 1989.

78. J. H. van't Hoff, *Arch. Nederl. Sci. Exactes. Nat.*, 445, 1874.

79. J. A. LeBel, *Bull. Soc. Chim. Fr.*, **22**, 337, 1874.

80. S. T. Chacon, M. H. Chisholm, K. Folting, J. C. Huffman and M. J. Hampden-Smith, *Organometallics.*, **10**, 3722, 1991.

81. R. Hoffmann, R. W. Alder and C. F. Wilcox, *J. Am. Chem. Soc.*, **92**, 4992, 1970.

82. G. Erker and M. Albrecht, *Organometallics.*, **11**, 3517, 1992.

83. G. Erker, M. Albrecht, C. Kruger and S. Werner, *J. Am. Chem. Soc.*, **114**, 8531, 1992.

84. R. Gleiter, I. Hyla-Kryspin, N. Shuqiang and G. Erker, *Angew. Chem. Int. Ed. Engl.*, **32**, 754, 1993.

85. Calculations carried out by R. J. Deeth., University of Bath.

86. K. H. Dotz, *Angew. Chem. Int. Ed. Engl.*, **14**, 644, 1975.

87. P. Hoffmann and M. Hammerle, *Angew. Chem. Int. Ed. Engl.*, **28**, 908, 1989.

88. F. N. Tebbe and R. L. Harlow, *J. Am. Chem. Soc.*, **102**, 6149, 1980.

89. R. J. McKinney, T. H. Tulip, D. L. Thorn, T. S. Coolbaugh and F. N. Tebbe, *ibid.*, **103**, 5584, 1981.

90. R. C. Hemand, R. P. Hughes, D. J. Robinson and A. L. Rheingold, *Organometallics.*, **7**, 2239, 1988.

91. J. C. Calabrese, D. C. Roe, D. L. Thorn and T. H. Tulip, *Organometallics.*, **3**, 1223, 1984.

92. T. A. Albright, J. K. Burchett and M. C. Whangbo, *Orbital Interactions in Chemistry,* Wiley, New York 1985.

93. W. A. Hermann, R. A. Fischer and E. Herdtweck, *Angew. Chem. Int. Ed. Engl.*, **26**, 1263, 1987.

94. A. Mayr, M. F. Asaro and T. J. Glines, *J. Am. Chem. Soc.*, **109**, 2215, 1987.

95. M. Crocker, M. Green, A.G.Orpen, H. P. Neumann and C.J. Schaverien, *J. Chem. Soc.; Chem. Commun.*, 1351, 1984.

96. M. Crocker, M. Green, K. R. Nagle, A. G. Orpen, H. P. Neumann, C. E. Morton and C. J. Schaverien, *Organometallics.*, **9**, 1422, 1990.

97. J. R. Morrow, T. L. Tonker and J. L. Templeton, *J. Am. Chem. Soc.*, **107**, 5004, 1985.

98. S. G. Feng, A. S. Gamble and J. L. Templeton, *Organometallics.*, **8**, 2024, 1989.

99. W. C. Zeise, *Ann. Phys*, **9**, 932, 1827.

100. K. Birnbaum, *J. Am. Chem. Soc.*, **145**, 67, 1868.

101. B. D. Dombek and A. M. Harrison, *J. Am. Chem. Soc.*, **105**, 2485, 1983.

102. J. F. Knighton, *J. Chem. Soc.; Chem. Commun.*, 729, 1983.

103. R. J. Whyman, *J. Chem. Soc.; Chem. Commun.*, 1439, 1983.

104. R. M. Laine, *J. Org. Chem.*, **45**, 3370, 1980.

105. C. P. Casey, E. W. Rutler and K. J. Haller, *J. Am. Chem. Soc.*, **109**, 6886, 1987.

106. C. P. Casey and E. W. Rutler, *J. Am. Chem. Soc.*, **111**, 8917, 1989.

107. R. R. Burch, E. L. Muetterties, R. G. Teller and J. M. Williams, *J. Am. Chem. Soc.*, **104**, 4257, 1982.

108. P. Abley and F. J. McQuillen, *J. Chem. Soc.; Chem. Commun.*, 1503, 1969.

109. C. Vaughan, PhD Thesis, 1993.

110. C. Carfagna, R. J. Deeth, S. J. Dossett, M. Green, M. F. Mahon and C. Vaughan, submitted to *J. Am. Chem. Soc.* 1994.

111. C. Mealli and D. M. Porserpio, *J. Chem. Ed.*, **67**, 399, 1990.

112. D. W. Brown, A. J. Floyd and M. Sainsbury, Organic Spectroscopy, Wiley, 1988.

113. W. D. Jones, *J. Am. Chem. Soc.*, **111**, 8722, 1989.

114. W. D. Harman and H. Taube, *J. Am. Chem. Soc.*, **110**, 5403, 1988.

115. W. D. Harman, M. Sekine and H. Taube, *J. Am. Chem. Soc.*, **110**, 5725, 1988.

116. K. B. Shui, C. C. Chou, S. L. Wong and S. C. Wei, *Organometallics.*, **9**, 286, 1990.

117. L. Brandt, M. Green and A. W. Parkins, *Angew. Chem. Int. Ed. Engl.*, **29**, 1046, 1990.

118. S. G. Feng, P. S. White and J. L. Templeton, *J. Am. Chem. Soc.*, **114**, 2951, 1992.

119. Calculations carried out by R. J. Deeth., University of Bath.

120. C. P. Casey and S. R. Marder, *Organometallics.*, **4**, 411, 1985.

121. J. Lewis and A. W. Parkins, *J. Chem. Soc. A.*, 953, 1969.

122. M. L. H. Green, A. G. Massey, J. T. Moelwyn-Hughes and P. L. I. Nagy, *J. Organometallic. Chem.*, **8**, 511, 1967.

123. A. J. Deeming, S. S. Ullah, A. J. P. Domingos, B. F. G. Johnson and J. Lewis, *J. Chem. Soc., Dalton. Trans.*, 2093, 1974.

124. A. J. P. Domingos, B. F. G. Johnson and J. Lewis, *J. Chem. Soc., Dalton. Trans.*, 145, 1974.

125. I. Y. Wu, J. H. Tsai, B. C. Huang, S. C. Chen and Y. C. Lin, *Organometallics.*, **12**, 3971, 1993.

126. P. J. Harris, S. A. R. Knox, R. J. McKinney and F. G. A. Stone, *J. Chem. Soc., Dalton. Trans.*, 1009, 1978.

127. R. R. Schrock, B. F. G. Johnson and J. Lewis, *J. Chem. Soc., Dalton. Trans.*, 951, 1974.

128. C. P. Casey, C. S. Yi and J. A. Gavney, *J. Organometallic. Chem.*, **111**, 443, 1993.

129. M. Green, M. F. Mahon, K. C. Molloy, C. B. M. Nation and C. M. Woolhouse, *J. Chem. Soc.; Chem. Commun.*, 1587, 1991.

130. N. G. Connelly, *Chem. Soc. Rev.*, 153, 1989.

131. J. C. Hayes and N. J. Cooper, *J. Am. Chem. Soc.*, **104**, 5570, 1982.

132. G. S. Bodner, J. A. Gladysz, M. F. Nielsen and V. D. Parker, *J. Am. Chem. Soc.*, **109**, 1757, 1987.

133. K. Stanley and M. C. Baird, *J. Am. Chem. Soc.*, **97**, 6598, 1975.

134. R. S. Cahn, C. Ingold and V. Prelog, *Angew. Chem. Int. Ed. Engl.*, **5**, 385, 1966.

135. H. Alt, M. Herberhold, C. G. Kreiter and H. Strack, *J. Organometallic. Chem.*, **77**, 353, 1974.

136. A. Davidson and N. Martinez, *J. Organometallic. Chem.*, **74**, C17, 1974.

137. Reich-Rohrwig and A. Wojcicki, *Inorg. Chem.*, **13**, 2475, 1974.

138. S. H. Forsen and R. A. Hoffman, *J. Chem. Phys.*, **39**, 2892, 1963; **40**, 1189, 1964.

139. L. Y. Lion and G. K. Roberts, Effects of chemical exchange on nmr spectra., Oxford Press, 1993.

140. R. Birdwhistell, P. Hackett and A. R. Manning, *J. Organometallic. Chem.*, **157**, 239, 1978.

141. R. B. King and R. H. Reimann, *Inorg. Chem.*, **15**, 179, 1976.

APPENDIX

Full tables of X-ray data for complexes **1-5** and **7**.

X-ray data for complex **1**.

Table 1.1 Fractional atomic co-ordinates and thermal parameters (Å).

Atom	x	y	z	Uiso or Ueq	(***)
Mo1	0.84836(5)	0.83509(4)	0.21459(2)	0.0391(2)	***
C1	0.7272(10)	1.0127(7)	0.1743(4)	0.067(4)	***
C2	0.7481(10)	1.0376(7)	0.2409(4)	0.071(5)	***
C3	0.6516(10)	0.9581(7)	0.2752(4)	0.073(4)	***
C4	0.5719(8)	0.8785(8)	0.2333(4)	0.076(5)	***
C5	0.6150(9)	0.9146(7)	0.1686(4)	0.071(5)	***
C6	0.9480(7)	0.7201(5)	0.1463(2)	0.039(3)	***
C7	0.7987(6)	0.6853(6)	0.1583(2)	0.045(3)	***
C8	0.6709(8)	0.6014(7)	0.1340(3)	0.064(4)	***
C9	1.0803(6)	0.6830(6)	0.1028(2)	0.040(3)	***
C10	1.1843(7)	0.7733(6)	0.0763(3)	0.048(3)	***
C11	1.3011(8)	0.7393(6)	0.0309(3)	0.054(4)	***
C12	1.3175(8)	0.6125(7)	0.0126(3)	0.062(4)	***
C13	1.2166(8)	0.5253(6)	0.0382(3)	0.056(4)	***
C14	1.0978(8)	0.5581(6)	0.0840(3)	0.049(3)	***
C15	0.9210(7)	0.7730(5)	0.3071(3)	0.044(3)	***
C16	1.0438(6)	0.8328(6)	0.2848(2)	0.047(3)	***
C17	1.1059(8)	0.9042(7)	0.2332(3)	0.054(4)	***
C18	0.8652(7)	0.7123(5)	0.3665(2)	0.045(3)	***
C19	0.9600(9)	0.7098(6)	0.4217(3)	0.057(4)	***
C20	0.9052(10)	0.6575(7)	0.4790(3)	0.063(4)	***
C21	0.7530(12)	0.6079(7)	0.4810(3)	0.071(5)	***

C22	0.6537(11)	0.6066(7)	0.4271(3)	0.070(4	***
C23	0.7098(8)	0.6613(7)	0.3699(3)	0.056(3)	***
H171	1.1279(71)	1.0018(21)	0.2389(25)	0.044(14)	
H172	1.1963(62)	0.8840(68)	0.1980(25)	0.073(22)	

Table 1.2 Fractional atomic co-ordinates for the hydrogen atoms.

Atom	x	y	z
H11	0.7880	1.0597	0.1348
H21	0.8259	1.1089	0.2613
H31	0.6415	0.9562	0.3274
H41	0.4908	0.8034	0.2470
H51	0.5683	0.8743	0.1243
H81	0.5639	0.6096	0.1640
H82	0.7142	0.5058	0.1352
H83	0.6412	0.6268	0.0847
H101	1.1743	0.8700	0.0913
H111	1.3800	0.8092	0.0100
H121	1.4082	0.5858	-0.0227
H131	1.2297	0.4285	0.0238
H141	1.0191	0.4871	0.1043
H191	1.0808	0.7491	0.4200
H201	0.9809	0.6571	0.5217
H211	0.7085	0.5671	0.5255
H221	0.5340	0.5654	0.4287
H231	0.6334	0.6617	0.3273

Table 1.3 Anisotropic thermal parameters (Å).

Atom	U11	U22	U33	U23	U13	U12
Mo1	0.0315(2)	0.0470(2)	0.0387(2)	-0.0005(2)	0.0007(2)	-0.0003(2)
C1	0.070(4)	0.056(4)	0.077(5)	0.012(4)	0.001(4)	0.014(4)
C2	0.059(4)	0.056(4)	0.097(5)	-0.008(4)	-0.007(4)	0.011(4)
C3	0.054(4)	0.085(5)	0.079(5)	-0.016(4)	-0.002(4)	0.028(4)
C4	0.029(3)	0.085(5)	0.112(6)	0.021(5)	0.012(4)	0.022(3)
C5	0.056(4)	0.073(5)	0.083(5)	0.003(4)	-0.023(4)	0.015(4)
C6	0.040(3)	0.043(3)	0.034(2)	0.001(2)	0.003(2)	-0.004(2)
C7	0.039(3)	0.058(4)	0.038(3)	0.006(3)	0.000(2)	-0.008(3)
C8	0.047(4)	0.077(4)	0.067(4)	-0.012(3)	0.003(3)	-0.012(4)
C9	0.034(2)	0.057(3)	0.029(2)	0.001(2)	-0.002(2)	0.000(3)
C10	0.048(4)	0.051(3)	0.044(3)	0.006(2)	0.005(3)	-0.006(3)
C11	0.047(4)	0.064(4)	0.052(3)	0.007(3)	0.012(3)	0.000(3)
C12	0.057(4)	0.081(4)	0.049(3)	0.001(3)	0.015(3)	0.007(4)
C13	0.057(4)	0.060(4)	0.052(3)	-0.010(3)	0.011(3)	0.003(3)
C14	0.048(3)	0.050(3)	0.049(3)	0.007(3)	-0.001(3)	-0.004(3)
C15	0.043(3)	0.047(3)	0.042(3)	-0.005(2)	0.000(2)	0.006(3)
C16	0.038(2)	0.058(3)	0.045(2)	-0.011(4)	-0.006(2)	-0.006(3)
C17	0.047(4)	0.061(4)	0.053(4)	-0.002(3)	-0.004(2)	-0.013(3)
C18	0.052(3)	0.044(3)	0.038(3)	-0.006(2)	0.002(3)	0.003(3)
C19	0.061(4)	0.064(4)	0.046(3)	-0.001(3)	-0.001(3)	0.014(3)
C20	0.089(5)	0.056(3)	0.044(3)	-0.003(3)	-0.007(3)	0.018(4)
C21	0.112(7)	0.054(4)	0.046(4)	0.007(3)	0.015(4)	0.007(4)
C22	0.079(5)	0.064(4)	0.065(4)	-0.002(3)	0.011(4)	-0.009(5)
C23	0.063(4)	0.061(3)	0.045(3)	-0.004(3)	0.001(3)	-0.006(3)

Table 1.4 Bond lengths (Å).

Mo1-C1	2.296(7)	Mo1-C2	2.375(7)
Mo1-C3	2.430(7)	Mo1-C4	2.355(6)
Mo1-C5	2.305(7)	Mo1-C6	2.039(5)
Mo1-C7	2.016(6)	Mo1-C15	2.105(5)
Mo1-C16	2.164(5)	Mo1-C17	2.278(6)
C1-C2	1.407(11)	C1-C3	2.246(12)
C1-C4	2.272(11)	C1-C5	1.401(11)
C2-C3	1.360(11)	C2-C4	2.238(12)
C2-C5	2.267(11)	C3-C4	1.377(11)
C3-C5	2.264(12)	C4-C5	1.432(11)
C6-C7	1.308(8)	C6-C9	1.466(7)
C7-C8	1.470(8)	C9-C10	1.400(8)
C9-C14	1.394(9)	C10-C11	1.389(8)
C11-C12	1.410(9)	C12-C13	1.355(10)
C13-C14	1.404(8)	C15-C16	1,281(8)
C15-C18	1.459(8)	C16-C17	1.404(9)
C17-H171	1.063(19)	C17-H172	1.061(19)
C18-C19	1.380(8)	C18-C23	1.393(9)
C19-C20	1.381(9)	C20-C21	1.361(12)
C21-C22	1.379(11)	C22-C23	1.393(9)

Table 1.5 Bond angles (°).

C2-Mo1-C1	35.0(3)	C3-Mo1-C1	56.7(3)
C3-Mo1-C2	32.9(3)	C4-Mo1-C1	58.5(3)
C4-Mo1-C2	56.5(3)	C4-Mo1-C3	33.4(3)
C5-Mo1-C1	35.5(3)	C5-Mo1-C2	57.9(3)
C5-Mo1-C3	57.1(3)	C5-Mo1-C4	35.8(3)
C6-Mo1-C3	114.9(2)	C6-Mo1-C2	147.6(3)
C6-Mo1-C3	161.4(2)	C6-Mo1-C4	128.3(3)
C6-Mo1-C5	105.9(3)	C7-Mo1-C1	111.0(3)
C7-Mo1-C2	141.4(3)	C7-Mo1-C3	126.0(3)
C7-Mo1-C4	93.1(3)	C7-Mo1-C5	83.5(3)
C7-Mo1-C6	37.6(2)	C15-Mo1-C1	135.2(3)
C15-Mo1-C2	100.3(3)	C15-Mo1-C3	83.9(2)
C15-Mo1-C4	100.9(3)	C15-Mo1-C5	136.5(3)
C15-Mo1-C6	108,8(2)	C15-Mo1-C7	109.2(2)
C16-Mo1-C1	125.0(3)	C16-Mo1-C2	96.7(3)
C16-Mo1-C3	99.1(2)	C16-Mo1-C4	127.7(3)
C16-Mo1-C5	154.1(3)	C16-Mo1-C6	98.9(2)
C16-Mo1-C7	121.7(2)	C16-Mo1-C15	34.9(2)
C3-C1-C2	35.1(4)	C4-C1-C2	70.5(5)
C4-C1-C3	35.5(3)	C5-C1-C2	107.7(7)
C5-C1-C3	72.6(5)	C5-C1-C4	37.2(5)
C3-C2-C1	108.5(8)	C4-C2-C1	73.1(5)
C4-C2-C3	35.4(4)	C5-C2-C1	36.1(5)
C5-C2-C3	72.4(5)	C5-C2-C4	37.0(3)
C2-C3-C1	36.5(5)	C4-C3-C1	73.3(5)

C4-C3-C2	109.7(7)	C5-C3-C1	36.2(3)
C5-C3-C2	72.7(5)	C5-C3-C4	37.1(4)
C2-C4-C1	36.4(3)	C3-C4-C1	71.2(5)
C3-C4-C2	34.9(5)	C5-C4-C1	36.2(4)
C5-C4-C2	72.6(5)	C5-C4-C3	107.4(7)
C2-C5-C1	36.3(4)	C3-C5-C1	71.2(5)
C3-C5-C2	34.9(3)	C4-C5-C1	106.6(7)
C4-C5-C2	70.4(5)	C4-C5-C3	35.5(5)
C9-C6-C7	137.5(6)	C8-C7-C6	141.4(6)
C10-C9-C6	120.5(5)	C14-C9-C6	120.3(5)
C14-C9-C10	119.1(5)	C11-C10-C9	120.4(6)
C12-C11-C10	119.8(6)	C13-C12-C11	119.7(6)
C14-C13-C12	121.3(6)	C13-C14-C9	119.8(6)
C18-C15-C16	140.4(6)	C17-C16-C15	146.1(6)
H171-C17-C16	123(3)	H172-C17-C16	131(4)
H172-C17-H171	99(5)	C19-C18-C15	121.5(6)
C23-C18-C15	120.3(5)	C23-C18-C19	118.1(5)
C20-C19-C18	121.8(7)	C21-C20-C19	119.0(6)
C22-C21-C20	121.7(7)	C23-C22-C21	118.7(8)
C22-C23-C18	120.7(6)		

Table 1.6 Intermolecular distances (Å).

H11	...C19	2.87	4	2.0	-1.0	0.0
H21	...C6	2.91	4	2.0	-1.0	0.0
H21	...C6	2.78	4	2.0	-1.0	0.0
C3	...H81	2.71	4	1.0	-1.0	0.0
C5	...H221	2.85	4	1.0	-1.0	0.0
C7	...H171	2.94	4	2.0	0.0	0.0
C9	...H111	2.85	3	0.0	1.0	0.0
C10	...H121	2.94	3	0.0	1.0	0.0
H101	...C22	2.92	4	2.0	-1.0	0.0
H111	...C14	2.99	3	-1.0	1.0	0.0
H141	...C15	2.97	4	2.0	0.0	0.0
H141	...C16	2.86	4	2.0	0.0	0.0
H191	...C21	2.91	3	-1.0	1.0	1.0

Table 1.7 Intramolecular distances (Å).

C1	...H21	2.22	C1	...H51	2.23
H11	...C2	2.22	H11	...C5	2.22
C2	...H31	2.17	H21	...C3	2.18
C3	...H41	2.19	H31	...C4	2.19
C4	...H51	2.25	H41	...C5	2.25
C5	...C7	2.88	H51	...C7	2.86
C6	...C8	2.62	C6	...H82	3.00
C6	...H83	3.00	C6	...C10	2.49
C6	...H101	2.70	C6	...C14	2.48
C6	...H141	2.70	C6	...C17	2.96
C6	...H172	2.89	C7	...H81	2.10
C7	...H82	2.09	C7	...H83	2.09
C7	...C9	2.59	C9	...H101	2.15
C9	...C11	2.42	C9	...C12	2.80
C9	...C13	2.42	C9	...H141	2.15
C10	...H111	2.15	C10	...C12	2.42
C10	...C13	2.77	C10	...C14	2.41
C10	...H172	2.77	H101	...C11	2.14
H101	...C17	3.00	H101	...H172	2.21
C11	...H121	2.16	C11	...C13	2.39
C11	...C14	2.78	H111	...C12	2.16
C12	...H131	2.10	C12	...C14	2.40
H121	...C13	2.12	C13	...H141	2.16
H131	...C14	2.15	C15	...C17	2.57
C15	...C19	2.48	C15	...H191	2.69

C15	...C23	2.47	C15	...H231	2.68
C16	...H171	2.15	C16	...H172	2.25
C16	...C18	2.58	C16	...H191	2.94
H171	...H172	1.61	C18	...H191	2.13
C18	...C20	2.41	C18	...C21	2.77
C18	...C22	2.42	C18	...H231	2.14
C19	...H201	2.14	C19	...C21	2.36
C19	...C22	2.76	C19	...C23	2.38
H191	...C20	2.13	C20	...H211	2.11
C20	...C22	2.39	C20	...C23	2.76
H201	...C21	2.12	C21	...H221	2.15
C21	...C23	2.39	H221	...C22	2.12
C22	...H231	2.14	H221	...C23	2.15

X-ray data for complex **2**.

Table 2.1 Fractional atomic co-ordinates ($x10^4$) and equivalent isotropic temperature factors ($Å^2 x10^3$).

Atom	x	y	z	U
Mo1	1645.3(3)	1151.3(3)	52.0(3)	30.4(3)
O1	1485(4)	166(4)	-1427(3)	68(2)
O2	2531(4)	-1019(2)	353(3)	44(1)
C1	1590(5)	521(5)	-882(4)	43(2)
C2	857(5)	2431(5)	-114(4)	56(3)
C3	686(5)	2174(5)	612(5)	53(3)
C4	116(5)	1433(5)	593(5)	51(3)
C5	-76(5)	1228(4)	-148(4)	50(3)
C6	398(5)	1859(5)	-591(5)	50(3)
C7	2613(5)	-248(4)	446(3)	33(2)
C8	3161(4)	366(4)	-14(3)	30(2)
C9	3213(4)	1160(4)	388(3)	29(2)
C10	2632(5)	1050(4)	1060(3)	35(2)
C11	2164(5)	237(4)	1043(3)	35(2)
C12	3106(5)	1913(4)	-19(4)	35(2)
C13	1604(6)	-202(5)	1652(4)	52(3)
C14	3804(4)	145(4)	-665(3)	32(2)
C15	4654(5)	625(4)	-822(3)	39(2)
C16	5267(5)	407(5)	-1415(4)	50(3)
C17	5065(6)	-294(5)	-1833(4)	52(3)
C18	4237(6)	-776(5)	-1667(3)	46(2)

C19	3600(5)	-561(4)	-1087(3)	41(2)
C20	2634(5)	1653(4)	1696(3)	37(2)
C21	1876(6)	1682(5)	2232(4)	52(3)
C22	1944(6)	2210(6)	2837(4)	63(3)
C23	2767(7)	2718(5)	2931(4)	67(3)
C24	3524(6)	2705(5)	2401(4)	67(3)
C25	3451(5)	2177(5)	1801(4)	50(3)

Table 2.2 Fractional atomic co-ordinates ($x10^4$).

	x	y	z
Mo1	1645.3(3)	1151.3(3)	52.0(3)
O1	1485(4)	166(4)	-1427(3)
O2	2531(4)	-1019(2)	353(3)
C1	1590(5)	521(5)	-882(4)
C2	857(5)	2431(5)	-114(4)
C3	686(5)	2174(5)	612(5)
C4	116(5)	1433(5)	593(5)
C5	-76(5)	1228(4)	-148(4)
C6	398(5)	1859(5)	-591(5)
C7	2613(5)	-248(4)	446(3)
C8	3161(4)	366(4)	-14(3)
C9	3213(4)	1160(4)	388(3)
C10	2632(5)	1050(4)	1060(3)
C11	2164(5)	237(4)	1043(3)
C12	3106(5)	1913(4)	-19(4)
C13	1604(6)	-202(5)	1652(4)

C14	3804(4)	145(4)	-665(3)
C15	4654(5)	625(4)	-822(3)
C16	5267(5)	407(5)	-1415(4)
C17	5065(6)	-294(5)	-1833(4)
C18	4237(6)	-776(5)	-1667(3)
C19	3600(5)	-561(4)	-1087(3)
C20	2634(5)	1653(4)	1696(3)
C21	1876(6)	1682(5)	2232(4)
C22	1944(6)	2210(6)	2837(4)
C23	2767(7)	2718(5)	2931(4)
C24	3524(6)	2705(5)	2401(4)
C25	3451(5)	2177(5)	1801(4)

Table 2.3 Anisotropic temperature factors (Å x10^3).

Atom	U11	U22	U33	U23	U13	U12
Mo1	24.8(3)	24.5(3)	42.1(3)	2.0(3)	-1.9(3)	0.3(2)
O1	63(4)	79(4)	63(3)	-23(3)	-20(3)	13(3)
O2	51(3)	25(2)	56(3)	-1(2)	4(2)	-3(2)
C1	34(4)	45(4)	50(4)	-5(3)	-9(4)	10(3)
C2	39(4)	33(4)	97(6)	16(5)	-4(4)	8(3)
C3	40(4)	43(5)	75(5)	-12(4)	-3(4)	7(4)
C4	26(4)	49(5)	78(5)	2(4)	18(4)	10(4)
C5	25(3)	39(4)	86(6)	-7(4)	-8(4)	-1(3)
C6	33(4)	46(5)	72(5)	5(4)	-8(4)	5(3)
C7	26(3)	37(4)	37(3)	5(3)	-8(3)	1(3)
C8	27(3)	30(3)	33(3)	7(3)	-5(3)	1(2)
C9	22(3)	26(3)	40(3)	-3(3)	-5(2)	-4(3)
C10	29(3)	34(3)	41(3)	3(3)	-3(3)	4(3)
C11	33(3)	35(4)	36(3)	3(3)	1(3)	1(3)
C12	32(3)	26(3)	46(4)	4(3)	-3(3)	-7(3)
C13	53(5)	47(5)	57(4)	8(3)	17(4)	0(4)
C14	26(3)	31(4)	38(3)	4(3)	-3(3)	8(3)
C15	31(4)	40(4)	45(4)	6(3)	-1(3)	6(3)
C16	38(4)	70(5)	42(4)	14(4)	8(3)	5(4)
C17	55(5)	67(5)	33(4)	15(3)	5(3)	31(5)
C18	60(5)	43(4)	33(4)	0(3)	-4(3)	17(4)
C19	43(4)	42(4)	36(3)	1(3)	-4(3)	5(3)
C20	40(4)	35(3)	35(3)	0(3)	0(3)	7(3)

C21	60(5)	53(5)	43(4)	-3(3)	4(4)	1(4)
C22	70(5)	77(6)	42(4)	-5(4)	13(4)	14(5)
C23	86(7)	58(6)	57(5)	-18(4)	-9(5)	17(5)
C24	70(6)	58(6)	73(5)	-27(4)	-10(5)	-13(5)
C25	45(4)	51(5)	53(4)	-14(3)	0(4)	1(4)

Table 2.4 Hydrogen fractional atomic co-ordinates ($x10^4$) and isotropic temperature factors ($Å^2 x10^3$).

Atom	x	y	z	U
H21	1229(5)	2921(5)	-262(4)	70(5)
H31	918(5)	2456(5)	1051(5)	70(5)
H41	-106(5)	1118(5)	1017(5)	70(5)
H51	-454(5)	753(4)	-325(4)	70(5)
H61	400(5)	1884(5)	-1123(5)	70(5)
H121	3366(47)	1968(46)	-513(14)	70(5)
H122	3062(51)	2438(22)	243(34)	70(5)
H131	1358(6)	205(5)	2001(4)	70(5)
H132	2051(6)	-586(5)	1900(4)	70(5)
H133	1045(6)	-508(5)	1446(4)	70(5)
H151	4816(5)	1105(4)	-522(3)	70(5)
H161	5840(5)	751(5)	-1536(4)	70(5)
H171	5499(6)	-446(5)	-2238(4)	70(5)
H181	4096(6)	-1270(5)	-1955(3)	70(5)
H191	3020(5)	-901(4)	-979(3)	70(5)
H211	1294(6)	1326(5)	2180(4)	70(5)
H221	1408(6)	2221(6)	3195(4)	70(5)
H231	2820(7)	3078(5)	3357(4)	70(5)
H241	4100(6)	3067(5)	2453(4)	70(5)
H251	3987(5)	2174(5)	1442(4)	70(5)

Table 2.5 Bond lengths (Å)

C1-Mo1	1.961(9)	C2-Mo1	2.308(9)
C3-Mo1	2.299(9)	C4-Mo1	2.293(8)
C5-Mo1	2.309(9)	C6-Mo1	2.310(9)
C7-Mo1	2.664(9)	C8-Mo1	2.368(8)
C9-Mo1	2.162(8)	C10-Mo1	2.247(8)
C11-Mo1	2.407(8)	C12-Mo1	2.284(8)
C1-O1	1.142(8)	C7-O2	1.243(8)
C3-C2	1.391(10)	C4-C2	2.261(12)
C5-C2	2.279(12)	C6-C2	1.393(11)
C4-C3	1.400(11)	C5-C3	2.272(12)
C6-C3	2.260(14)	C5-C4	1.400(11)
C6-C4	2.272(13)	C6-C5	1.428(11)
C8-C7	1.471(9)	C11-C7	1.453(9)
C9-C8	1.458(9)	C14-C8	1.492(9)
C10-C9	1.448(9)	C12-C9	1.412(9)
C11-C10	1.435(9)	C20-C10	1.495(9)
C13-C11	1.498(9)	C15-C14	1.390(10)
C19-C14	1.384(9)	C16-C15	1.387(10)
C17-C16	1.371(11)	C18-C17	1.372(11)
C19-C18	1.386(10)	C21-C20	1.395(10)
C25-C20	1.379(10)	C22-C21	1.380(11)
C23-C22	1.367(12)	C24-C23	1.385(12)
C25-C24	1.374(10)	H21-C2	0.96
H31-C3	0.960	H41-C4	0.960
H51-C5	0.960	H61-C6	0.960

H121-C12	0.960(2)	H122-C12	0.960(2)
H131-C13	0.960	H132-C13	0.960
H133-C13	0.960	H151-C15	0.960
H161-C16	0.960	H171-C17	0.960
H181-C18	0.960	H191-C19	0.960
H211-C21	0.960	H221-C22	0.960
H231-C23	0.960	H241-C24	0.960
H251-C25	0.960		

Table 2.6 Bond angles (°).

C2-Mo1-C1	108.8(4)	C3-Mo1-C1	135.9(3)
C3-Mo1-C2	35.1(2)	C4-Mo1-C1	115.6(4)
C4-Mo1-C2	58.9(4)	C4-Mo1-C3	35.6(2)
C5-Mo1-C1	81.7(4)	C5-Mo1-C2	59.2(4)
C5-Mo1-C3	59.1(4)	C5-Mo1-C4	35.4(3)
C6-Mo1-C1	77.9(4)	C6-Mo1-C2	35.1(2)
C6-Mo1-C3	58.7(4)	C6-Mo1-C4	59.2(4)
C6-Mo1-C5	36.0(2)	C7-Mo1-C1	79.6(3)
C7-Mo1-C2	171.6(2)	C7-Mo1-C3	137.8(2)
C7-Mo1-C4	118.3(3)	C7-Mo1-C5	124.0(3)
C7-Mo1-C6	152.1(2)	C8-Mo1-C1	73.6(3)
C8-Mo1-C2	147.4(2)	C8-Mo1-C3	149.9(2)
C8-Mo1-C4	150.9(2)	C8-Mo1-C5	148.8(2)
C8-Mo1-C6	146.9(2)	C8-Mo1-C7	33.4(2)
C9-Mo1-C1	106.3(3)	C9-Mo1-C2	117.6(4)
C9-Mo1-C3	113.7(3)	C9-Mo1-C4	136.7(3)
C9-Mo1-C5	172.0(2)	C9-Mo1-C6	145.4(2)
C9-Mo1-C7	58.0(3)	C9-Mo1-C8	37.3(2)
C10-Mo1-C1	132.9(2)	C10-Mo1-C2	115.5(3)
C10-Mo1-C3	90.9(3)	C10-Mo1-C4	100.6(4)
C10-Mo1-C5	134.8(2)	C10-Mo1-C6	149.0(3)
C10-Mo1-C7	56.3(3)	C10-Mo1-C8	60.7(3)
C10-Mo1-C9	38.3(2)	C11-Mo1-C1	109.9(4)
C11-Mo1-C2	139.4(2)	C11-Mo1-C3	105.1(3)
C11-Mo1-C4	93.1(3)	C11-Mo1-C5	115.5(3)

C11-Mo1-C6	150.7(2)	C11-Mo1-C7	32.8(2)
C11-Mo1-C8	58.4(3)	C11-Mo1-C9	61.4(3)
C11-Mo1-C10	35.7(2)	C12-Mo1-C1	104.7(4)
C12-Mo1-C2	84.7(3)	C12-Mo1-C3	96.7(4)
C12-Mo1-C4	131.9(3)	C12-Mo1-C5	142.9(2)
C12-Mo1-C6	108.6(3)	C12-Mo1-C7	92.9(3)
C12-Mo1-C8	63.9(3)	C12-Mo1-C9	36.8(2)
C12-Mo1-C10	65.8(3)	C12-Mo1-C11	96.9(3)
C4-C2-C3	36.0(4)	C5-C2-C3	71.9(6)
C5-C2-C4	35.9(3)	C6-C2-C3	108.6(8)
C6-C2-C4	72.5(6)	C6-C2-C5	36.6(4)
C4-C3-C2	108.2(8)	C5-C3-C2	72.5(6)
C5-C3-C4	35.7(4)	C6-C3-C2	35.7(4)
C6-C3-C4	72.5(6)	C6-C3-C5	36.7(3)
C3-C4-C2	35.7(4)	C5-C4-C2	72.8(6)
C5-C4-C3	108.5(8)	C6-C4-C2	35.8(3)
C6-C4-C3	71.5(6)	C6-C4-C5	37.0(4)
C3-C5-C2	35.6(3)	C4-C5-C2	71.3(6)
C4-C5-C3	35.8(4)	C6-C5-C2	35.6(4)
C6-C5-C3	71.2(6)	C6-C5-C4	106.9(7)
C3-C6-C2	35.7(4)	C4-C6-C2	71.7(6)
C4-C6-C3	36.0(3)	C5-C6-C2	107.8(8)
C5-C6-C3	72.1(6)	C5-C6-C4	36.1(4)
C8-C7-O2	128.5(7)	C11-C7-O2	126.0(7)
C11-C7-C8	105.5(6)	C9-C8-C7	108.6(6)
C14-C8-C7	124.6(6)	C14-C8-C9	124.6(6)
C10-C9-C8	106.6(6)	C12-C9-C8	118.2(6)

C12-C9-C10	119.0(6)	C11-C10-C9	108.7(6)
C20-C10-C9	124.4(6)	C20-C10-C11	126.6(6)
C10-C11-C7	108.5(6)	C13-C11-C7	119.9(7)
C13-C11-C10	128.2(7)	C15-C14-C8	119.6(7)
C19-C14-C8	120.9(6)	C19-C14-C15	119.4(7)
C16-C15-C14	119.6(8)	C17-C16-C15	120.9(8)
C18-C17-C16	119.4(8)	C19-C18-C17	120.8(8)
C18-C19-C14	119.9(7)	C21-C20-C1-	123.5(7)
C25-C20-C10	119.6(7)	C25-C20-C21	116.8(7)
C22-C21-C20	121.4(8)	C23-C22-C21	120.7(8)
C24-C23-C22	118.8(8)	C25-C24-C23	120.2(9)
C24-C25-C20	122.1(8)	C3-C2-H21	125.8(5)
C4-C2-H21	161.8(3)	C5-C2-H21	162.3(3)
C6-C2-H21	125.7(5)	H31-C3-C2	125.8(5)
C4-C3-H31	126.0(6)	C5-C3-H31	161.7(3)
C6-C3-H31	161.6(3)	H41-C4-C2	161.5(3)
H41-C4-C3	125.7(6)	C5-C4-H41	125.8(5)
C6-C4-H41	162.7(3)	H51-C5-C2	162.1(3)
H51-C5-C3	162.3(3)	H51-C5-C4	126.5(5)
C6-C5-H51	126.5(5)	H61-C6-C2	126.1(5)
H61-C6-C3	161.8(3)	H61-C6-C4	162.2(3)
H61-C6-C5	126.1(5)	H121-C12-C9	121.6(46)
H122-C12-C9	119.2(45)	H122-C12-H121	113.6(60)
H131-C13-C11	109.5(5)	H132-C13-C11	109.5(5)
H132-C13-H131	109.5	H133-C13-C11	109.5(5)
H133-C13-H131	109.5	H133-C13-H132	109.5
H151-C15-C14	120.2(5)	C16-C15-H151	120.2(6)

H161-C16-C15	119.6(6)	C17-C16-H161	119.5(5)
H171-C17-C16	120.4(5)	C18-C17-H171	120.2(5)
H181-C18-C17	119.6(5)	C19-C18-C181	119.5(5)
H191-C19-C14	120.1(5)	H191-C19-C18	120.1(5)
H211-C21-C20	119.3(5)	C22-C21-H211	119.3(6)
H221-C22-C21	119.6(6)	C23-C22-H221	119.7(6)
H231-C23-C22	120.6(6)	C24-C23-H231	120.6(6)
H241-C24-C23	119.9(6)	C25-C24-H241	119.9(6)
H251-C25-C20	119.0(5)	H251-C25-C24	118.9(6)

Table 2.7 Selected non-bonded distances (Å).

Intramolecular:

O1	...Mo1	3.103	H21	...Mo1	2.925
H31	...Mo1	2.913	H41	...Mo1	2.901
H51	...Mo1	2.929	H61	...Mo1	2.926
H121	...Mo1	2.848	H122	...Mo1	2.783
C13	...Mo1	3.603	C14	...Mo1	3.521
C20	...Mo1	3.338	C19	...O1	3.091
C8	...O2	2.447	C11	...O2	2.403
C13	...O2	2.946	C14	...O2	3.105
C19	...O2	3.047	H191	...O2	2.496
C5	...C1	2.807	C6	...C1	2.701
H61	...C1	2.714	C7	...C1	3.011
C8	...C1	2.615	C14	...C1	3.017
C19	...C1	3.191	H31	...C2	2.102
H61	...C2	2.107	C12	...C2	3.094
C3	...H21	2.102	C6	...H21	2.102
H41	...C3	2.110	C4	...H31	2.112
C21	...H31	2.770	H51	...C4	2.117
C5	...H41	2.110	H61	...C5	2.139
C6	...H51	2.143	C9	...C7	2.379
C10	...C7	2.344	C13	...C7	2.554
H132	...C7	2.779	C14	...C7	2.624
C19	...C7	3.098	C10	...C8	2.330
C11	...C8	2.328	C12	...C8	2.463

H121	...C8	2.717	C15	...C8	2.491
H151	...C8	2.651	C19	...C8	2.502
H191	...C8	2.669	C11	...C9	2.342
H121	...C9	2.082	H122	...C9	2.058
C14	...C9	2.612	C15	...C9	3.021
H151	...C9	2.684	C20	...C9	2.603
C25	...C9	3.035	H251	...C9	2.696
C12	...C10	2.464	H122	...C10	2.714
C13	...C10	2.638	H131	...C10	2.744
C21	...C10	2.545	H211	...C10	2.722
C25	...C10	2.484	H251	...C10	2.624
H131	...C11	2.031	H132	...C11	2.030
H133	...C11	2.031	C20	...C11	2.617
C21	...C11	3.166	C14	...C12	3.181
H151	...C12	2.758	C20	...C12	3.184
H122	...H121	1.606	C21	...C13	3.195
H211	...C13	2.643	H132	...H131	1.568
H133	...H131	1.568	C21	...H131	2.483
H211	...H131	1.814	H133	...H132	1.568
H151	...C14	2.048	C16	...C14	2.400
C17	...C14	2.778	C18	...C14	2.397
H191	...C14	2.041	H161	...C15	2.039
C17	...C15	2.400	C18	...C15	2.756
C19	...C15	2.395	C16	...H151	2.046
H161	...H151	2.344	H171	...C16	2.033
C18	...C16	2.368	C19	...C16	2.755
C17	...H161	2.025	H171	...H161	2.330

H181	...C17	2.026	C19	...C17	2.398
C18	...H171	2.032	H181	...H171	2.330
H191	...C18	2.043	C19	...H181	2.038
H191	...H181	2.340	H211	...C20	2.044
C22	...C20	2.419	C23	...C20	2.804
C24	...C20	2.409	H251	...C20	2.026
H221	...C21	2.034	C23	...C21	2.387
C24	...C21	2.739	C25	...C21	2.362
C22	...H211	2.031	H221	...H211	2.325
H231	...C22	2.031	C24	...C22	2.369
C25	...C22	2.735	C23	...H221	2.022
H231	...H221	2.331	H241	...C23	2.041
C25	...C23	2.391	C24	...H231	2.047
H241	...H231	2.352	H251	...C24	2.021
C25	...H241	2.031	H251	...H241	2.316

Intermolecular:

H21	...O2	2.359	H133	...H51	2.203

X-ray data for complex **3**.

Table 3.1 Fractional atomic co-ordinates and thermal parameters (Å).

Atom	x	y	z	Uiso or Ueq	(***)
Mo1	0.85464(7)	-0.41268(4)	0.37054(2)	0.0259(2)	***
O1	1.1881(7)	-0.5263(4)	03778(3)	0.054(4)	***
O2	1.2458(6)	-0.2897(4)	0.3503(3)	0.050(3)	***
C1	1.0652(10)	-0.4825(5)	0.3777(3)	0.306(4)	***
C2	0.6855(10)	-0.4266(5)	0.2787(3)	0.042(4)	***
C3	0.5739(9)	-0.4245(5)	0.3270(4)	0.044(4)	***
C4	0.6072(10)	-0.4993(5)	0.3646(4)	0.046(5)	***
C5	0.7383(9)	-0.5490(5)	0.3411(3)	0.038(4)	***
C6	0.7867(10)	-0.5043(5)	0.2859(3)	0.040(4)	***
C7	1.1016(8)	-0.2936(4)	0.3725(3)	0.030(4)	***
C8	1.0675(9)	-0.3360(5)	0.4311(3)	0.035(4)	***
C9	0.8920(9)	-0.3152(5)	0.4429(3)	0.034(4)	***
C10	0.8168(9)	-0.2676(4)	0.3893(3)	0.033(4)	***
C11	0.9371(8)	-0.2657(4)	0.3448(3)	0.029(4)	***
C12	1.2045(11)	-0.3703(6)	0.4781(4)	0.052(5)	***
C13	0.7973(10)	-0.3820(5)	0.4724(3)	0.048(5)	***
C14	0.6424(9)	-0.2234(5)	0.3839(4)	0.045(5)	***
C15	0.9159(10)	-0.2166(5)	0.2831(3)	0.042(4)	***
Mo2	0.20610(7)	0.08572(4)	0.37142(2)	0.0250(3)	***
O'1	-0.1206(7)	-0.0316(4)	0.3758(3)	0.052(4)	***
O'2	-0.1926(6)	0.2127(4)	0.3509(2)	0.045(3)	***
C'1	0.0007(10)	0.0136(5)	0.3759(3)	0.035(4)	***

C'2	0.3295(9)	0.0752(5)	0.2784(3)	0.042(4)	***
C'3	0.4652(9)	0.0788(5)	0.3273(4)	0.042(4)	***
C'4	0.4533(10)	0.0015(5)	0.3640(4)	0.042(5)	***
C'5	0.3123(10)	-0.0481(5)	0.3399(4)	0.041(4)	***
C'6	0.2355(9)	-0.0037(5)	0.2860(3)	0.038(4)	***
C'7	-0.0388(9)	0.2052(4)	0.3745(3)	0.032(4)	***
C'8	0.0174(8)	0.1590(4)	0.4322(3)	0.030(4)	***
C'9	0.1985(9)	0.1769(4)	0.4474(3)	0.030(4)	***
C'10	0.2552(8)	0.2287(4)	0.3965(3)	0.030(4)	***
C'11	0.1152(8)	0.2349(4)	0.3500(3)	0.029(4)	***
C'12	-0.1026(10)	0.1220(5)	0.4759(3)	0.042(4)	***
C'13	0.3055(10)	0.1078(5)	0.4737(3)	0.039(4)	***
C'14	0.4266(9)	0.2735(5)	0.3959(4)	0.046(5)	***
C'15	0.1117(10)	0.2878(5)	0.2904(3)	0.043(4)	***
H131	0.8835(86)	-0.4196(51)	0.5039(31)	0.079(7)	
H132	0.6605(30)	-0.3801(61)	0.4756(40)	0.079(7)	
H13a	0.2568(106)	0.0627(47)	0.5062(32)	0.079(7)	
H13b	0.4429(29)	0.1133(61)	0.4788(40)	0.079(7)	

Table 2.2 Fractional atomic co-ordinates for the hydrogen atoms.

Atom	x	y	z
H21	0.6934	-0.3771	0.2430
H31	0.4782	-0.3744	0.3328
H41	0.5440	-0.5152	0.4056
H51	0.7922	-0.6101	0.3601
H61	0.8820	-0.5259	0.2561
H121	1.1461	-0.3984	0.5170
H122	1.2879	-0.3164	0.4940
H123	1.2783	-0.4206	0.4570
H141	0.5790	-0.2362	0.4253
H142	0.5657	-0.2495	0.3441
H143	0.6581	-0.1528	0.3784
H151	0.7819	-0.2021	0.2711
H152	0.9636	-0.2573	0.2474
H153	0.9877	-0.1555	0.2871
H'21	0.3027	0.1239	0.2423
H'31	0.5595	0.1308	0.3348
H'41	0.5394	-0.0162	0.4039
H'51	0.2684	-0.1093	0.3589
H'61	0.1259	-0.0264	0.2564
H12a	-0.2295	0.1154	0.4523
H12b	-0.1075	0.1661	0.5150
H12c	-0.0569	0.0578	0.4920
H14a	0.5062	0.2561	0.4375

H14b	0.4083	0.3444	0.3943
H14c	0.4883	0.2525	0.3557
H15a	0.2413	0.3030	0.2805
H152	0.0417	0.3486	0.2955
H15c	0.0493	0.2495	0.2526

Table 3.3 Anisotropic thermal parameters (Å).

Atom	U11	U22	U33	U23	U13	U12
Mo1	0.0299(3)	0.0224(3)	0.0254(3)	-0.0019(3)	0.0041(2)	-0.0024(3)
O1	0.047(3)	0.052(4)	0.061(4)	-0.004(3)	-0.001(3)	0.012(3)
O2	0.033(3)	0.051(3)	0.067(4)	-0.007(3)	0.014(3)	-0.001(3)
C1	0.046(5)	0.031(4)	0.032(4)	-0.005(3)	-0.003(3)	-0.003(4)
C2	0.049(5)	0.035(4)	0.041(4)	-0.003(3)	-0.009(3)	-0.012(4)
C3	0.031(4)	0.043(5)	0.058(5)	-0.014(4)	0.002(3)	-0.008(4)
C4	0.043(5)	0.044(5)	0.052(5)	-0.007(4)	0.019(4)	-0.018(4)
C5	0.043(4)	0.025(4)	0.046(4)	-0.006(3)	0.004(3)	-0.008(3)
C6	0.051(5)	0.033(4)	0.037(4)	-0.016(3)	0.002(3)	-0.011(4)
C7	0.029(4)	0.023(3)	0.037(4)	-0.003(3)	0.002(3)	-0.004(3)
C8	0.041(4)	0.030(4)	0.033(4)	-0.009(3)	-0.006(3)	-0.006(3)
C9	0.046(4)	0.028(4)	0.030(4)	-0.011(3)	0.006(3)	-0.005(3)
C10	0.032(4)	0.026(4)	0.040(4)	-0.011(3)	-0.004(3)	-0.003(3)
C11	0.036(4)	0.023(4)	0.029(4)	-0.005(3)	0.005(3)	-0.009(3)
C12	0.065(6)	0.047(5)	0.043(5)	-0.001(4)	-0.025(4)	0.006(4)
C13	0.076(6)	0.043(5)	0.026(4)	-0.004(3)	0.013(4)	-0.004(4)
C14	0.036(4)	0.043(5)	0.056(5)	-0.014(4)	0.005(3)	0.009(4)

C15	0.057(5)	0.033(4)	0.036(4)	0.006(3)	0.000(3)	-0.002(4)
Mo2	0.0271(3)	0.0221(3)	0.0259(3)	-0.0018(3)	0.0030(2)	0.0010(3)
O'1	0.047(3)	0.052(4)	0.058(4)	-0.010(3)	0.017(3)	-0.014(3)
O'2	0.032(3)	0.049(3)	0.054(3)	-0.004(3)	-0.002(2)	-0.001(2)
C'1	0.042(4)	0.035(4)	0.028(4)	-0.002(3)	0.009(3)	0.004(4)
C'2	0.049(4)	0.039(5)	0.038(4)	0.000(3)	0.022(3)	0.010(4)
C'3	0.028(4)	0.042(5)	0.057(5)	-0.017(4)	0.009(3)	0.005(4)
C'4	0.040(4)	0.042(5)	0.044(4)	-0.008(4)	-0.001(3)	0.013(4)
C'5	0.045(5)	0.025(4)	0.054(5)	-0.006(3)	0.010(4)	0.009(3)
C'6	0.043(4)	0.036(4)	0.037(4)	-0.011(3)	0.009(3)	0.010(3)
C'7	0.033(4)	0.024(4)	0.038(4)	-0.005(3)	0.005(3)	0.006(3)
C'8	0.031(4)	0.025(4)	0.034(4)	-0.011(3)	0.007(3)	-0.002(3)
C'9	0.043(4)	0.028(4)	0.020(3)	-0.006(3)	0.003(3)	-0.001(3)
C'10	0.036(4)	0.025(4)	0.028(3)	-0.003(3)	0.010(3)	0.005(3)
C'11	0.035(4)	0.018(3)	0.035(4)	-0.005(3)	0.002(3)	0.004(3)
C'12	0.048(5)	0.038(4)	0.041(4)	-0.004(3)	0.018(3)	-0.004(4)
C'13	0.042(4)	0.044(5)	0.032(4)	-0.005(3)	-0.004(3)	0.004(4)
C'14	0.042(4)	0.038(5)	0.058(5)	-0.020(4)	0.007(4)	-0.016(4)
C'15	0.058(5)	0.035(4)	0.035(4)	0.006(3)	0.011(3)	0.005(4)

Table 3.4 Bond lengths (Å).

Mo1-C1	1.950(8)	Mo1-C2	2.296(7)
Mo1-C3	2.318(7)	Mo1-C4	2.331(8)
Mo1-C5	2.316(7)	Mo1-C6	2.318(7)
Mo1-C7	2.637(7)	Mo1-C8	2.332(7)
Mo1-C9	2.150(7)	Mo1-C10	2.251(7)
Mo1-C11	2.390(7)	Mo1-C13	2.335(7)
O1-C1	1.168(10)	02-C7	1.268(9)
C2-C3	1.420(11)	C2-C4	2.289(11)
C2-C6	1.417(11)	C3-C4	1.403(11)
C3-C5	2.283(11)	C3-C6	2.297(11)
C4-C5	1.403(11)	C5-C6	1.451(11)
C7-C8	1.466(10)	C7-C11	1.434(9)
C8-C9	1.454(10)	C8-C12	1.501(10)
C9-C10	1.444(9)	C9-C13	1.435(11)
C10-C11	1.406(10)	C10-C14	1.515(10)
C11-C15	1.523(10)	C13-H131	1.08(7)

C13-H132	1.08(3)	Mo2-C'1	1.951(8)
Mo2-C'2	2.314(8)	Mo2-C'3	2.320(7)
Mo2-C'4	2.332(8)	Mo2-C'5	2.310(8)
Mo2-C'6	2.317(7)	Mo2-C'7	2.637(7)
Mo2-C'8	2.342(7)	Mo2-C'9	2.150(6)
Mo2-C'10	2.251(6)	Mo2-C'11	2.395(6)
Mo2-C'13	2.302(7)	O'1-C'1	1.169(9)
O'2-C'7	1.269(8)	C'2-C'3	1.431(10)
C'2-C'4	2.299(10)	C'2-C'5	2.299(11)
C'2-C'6	1.417(11)	C'3-C'4	1.419(11)
C'3-C'5	2.287(11)	C'4-C'5	1.395(10)
C'4-C'6	2.290(10)	C'5-C'6	1.430(10)
C'7-C'8	1.463(9)	C'7-C'11	1.431(10)
C'8-C'9	1.451(9)	C'8-C'12	1.499(10)
C'9-C'10	1.453(9)	C'9-C'13	1.424(10)
C'10-C'11	1.423(9)	C'10-C'14	1.503(10)
C'11-C'15	1.515(10)	C'13-H13a	1.07(7)
C'13-H13b	1.074(25)		

Table 3.5 Bond angles (°).

C2-Mo1-C2	115.9(3)	C3-Mo1-C1	138.9(3)
C3-Mo1-C2	35.8(3)	C4-Mo1-C1	113.2(3)
C4-Mo1-C2	59.3(3)	C4-Mo1-C3	35.1(3)
C5-Mo1-C1	81.4(3)	C5-Mo1-C2	60.0(3)
C5-Mo1-C3	59.0(3)	C5-Mo1-C4	35.1(3)
C6-Mo1-C1	82.7(3)	C6-Mo1-C2	35.8(3)
C6-Mo1-C3	59.4(3)	C6-Mo1-C4	59.4(3)
C6-Mo1-C5	36.5(3)	C7-Mo1-C1	75.8(3)
C7-Mo1-C2	116.2(2)	C7-Mo1-C3	136.5(2)
C7-Mo1-C4	170.9(2)	C7-Mo1-C5	151.6(2)
C7-Mo1-C6	122.4(2)	C8-Mo1-C1	70.6(3)
C8-Mo1-C2	149.2(3)	C8-Mo1-C3	150.4(3)
C8-Mo1-C4	149.0(3)	C8-Mo1-C5	147.0(2)
C8-Mo1-C6	147.3(3)	C8-Mo1-C7	33.6(2)
C9-Mo1-C1	104.7(3)	C9-Mo1-C2	136.3(3)
C9-Mo1-C3	114.3(3)	C9-Mo1-C4	118.8(3)
C9-Mo1-C5	146.4(3)	C9-Mo1-C6	172.1(3)

C9-Mo1-C7	58.0(2)	C9-Mo1-C8	37.6(3)
C6-C2-C3	108.1(7)	C4-C3-C2	108.4(7)
C5-C4-C3	108.9(7)	C6-C5-C4	107.6(6)
C5-C6-C2	107.0(7)	C8-C7-O2	126.4(6)
C11-C7-O2	128.1(6)	C11-C7-C8	105.3(6)
C9-C8-C7	107.7(6)	C12-C8-C7	124.2(6)
C12-C8-C9	125.7(6)	C10-C9-C8	106.8(6)
C13-C9-C8	117.4(6)	C13-C9-C10	121.1(6)
C11-C10-C9	108.1(6)	C14-C10-C9	125.5(6)
C14-C10-C11	126.3(6)	C10-C11-C7	109.8(6)
C15-C11-C7	122.2(6)	C15-C11-C10	125.7(6)
H131-C13-C9	109(4)	C'2-Mo2-C'1	114.5(3)
C'3-Mo2-C'1	138.5(3)	C'3-Mo2-C'2	36.0(3)
C'4-Mo2-C'1	113.0(3)	C'4-Mo2-C'2	59.3(3)
C'4-Mo2-C'3	35.5(3)	C'5-Mo2-C'1	81.2(3)
C'5-Mo2-C'2	59.6(3)	C'5-Mo2-C'3	59.2(3)
C'5-Mo2-C'4	35.0(3)	C'6-Mo2-C'1	81.7(3)
C'6-Mo2-C'2	35.6(3)	C'6-Mo2-C'3	59.5(3)

C'6-Mo2-C'4	59.0(3)	C'6-Mo2-C'5	36.0(3)
C'7-Mo2-C'1	77.1(3)	C'7-Mo2-C'2	115.4(2)
C'7-Mo2-C'3	134.9(3)	C'7-Mo2-C'4	169.7(2)
C'7-Mo2-C'5	152.5(2)	C'7-Mo2-C'6	122.9(2)
C'8-Mo2-C'1	70.9(3)	C'8-Mo2-C'2	148.7(2)
C'8-Mo2-C'3	150.6(3)	C'8-Mo2-C'4	149.9(2)
C'8-Mo2-C'5	147.2(3)	C'8-Mo2-C'6	146.7(2)
C'8-Mo2-C'7	33.5(2)	C'9-Mo2-C'1	103.9(3)
C'9-Mo2-C'2	138.7(3)	C'9-Mo2-C'3	115.4(3)
C'9-Mo2-C'4	118.8(3)	C'9-Mo2-C'5	145.2(3)
C'9-Mo2-C'6	174.3(3)	C'9-Mo2-C'7	58.2(2)
C'9-Mo2-C'8	37.4(2)	H132-C13-C9	124(5)
C'4-C'3-C'2	107.5(7)	C'5-C'4-C'3	108.7(6)
C'6-C'5-C'4	108.3(7)	C'5-C'6-C'2	107.7(6)
C'8-C'7-O'2	126.0(6)	C'11-C'7-0'2	128.5(6)
C'11-C'7-C'8	105.5(6)	C'9-C'8-C'7	108.5(6)
C'12-C'8-C'7	124.0(6)	C'12-C'8-C'9	125.5(6)
C'10-C'9-C'8	106.6(5)	C'13-C'9-C'8	118.8(6)
C'13-C'9-C'10	119.2(6)	C'11-C'10-C'9	107.6(6)

C'14-C'10-C'9	125.6(6)	C'14-C'10-C'11	126.6(6)
C'10-C'11-C'7	109.8(6)	C'15-C'11-C'7	121.9(6)
C'15-C'11-C'10	126.2(6)	H13a-C'13-C'9	120(4)
H13b-C'13-C'9	122(5)	H13b-C'13-H13a	113(6)

Table 3.6 Intermolecular distances (Å).

O1	...H41	2.80	1	-1.0	0.0	0.0
O1	...H14b	2.61	1	-1.0	1.0	0.0
O1	...H152	2.77	1	-1.0	1.0	0.0
O1	...H131	2.79	-1	2.0	-1.0	1.0
O2	...H31	2.30	1	-1.0	0.0	0.0
O2	...H142	2.59	1	-1.0	0.0	0.0
O2	...H'51	2.71	1	-1.0	0.0	0.0
O2	...H'21	2.41	2	1.0	0.0	0.0
O2	...H15c	2.91	2	1.0	0.0	0.0
C1	...H131	2.95	-1	2.0	-1.0	1.0
C2	...H'61	2.91	2	0.0	0.0	0.0
H21	...O'2	2.44	2	0.0	0.0	0.0
H21	...C'7	2.99	2	0.0	0.0	0.0
C3	...H'61	2.75	2	0.0	0.0	0.0
C4	...H14b	2.93	1	0.0	1.0	0.0

H51	...O'2	2.69	1	-1.0	1.0	0.0
C6	...H152	2.98	1	-1.0	1.0	0.0
H61	...C'2	2.88	2	1.0	0.0	0.0
H61	...C'3	2.75	2	1.0	0.0	0.0
C7	...H'21	2.94	2	1.0	0.0	0.0
C8	...H12b	2.82	-1	1.0	0.0	1.0
C9	...H12b	2.91	-1	1.0	0.0	1.0
H141	...C'13	3.00	-1	1.0	0.0	1.0
H143	...O'1	2.52	1	-1.0	0.0	0.0
H151	...O'2	2.96	2	0.0	0.0	0.0
H152	...O'2	2.90	2	0.0	0.0	0.0
H153	...O'1	2.86	1	-1.0	0.0	0.0
O'1	...H'41	2.79	1	1.0	0.0	0.0
O'1	...H13a	2.89	-1	0.0	0.0	1.0
O'2	...H'31	2.30	1	1.0	0.0	0.0
O'2	...H14c	2.58	1	1.0	0.0	0.0
H'41	...H13a	2.50	-1	1.0	0.0	1.0
H12c	...H13a	2.40	-1	0.0	0.0	1.0

Table 3.7 Intramolecular distances (Å).

Mo1	...C1	1.95	Mo1	...C2	2.30
Mo1	...C3	2.32	Mo1	...C4	2.33
Mo1	...C5	2.32	Mo1	...C6	2.32
Mo1	...C7	2.64	Mo1	...C8	2.33
Mo1	...C9	2.15	Mo1	...C10	2.25
Mo1	...C11	2.39	Mo1	...C13	2.34
O1	...H123	2.40	O2	...C8	2.44
O2	...C11	2.43	C1	...C5	2.80
C1	...H51	2.88	C1	...C6	2.83
C1	...H61	2.95	C1	...C7	2.87
C1	...C8	2.49	C1	...C12	2.89
C1	...H123	2.47	C2	...H31	2.23
C2	...C4	2.29	C2	...C5	2.31
C2	...H61	2.23	H21	...C3	2.23
H21	...C6	2.23	C3	...H41	2.21
C3	...C5	2.28	C3	...C6	2.30
C3	...H142	2.67	H31	...C4	2.22
H31	...C14	2.80	C4	...H51	2.22
C4	...C6	2.30	H41	...C5	2.21
H41	...H132	2.65	C5	...H61	2.27

H51	...C6	2.26	C7	...C9	2.36
C7	...C10	2.32	C7	...C12	2.62
C7	...H122	2.91	C7	...H123	2.91
C7	...C15	2.59	C7	...H152	2.88
C7	...H153	2.87	C8	...C10	2.33
C8	...C11	2.31	C8	...H121	2.12
C8	...H122	2.12	C8	...H123	2.12
C8	...C13	2.47	C8	...H131	2.56
C9	...C11	2.31	C9	...C12	2.63
C9	...H121	2.74	C9	...C14	2.63
C9	...H141	2.72	C9	...H131	2.06
C9	...H132	2.23	C10	...C13	2.51
C10	...H141	2.41	C10	...H142	2.13
C10	...H143	2.13	C10	...C15	2.61
C10	...H151	2.73	C10	...H132	2.88
C11	...C14	2.61	C11	...H142	2.91
C11	...H143	2.91	C11	...H151	2.14
C11	...H152	2.14	C11	...H153	2.14
C12	...H131	2.73	H121	...C13	2.82
H121	...H131	2.07	C13	...H141	2.91
C14	...H151	2.78	H141	...H132	2.49
H143	...C'4	2.83			

X-ray data for complex **4**.

Table 1.1 Fractional atomic co-ordinates and thermal parameters (Å).

Atom	x	y	z	Uiso or Ueq	(***)
Mo1	0.28522(4)	0.10146(4)	0.13345(2)	0.0330(3)	***
O1	0.2826(6)	-0.2125(5)	0.2066(2)	0.075(3)	***
O2	-0.1150(4)	-0.0089(4)	0.0886(1)	0.048(2)	***
C1	0.2834(6)	-0.0961(6)	0.1800(2)	0.047(3)	***
C2	0.5507(6)	0.1610(8)	0.1267(3)	0.058(3)	***
C3	0.4550(7)	0.2050(8)	0.0724(3)	0.062(4)	***
C4	0.3797(7)	0.0687(8)	0.0455(8)	0.065(4)	***
C5	0.4321(7)	-0.0613(7)	0.0815(3)	0.061(3)	***
C6	0.5358(6)	-0.0032(8)	0.1319(3)	0.059(4)	***
C7	-0.0073(6)	0.0990(5)	0.1144(2)	0.037(2)	***
C8	0.0566(5)	0.1204(6)	0.1761(2)	0.039(2)	***
C9	0.1527(6)	0.2640(6)	0.1812(2)	0.041(3)	***
C10	0.1395(6)	0.3292(6)	0.1215(2)	0.042(3)	***
C11	0.0443(5)	0.2226(5)	0.0814(2)	0.038(2)	***
C12	0.0067(8)	0.0282(8)	0.2257(2)	0.059(3)	***
C13	0.3087(7)	0.2604(7)	0.2175(3)	0.051(3)	***
C14	0.2058(7)	0.4870(6)	0.1063(3)	0.056(3)	***
C15	-0.0135(7)	0.2495(7)	0.0164(2)	0.053(3)	***
B1	0.7281(8)	-0.4071(7)	0.1123(3)	0.050(4)	***
F1	0.8329(5)	-0.2862(5)	0.1374(2)	0.081(3)	***
F2	0.5991(6)	-0.4048(6)	0.1404(3)	0.117(4)	***
F3	-0.1988(5)	0.4540(6)	0.1242(3)	0.123(4)	***

F4	0.6804(10)	-0.3791(9)	0.0558(2)	0.156(6)	***
H121	-0.0467(75)	-0.0848(40)	0.2136(29)	0.075(5)	
H122	0.0985(59)	0.0237(83)	0.2644(18)	0.075(5)	
H123	-0.1009(49)	0.0818(68)	0.2361(29)	0.075(5)	
H131	0.3267(76)	0.1928(67)	0.2581(17)	0.075(5)	
H132	0.3967(62)	0.3468(61)	0.2127(30)	0.075(5)	
H141	0.1193(60)	0.5715(58)	0.1156(29)	0.075(5)	
H142	0.2990(53)	0.5091(88)	0.1433(18)	0.075(5)	
H143	0.1965(77)	0.4697(83)	0.0597(10)	0.075(5)	
H151	-0.0374(79)	0.1304(36)	0.0007(29)	0.075(5)	
H152	0.0650(65)	0.3229(67)	-0.0030(27)	0.075(5)	
H153	-0.1331(37)	0.2946(71)	0.0126(27)	0.075(5)	
H2	-0.1341(90)	-0.1067(49)	0.1083(29)	0.075(5)	

Table 4.2 Fractional atomic co-ordinates for the hydrogen atoms.

Atom	x	y	z
H21	0.6222	0.2390	0.1582
H31	0.4418	0.3234	0.0544
H41	0.2955	0.0651	0.0041
H51	0.3989	-0.1834	0.0724
H61	0.5946	-0.0741	0.1687

Table 4.3 Anisotropic thermal parameters (Å).

Atom	U11	U22	U33	U23	U13	U12
Mo1	0.0303(3)	0.0348(3)	0.0340(3)	0.0000(2)	0.0076(2)	0.0025(2)
O1	0.088(3)	0.048(2)	0.087(3)	0.025(2)	0.022(2)	0.006(2)
O2	0.040(2)	0.052(2)	0.051(2)	-0.003(2)	0.007(1)	-0.010(2)
C1	0.043(3)	0.050(3)	0.047(3)	-0.004(2)	0.009(2)	0.003(2)
C2	0.038(3)	0.064(4)	0.073(4)	-0.004(3)	0.023(3)	-0.005(2)
C3	0.051(3)	0.064(4)	0.072(4)	0.018(3)	0.033(3)	0.006(3)
C4	0.049(3)	0.100(5)	0.045(3)	-0.001(3)	0.022(3)	0.007(3)
C5	0.052(3)	0.054(3)	0.076(4)	-0.006(3)	0.030(3)	0.015(3)
C6	0.036(3)	0.070(4)	0.071(4)	0.009(3)	0.010(3)	0.014(3)
C7	0.034(2)	0.039(3)	0.037(2)	-0.004(2)	0.010(2)	0.006(2)
C8	0.030(2)	0.048(3)	0.039(3)	-0.004(2)	0.014(2)	0.002(2)
C9	0.038(2)	0.043(3)	0.043(3)	-0.014(2)	0.009(2)	0.007(2)
C10	0.044(3)	0.031(2)	0.051(3)	-0.002(2)	0.013(2)	0.004(2)

C11	0.035(2)	0.040(2)	0.040(2)	-0.001(2)	0.004(2)	0.008(2)
C12	0.062(3)	0.074(4)	0.039(3)	0.000(3)	0.020(2)	-0.008(3)
C13	0.046(3)	0.057(3)	0.051(3)	-0.005(2)	0.005(2)	-0.007(2)
C14	0.062(4)	0.031(3)	0.075(4)	0.004(3)	0.003(3)	0.004(2)
C15	0.055(3)	0.060(3)	0.044(3)	0.010(3)	-0.004(2)	0.002(3)
B1	0.045(3)	0.049(4)	0.056(4)	0.003(3)	0.009(3)	0.007(3)
F1	0.086(3)	0.058(2)	0.100(3)	0.008(2)	0.005(2)	-0.025(2)
F2	0.082(3)	0.118(4)	0.150(5)	-0.036(3)	0.057(3)	-0.021(3)
F3	0.079(3)	0.049(2)	0.240(7)	-0.012(3)	0.007(4)	0.012(2)
F4	0.207(7)	0.199(7)	0.062(3)	0.011(3)	-0.015(4)	-0.063(5)

Table 4.4 Bond lengths (Å).

Mo1-C1	1.983(5)	Mo1-C2	2.311(5)
Mo1-C3	2.331(5)	Mo1-C4	2.303(6)
Mo1-C5	2.308(5)	Mo1-C6	2.284(5)
Mo1-C7	2.414(5)	Mo1-C8	2.300(4)
Mo1-C9	2.176(4)	Mo1-C10	2.271(5)
Mo1-C11	2.389(4)	Mo1-C13	2.328(6)
O1-C1	1.158(6)	O2-C7	1.345(6)
O2-H2	0.967(19)	C2-C3	1.408(9)
C2-C6	1.401(9)	C3-C4	1.403(9)
C4-C5	1.398(9)	C5-C6	1.408(9)
C7-C8	1.433(7)	C7-C11	1.400(7)
C8-C9	1.450(7)	C8-C12	1.496(7)
C9-C10	1.461(7)	C9-C13	1.423(7)
C10-C11	1.427(7)	C10-C14	1.508(8)
C11-C15	1.502(7)	C12-H121	1.071(19)
C12-H122	1.069(19)	C12-H123	1.072(19)
C13-H131	1.078(19)	C13-H132	1.057(19)
C14-H141	1.065(19)	C14-H142	1.066(19)
C14-H143	1.065(19)	C15-H151	1.076(19)
C15-H151	1.057(19)	C15-H153	1.061(19)
B1-F1	1.404(7)	B1-F2	1.350(8)
B1-F3	1.331(7)	B1-F4	1.310(8)
F1-H2	1.699(21)		

Table 4.5 Bond angles (°).

C2-Mo1-C1	108.4(2)	C3-Mo1-C1	134.5(2)
C3-Mo1-C2	35.3(2)	C4-Mo1-C1	113.9(2)
C4-Mo1-C2	59.2(2)	C4-Mo1-C3	35.2(2)
C5-Mo1-C1	80.2(2)	C5-Mo1-C2	59.4(2)
C5-Mo1-C3	58.6(2)	C5-Mo1-C4	35.3(2)
C6-Mo1-C1	77.0(2)	C6-Mo1-C2	35.5(2)
C6-Mo1-C3	58.6(2)	C6-Mo1-C4	59.0(2)
C6-Mo1-C5	35.7(2)	C7-Mo1-C1	89.3(2)
C7-Mo1-C2	161.5(2)	C7-Mo1-C3	126.9(2)
C7-Mo1-C4	109.4(2)	C7-Mo1-C5	121.1(2)
C7-Mo1-C6	154.3(2)	C8-Mo1-C1	75.3(2)
C8-Mo1-C2	153.5(2)	C8-Mo1-C3	150.2(2)
C8-Mo1-C4	144.7(2)	C8-Mo1-C5	144.8(2)
C8-Mo1-C6	150.2(2)	C8-Mo1-C7	35.3(2)
C9-Mo1-C1	102.1(2)	C9-Mo1-C2	118.5(2)
C9-Mo1-C3	118.8(2)	C9-Mo1-C4	142.9(2)
C9-Mo1-C5	177.4(2)	C9-Mo1-C6	143.4(2)
C9-Mo1-C7	60.4(2)	C9-Mo1-C8	37.7(2)
H2-O2-C7	122(4)	C6-C2-C3	107.0(6)
C4-C3-C2	108.3(6)	C5-C4-C3	108.4(6)
C6-C5-C4	107.2(6)	C5-C6-C2	109.1(6)
C8-C7-O2	128.7(4)	C10-C7-O2	156.6(4)
C11-C7-O2	121.1(4)	C11-C7-C8	109.8(4)
C9-C8-C7	107.0(4)	C12-C8-C7	125.3(5)
C12-C8-C9	126.8(5)	C10-C9-C8	106.8(4)

C13-C9-C8	118.0(5)	C13-C9-C10	117.9(5)
C9-C10-C7	72.5(3)	C11-C10-C9	107.8(4)
C14-C10-C7	161.5(4)	C14-C10-C9	125.3(5)
C14-C10-C11	126.7(5)	C10-C11-C7	108.4(4)
C15-C11-C7	124.8(4)	C15-C11-C10	126.2(4)
H121-C12-C8	115(4)	H122-C12-C8	113(4)
H123-C12-H121	96(5)	H123-C12-H122	110(5)
H131-C13-C9	119(3)	H132-C13-C9	121(4)
H132-C13-H131	117(5)	H141-C14-C10	105(3)
H142-C14-C10	103(4)	H142-C14-H141	99(5)
H143-C14-C10	98(4)	H143-C14-H141	111(5)
H143-C14-H142	137(5)	H151-C15-C11	101(4)
H152-C15-C11	113(4)	H152-C15-H151	120(5)
H153-C15-C11	106(3)	H153-C15-H151	101(5)
H153-C15-H152	114(5)	F2-B1-F1	106.9(5)
F3-B1-F1	109.0(5)	F3-B1-F2	107.1(6)
F4-B1-F1	109.5(5)	F4-B1-F2	109.7(6)
F4-B1-F3	114.3(7)	H2-F1-B1	129(2)
F1-H2-O2	175(7)		

Table 4.6 Intermolecular distances (Å).

H151	...H151	2.29	-1	0.0	0.0	0.0
O1	...H141	2.93	1	0.0	1.0	0.0
O1	...H142	2.78	1	0.0	1.0	0.0
O1	...H123	2.78	-2	0.0	1.0	1.0
O2	...F1	2.66	1	1.0	0.0	0.0
O2	...H41	2.43	-1	0.0	0.0	0.0
O2	...H151	2.79	-1	0.0	0.0	0.0
H21	...F3	2.56	1	-1.0	0.0	0.0
H31	...F4	2.60	-1	1.0	0.0	0.0
H61	...C13	2.94	-2	1.0	1.0	1.0
H61	...H131	2.60	-2	1.0	1.0	1.0
C9	...H121	2.99	-2	0..0	0.0	1.0
B1	...H2	2.80	1	-1.0	0.0	0.0
B1	...H122	3.00	-2	1.0	1.0	1.0
F1	...F3	2.23	1	-1.0	1.0	0.0
F1	...H121	2.52	1	-1.0	0.0	0.0
F1	...H141	2.80	1	-1.0	1.0	0.0
F1	...H122	2.74	-2	1.0	1.0	1.0
F1	...H131	2.94	-2	10.	10.	1.0
F2	...F3	2.16	1	-1.0	1.0	0.0
F2	...H142	2.63	1	0.0	1.0	0.0
F2	...H131	2.44	-2	1.0	1.0	1.0
F2	...H131	2.44	-2	1.0	1.0	1.0
F3	...F4	2.22	1	1.0	-1.0	0.0
F3	...H122	2.61	-2	0.0	0.0	1..0

F4	...H2	2.92	1	-1.0	0.0	0.0
F4	...H152	2.67	-1	1.0	0.0	0.0
H143	...H153	2.59	-1	0.0	1.0	0.0
H151	...H151	2.29	-1	0.0	0.0	0.0

Table 4.7 Intramolecular distances (Å).

Mo1	...H41	2.99	Mo1	...H61	2.97
O1	...H121	2.99	O1	...H122	2.97
O2	...C8	2.51	O2	...C11	2.39
O2	...C15	2.95	O2	...H121	2.89
O2	...H151	2.51	C1	...C5	2.77
C1	...H51	2.90	C1	...C6	2.66
C1	...H61	2.67	C1	...C8	2.63
C1	...C12	2.90	C1	...H121	3.00
C1	...H122	2.86	C2	...H31	2.22
C2	...H61	2.21	C2	...H132	2.98
H21	...C3	2.23	H21	...C6	2.22
H21	...H132	2.60	C3	...H41	2.21
H31	...C4	2.22	H31	...C4	2.84
H31	..H143	2.42	C4	...H51	2.22
H41	...C5	2.21	C5	...H61	2.22
H51	...C6	2.23	H51	...F2	2.80
H51	...F4	2.96	H61	...F1	2.86
H61	...F2	2.87	C7	...C9	2.32
C7	...C12	2.60	C7	...C15	2.57
C7	...H121	2.82	C7	...H151	2.59
C7	...H153	2.90	C7	...H2	2.03
C8	...C10	2.34	C8	...C11	2.32
C8	...C13	2.46	C8	...H121	2.18
C8	...H122	2.15	C8	...H123	2.09
C8	...H131	2.75	C8	...H2	2.79

C9	...C11	2.33	C9	...C12	2.63
C9	...C14	2.64	C9	...H122	2.87
C9	...H131	2.17	C9	...H132	2.16
C9	...H141	2.99	C9	...H142	2.63
C10	...C13	2.47	C10	...C15	2.61
C10	...H132	2.73	C10	...H141	2.06
C10	...H142	2.03	C10	...H143	1.97
C10	...H152	2.81	C11	...C14	2.62
C11	...H143	2.54	C11	...H151	2.01
C11	...H152	2.15	C11	...H153	2.06
C12	...H131	3.00	C12	...H2	2.97
C13	...H122	2.98	C13	...H142	2.70
C14	...H132	2.93	C14	...H152	2.93
C15	...H143	2.64	F1	...F2	2.21
F1	...F4	2.22	F2	...F4	2.17
F3	...H141	2.88	H121	...H122	1.78
H121	...H123	1.59	H121	...H2	2.40
H122	...H123	1.76	H122	...H131	2.41
H131	...H132	1.82	H132	...H142	2.15
H141	...H142	1.62	H141	...H143	1.76
H142	...H143	1.99	H143	...H152	2.07
H151	...H152	1.85	H151	...H153	1.65
H152	...H153	1.77			

X-ray data for complex **5**.

Table 5.1 Fractional atomic co-ordinates ($x10^4$) and equivalent isotropic temperature factors ($Å^2 x10^3$).

Atom	x	y	z	U
Re1	1791.1(3)	3.657.1(2)	2068.8(2)	39.5(2)
Br1	2088(1)	5696(1)	1633(1)	66.2(4)
C1	-495(8)	3474(9)	2007(8)	66(4)
C2	-9(8)	2301(7)	1902(7)	60(4)
C3	291(7)	1995(7)	951(7)	54(3)
C4	59(8)	2969(8)	494(7)	60(4)
C5	-435(8)	3875(9)	1131(7)	63(4)
C6	2109(7)	4696(6)	3635(6)	44(3)
C7	2389(7)	3602(6)	3672(6)	42(3)
C8	3076(6)	2411(6)	1862(5)	37(3)
C9	3562(7)	3455(6)	1786(6)	42(3)
C10	2073(8)	5858(7)	4354(6)	49(3)
C11	1444(10)	6820(7)	3999(8)	66(4)
C12	1409(12)	7879(9)	4734(10)	89(6)
C13	2015(12)	8026(9)	5827(9)	86(6)
C14	2625(11)	7083(10)	6191(8)	84(5)
C15	2647(9)	6016(8)	5470(7)	60(4)
C16	2815(7)	2739(6)	4315(6)	44(3)
C17	1926(9)	2211(8)	4697(7)	63(4)
C18	2366(14)	1394(10)	5314(8)	90(6)
C19	3628(14)	1143(9)	5592(8)	89(5)
C20	4500(12)	1658(10)	5241(9)	90(6)

C21	4100(9)	2454(8)	4593(7)	67(4)
C22	3351(7)	1155(7)	1838(6)	47(3)
C23	2618(8)	354(6)	2150(7)	55(3)
C24	2922(9)	-805(8)	2130(8)	69(5)
C25	3947(10)	-1216(8)	1785(8)	78(5)
C26	4673(9)	-438(8)	1483(9)	76(5)
C27	4382(8)	730(7)	1512(7)	57(4)
C28	4633(7)	4108(6)	1633(6)	42(3)
C29	5089(8)	3573(7)	819(7)	55(4)
C30	6143(8)	4198(9)	691(8)	67(4)
C31	6761(8)	5314(8)	1381(9)	69(5)
C32	6331(8)	5838(8)	2221(8)	66(4)
C33	5265(8)	5245(7)	2351(7)	54(3)
P1	-1322(2)	8935(2)	1820(2)	64(1)
F1	-320(7)	9773(6)	2919(5)	124(4)
F2	-582(7)	7784(6)	1910(6)	118(4)
F3	-2330(7)	8173(7)	706(5)	125(3)
F4	-2072(7)	10133(6)	1705(7)	124(4)
F5	-2282(8)	8596(6)	2368(6)	127(5)
F6	-483(7)	9356(6)	1199(6)	115(3)

Table 5.2 Fractional atomic co-ordinates (x 10^4).

	x	y	z
Re1	1791.1(3)	3657.1(2)	2068.8(2)
Br1	2088(1)	5696(1)	1633(1)
C1	-495(8)	3474(9)	2007(8)
C2	-9(8)	2301(7)	1902(7)
C3	291(7)	1995(7)	951(7)
C4	59(8)	2969(8)	494(7)
C5	-435(8)	3875(9)	1131(7)
C6	2109(7)	4696(6)	3635(6)
C7	2389(7)	3602(6)	3672(6)
C8	3076(6)	2411(6)	1862(5)
C9	3526(7)	3455(6)	1786(6)
C10	2073(8)	5858(7)	4354(6)
C11	1444(10)	6820(7)	3999(8)
C12	1409(12)	7879(9)	4734(10)
C13	2015(12)	8026(9)	5827(9)
C14	2625(11)	7083(10)	6191(8)
C15	2647(9)	6016(8)	5470(7)
C16	2815(7)	2739(6)	4315(6)
C17	1926(9)	2211(8)	4697(7)
C18	2366(14)	1394(10)	5314(8)
C19	3628(14)	1143(9)	5592(8)
C20	4500(12)	1658(10)	5241(9)
C21	4100(9)	2454(8)	4593(7)
C22	3351(7)	1155(7)	1838(6)

C23	2618(8)	354(6)	2150(7)
C24	2922(9)	-805(8)	2130(8)
C25	3947(10)	-1216(8)	1785(8)
C26	4673(9)	-438(8)	1483(9)
C27	4382(8)	730(7)	1512(7)
C28	4633(7)	4108(6)	1633(6)
C29	5098(8)	3573(7)	819(7)
C30	6143(8)	4198(9)	691(8)
C31	6761(8)	5314(8)	1381(9)
C32	6331(8)	5838(8)	2221(8)
C33	5265(8)	5245(7)	2351(7)
P1	-1322(2)	8935(2)	1820(2)
F1	-320(7)	9773(6)	2919(5)
F2	-582(7)	7784(6)	1910(6)
F3	-2330(7)	8173(7)	706(5)
F4	-2072(7)	10133(6)	1705(7)
F5	-2282(8)	8596(6)	2368(6)
F6	-483(7)	9356(6)	1199(6)

Table 5.3 Anisotropic temperature factors (Å x10^3).

Atom	U11	U22	U33	U23	U13	U12
Re1	42.2(2)	35.0(2)	41.6(2)	16.1(1)	20.0(1)	8.1(2)
Br1	73.1(5)	48.4(5)	77.5(6)	37.4(4)	41.2(5)	21.2(4)
C1	39(4)	94(7)	72(6)	24(5)	27(4)	13(4)
C2	51(5)	53(5)	75(6)	14(4)	26(4)	-2(4)
C3	47(4)	49(4)	59(5)	9(4)	15(4)	2(4)
C4	55(5)	70(6)	51(5)	13(4)	16(4)	7(4)
C5	41(4)	77(6)	71(6)	31(5)	14(4)	14(4)
C6	51(4)	41(4)	47(4)	17(3)	22(3)	9(3)
C7	49(4)	43(4)	37(4)	12(3)	18(3)	0(3)
C8	41(4)	38(4)	34(4)	10(3)	15(3)	8(3)
C9	45(4)	38(4)	44(4)	11(3)	18(3)	10(3)
C10	58(5)	46(4)	48(4)	14(3)	25(4)	10(4)
C11	92(7)	44(5)	67(6)	15(4)	33(5)	19(4)
C12	128(9)	55(6)	114(9)	25(6)	76(8)	38(6)
C13	115(9)	60(6)	85(8)	-1(6)	54(7)	16(6)
C14	91(7)	93(8)	54(6)	-2(5)	25(5)	-1(6)
C15	70(5)	54(5)	59(5)	13(4)	28(4)	7(4)
C16	55(4)	38(4)	42(4)	12(3)	18(3)	5(3)
C17	79(6)	67(6)	50(5)	25(4)	26(4)	3(5)
C18	135(11)	77(7)	71(7)	46(6)	37(7)	-6(7)
C19	135(11)	60(6)	61(6)	30(5)	10(7)	19(7)
C20	89(8)	83(7)	88(8)	39(6)	5(6)	35(6)
C21	68(6)	71(6)	74(6)	36(5)	28(5)	20(5)

C22	46(4)	42(4)	49(4)	11(3)	13(3)	5(3)
C23	55(5)	34(4)	76(6)	18(4)	23(4)	2(3)
C24	72(6)	45(5)	93(7)	25(5)	28(5)	2(4)
C25	82(7)	43(5)	96(8)	15(5)	17(6)	20(5)
C26	63(6)	56(6)	114(8)	20(5)	38(6)	24(5)
C27	55(5)	46(4)	73(6)	11(4)	27(4)	8(4)
C28	43(4)	35(4)	49(4)	12(3)	18(3)	3(3)
C29	52(5)	53(5)	66(5)	15(4)	32(4)	1(4)
C30	63(5)	74(6)	79(6)	22(5)	43(5)	9(5)
C31	45(5)	61(6)	109(8)	32(5)	31(5)	1(4)
C32	46(5)	46(5)	94(7)	18(5)	9(5)	-9(4)
C33	59(5)	47(4)	55(5)	15(4)	17(4)	3(4)
P1	61(1)	66(1)	61(1)	4(1)	26(1)	-12(1)
F1	136(6)	114(5)	73(4)	-9(4)	-2(4)	-5(4)
F2	131(5)	100(5)	131(6)	43(4)	45(5)	49(4)
F3	109(5)	127(5)	91(4)	-4(4)	4(4)	-39(4)
F4	118(5)	99(5)	174(7)	48(5)	67(5)	25(4)
F5	152(6)	121(5)	152(6)	41(5)	110(5)	-1(4)
F6	143(6)	89(4)	129(5)	4(4)	89(5)	-20(4)

Table 5.4 Hydrogen fractional atomic co-ordinates (x 10^4) and isotropic temperature factors ($Å^2$ x10^3).

	x	y	z	U
H11	-801(8)	3898(9)	2570(8)	86(6)
H21	93(8)	1808(7)	2401(7)	86(6)
H31	601(7)	1245(7)	669(7)	86(6)
H41	209(8)	3021(8)	-153(7)	86(6)
H51	-687(8)	4640(9)	985(7)	86(6)
H111	1036(10)	6737(7)	3238(8)	86(6)
H121	956(12)	8526(9)	4484(10)	86(6)
H131	2014(12)	8783(9)	6336(9)	86(6)
H141	3036(11)	7179(10)	6954(8)	86(6)
H151	3063(9)	5360(8)	5732(7)	86(6)
H171	1031(9)	2410(8)	4533(7)	86(6)
H181	1752(14)	998(10)	5549(8)	86(6)
H191	3914(14)	595(9)	6041(8)	86(6)
H201	5402(12)	1474(10)	5442(9)	86(6)
H211	4720(9)	2805(8)	4337(7)	86(6)
H231	1897(8)	628(6)	2379(7)	86(6)
H241	2424(9)	-1344(8)	2355(8)	86(6)
H251	4149(10)	-2042(8)	1758(8)	86(6)
H261	5390(9)	-718(8)	1252(9)	86(6)
H271	4900(8)	1267(7)	1301(7)	86(6)
H291	4685(8)	2773(7)	342(7)	86(6)
H301	6439(8)	3837(9)	105(8)	86(6)
H311	7490(8)	5733(8)	1284(9)	86(6)

H321	6773(8)	6618(8)	2717(8)	86(6)
H331	4963(8)	5615(7)	2933(7)	86(6)

Table 5.5 Bond lengths (Å).

Br-Re	2.545(4)	C1-Re1	2.426(11)
C2-Re1	2.333(11)	C3-Re1	2.277(9)
C4-Re1	2.255(9)	C5-Re1	2.361(10)
C6-Re1	2.072(9)	C7-Re1	2.074(9)
C8-Re1	2.041(9)	C9-Re1	2.031(10)
C2-C1	1.432(14)	C5-C1	1.392(17)
C3-C2	1.400(15)	C4-C3	1.381(15)
C5-C4	1.410(14)	C7-C6	1.290(11)
C10-C6	1.442(11)	C16-C7	1.451(12)
C9-C8	1.296(12)	C22-C8	1.454(11)
C28-C9	1.473(12)	C11-C10	1.401(13)
C15-C10	1.397(12)	C12-C11	1.369(15)
C13-C12	1.375(18)	C14-C13	1.377(17)
C15-C14	1.362(14)	C17-C16	1.403(15)
C21-C16	1.377(13)	C18-C17	1.387(16)
C19-C18	1.342(21)	C20-C19	1.353(22)
C21-C20	1.389(17)	C23-C22	1.403(14)
C27-C22	1.382(14)	C24-C23	1.356(13)
C25-C24	1.385(17)	C26-C25	1.371(18)
C27-C26	1.359(14)	C29-C28	1.372(13)
C33-C28	1.395(10)	C30-C29	1.392(15)
C31-C30	1.362(12)	C32-C31	1.381(17)

C33-C32	1.387(15)	F1-P1	1.567(8)
F2-P1	1.557(9)	F3-P1	1.553(8)
F4-P1	1.613(10)	F5-P1	1.542(12)
F6-P1	1.554(11)	H11-C1	0.960(15)
H21-C2	0.960(16)	H31-C3	0.960(13)
H41-C4	0.960(16)	H51-C5	0.960(15)
H111-C11	0.960(14)	H121-C12	0.960(17)
H131-C13	0.960(16)	H141-C14	0.960(15)
H151-C15	0.960(14)	H171-C17	0.960(15)
H181-C8	0.960(22)	H191-C19	0.960(18)
H201-C20	0.960(18)	H211-C21	0.960(17)
H231-C23	0.960(14)	H241-C24	0.960(17)
H251-C25	0.960(14)	H261-C26	0.960(17)
H271-C27	0.960(15)	H291-C29	0.960(11)
H301-C30	0.960(16)	H311-C31	0.960(16)
H321-C32	0.960(11)	H331-C33	0.960(14)

Table 5.6 Bond angles (°).

C1-Re1-Br1	103.5(4)	C2-Re1-Br1	135.9(2)
C2-Re1-C1	35.0(3)	C3-Re1-Br1	125.2(3)
C3-Re1-C1	58.5(4)	C3-Re1-C2	35.3(3)
C4-Re1-Br1	89.9(4)	C4-Re1-C1	57.9(4)
C4-Re1-C2	58.4(5)	C4-Re1-C3	35.5(3)
C5-Re1-Br1	78.7(4)	C5-Re1-C1	33.8(4)
C5-Re1-C2	57.6(4)	C5-Re1-C3	58.7(4)
C5-Re1-C4	35.5(3)	C6-Re1-Br1	86.5(3)
C6-Re1-C1	81.8(4)	C6-Re1-C2	97.0(4)
C6-Re1-C3	132.3(3)	C6-Re1-C4	137.4(3)
C6-Re1-C5	102.7(4)	C7-Re1-Br1	119.7(3)
C7-Re1-C1	88.3(4)	C7-Re1-C2	82.4(4)
C7-Re1-C3	111.5(4)	C7-Re1-C4	140.6(3)
C7-Re1-C5	120.6(4)	C7-Re1-C6	36.2(3)
C8-Re1-Br1	118.5(3)	C8-Re1-C1	133.7(3)
C8-Re1-C2	98.8(4)	C8-Re1-C3	80.7(4)
C8-Re1-C4	101.4(4)	C8-Re1-C5	136.3(3)
C8-Re1-C6	117.4(4)	C8-Re1-C7	87.2(4)
C9-Re1-Br1	81.9(3)	C9-Re1-C1	165.8(3)
C9-Re1-C2	134.7(3)	C9-Re1-C3	107.6(4)
C9-Re1-C4	109.6(4)	C9-Re1-C5	139.0(3)
C9-Re1-C6	111.9(4)	C9-Re1-C7	100.4(4)
C9-Re1-C8	37.1(3)	C5-C1-C2	106.4(10)
C3-C2-C1	108.7(10)	C4-C3-C2	107.4(9)
C5-C4-C3	109.1(10)	C4-C5-C1	108.4(10)

C10-C6-C7	139.6(8)	C16-C7-C6	148.4(7)
C22-C8-C9	143.9(8)	C28-C9-C8	144.2(7)
C11-C10-C6	123.7(8)	C15-C10-C6	118.3(8)
C15-C10-C11	117.9(8)	C12-C11-C10	120.3(10)
C13-C12-C11	120.6(11)	C14-C13-C12	119.8(11)
C15-C14-C13	120.2(10)	C14-C15-C10	121.1(10)
C17-C16-C7	120.1(8)	C21-C16-C7	121.1(9)
C21-C16-C17	118.8(9)	C18-C17-C16	118.7(11)
C19-C18-C17	121.7(14)	C20-C19-C18	120.2(12)
C21-C20-C19	120.4(12)	C20-C21-C16	120.2(11)
C23-C22-C8	122.4(8)	C27-C22-C8	119.4(9)
C27-C22-C23	118.3(8)	C24-C23-C22	120.4(10)
C25-C24-C23	120.3(11)	C26-C25-C24	119.7(10)
C27-C26-C25	120.3(11)	C26-C27-C22	121.0(11)
C29-C28-C9	120.2(7)	C33-C28-C9	119.9(8)
C33-C28-C29	119.8(9)	C30-C29-C28	119.4(8)
C31-C30-C29	121.3(11)	C32-C31-C30	119.4(11)
C33-C32-C31	120.4(8)	C32-C33-C28	119.6(9)
F2-P1-F1	93.7(5)	F3-P1-F1	176.6(4)
F3-P1-F2	89.2(5)	F4-P1-F1	86.5(5)
F4-P1-F2	178.6(5)	F4-P1-F3	90.5(5)
F5-P1-F1	92.2(5)	F5-P1-F2	94.2(6)
F5-P1-F3	89.2(5)	F5-P1-F4	87.2(6)
F6-P1-F1	90.4(5)	F6-P1-F2	91.7(5)
F6-P1-F3	87.9(5)	F6-P1-F4	86.9(5)
F6-P1-F5	173.4(4)	C2-C1-H11	126.8(14)
C5-C1-H11	126.8(13)	H21-C2-C1	125.6(12)

C3-C2-H21	125.6(11)	H31-C3-C2	126.3(12)
C4-C3-H31	126.3(12)	H41-C4-C3	125.4(12)
C5-C4-H41	125.5(12)	H51-C5-C1	125.8(12)
H51-C5-C4	125.8(13)	H111-C11-C10	119.9(10)
C12-C11-H111	119.9(12)	H121-C12-C11	119.7(15)
C13-C12-C121	119.7(14)	H131-C13-C12	120.1(14)
C14-C13-H131	120.1(14)	H141-C14-C13	119.9(13)
C15-C14-H141	119.9(14)	H151-C15-C10	119.4(10)
H151-C15-C14	119.4(11)	H171-C17-C16	120.7(12)
C18-C17-H171	120.7(14)	H181-C18-C17	119.2(16)
C19-C18-H181	119.1(15)	H191-C19-C18	119.9(19)
C20-C19-H191	119.9(18)	H201-C20-C19	119.8(16)
C21-C20-H201	119.8(16)	H211-C21-C16	119.9(12)
H211-C21-C20	119.9(12)	H231-C23-C22	119.8(10)
C24-C23-H231	119.8(12)	H241-C24-C23	119.9(13)
C25-C24-H241	119.9(12)	H251-C25-C24	120.1(15)
C26-C25-H251	120.1(15)	H261-C26-C25	119.8(12)
C27-C26-H261	119.8(14)	H271-C27-C22	119.5(11)
H271-C27-C26	119.5(12)	H291-C29-C28	120.3(12)
C30-C29-H291	120.3(12)	H301-C30-C29	119.4(10)
C31-C30-H301	119.4(13)	H311-C31-C30	120.3(13)
C32-C31-H311	120.3(11)	H321-C32-C31	119.8(13)
C33-C32-H321	119.8(13)	H331-C33-C28	120.2(11)
H331-C33-C32	120.2(9)		

Table 5.7 Selected non-bonded distances (Å).

Intramolecular:

H11	...Re1	3.081	H21	...Re1	2.931
H31	...Re1	2.876	H41	...Re1	2.824
H51	...Re1	2.983	C10	...Re1	3.386
C16	...Re1	3.317	C22	...Re1	3.338
C28	...Re1	3.337	H21	...C1	2.139
C3	...C1	2.301	C4	...C1	2.272
H51	...C1	2.103	C6	...C1	2.956
C7	...C1	3.145	C2	...H11	2.149
C5	...H11	2.112	H31	...C2	2.115
C4	...C2	2.240	C5	...C2	2.260
C7	...C2	2.909	C3	...H21	2.109
H41	...C3	2.089	C5	...C3	2.274
C8	...C3	2.802	C4	...H31	2.097
C8	...H31	2.695	H51	...C4	2.120
C5	...H41	2.117	C11	...C6	2.507
H111	...C6	2.705	C15	...C6	2.437
H151	...C6	2.589	C16	...C6	2.638
C8	...C7	2.839	C9	...C7	3.155
C10	...C7	2.564	C15	...C7	3.117
C17	...C7	2.473	H171	...C7	2.656
C21	...C7	2.463	H211	...C7	2.638
C23	...C8	2.503	H231	...C8	2.687
C27	...C8	2.448	H271	...C8	2.604

C28	...C8	2.635	C22	...C9	2.614
C29	...C9	2.467	H291	...C9	2.634
C33	...C9	2.483	H331	...C9	2.650
H111	...C10	2.055	C12	...C10	2.402
C13	...C10	2.776	C14	...C10	2.403
H151	...C10	2.048	H121	...C11	2.024
C13	...C11	2.384	C14	...C11	2.758
C15	...C11	2.397	C12	...H111	2.026
H121	...H111	2.323	F2	...H111	2.604
H131	...C12	2.033	C14	...C12	2.382
C15	...C12	2.746	C13	...H121	2.030
H131	...H121	2.332	H141	...C13	2.034
C15	...C13	2.374	C14	...H131	2.036
H141	...H131	2.337	H151	...C14	2.015
C15	...H141	2.020	H151	...H14	2.313
H171	...C16	2.065	C18	...C16	2.399
C19	...C16	2.766	C20	...C16	2.398
H211	...C16	2.034	H181	...C17	2.035
C19	...C17	2.383	C20	...C17	2.752
C21	...C17	2.393	C18	...H171	2.050
H181	...H171	2.344	H191	...C18	2.001
C20	...C18	2.336	C21	...C18	2.731
C19	...H181	1.994	H191	...H181	2.288
H201	...C19	2.011	C21	...C19	2.379
C20	...H191	2.011	H201	...H191	2.308
H211	...C20	2.044	C21	...H201	2.044
H211	...H201	2.344	H231	...C22	2.056

C24	...C22	2.394	C25	...C22	2.764
C26	...C22	2.387	H271	...C22	2.034
H241	...C23	2.014	C25	...C23	2.377
C26	...C23	2.748	C27	...C23	2.391
C24	...H231	2.014	H241	...H231	2.312
H251	...C24	2.043	C26	...C24	2.383
C27	...C24	2.744	C25	...H241	2.040
H251	...H241	2.345	H261	...C25	2.028
C27	...C25	2.369	C26	...H251	2.031
H261	...H251	2.331	H271	...C26	2.014
C27	...H261	2.017	H271	...H261	2.310
H291	...H271	2.355	H291	...C28	2.033
C30	...C28	2.387	C31	...C28	2.774
C32	...C28	2.404	H331	...C28	2.053
H301	...C29	2.042	C31	...C29	2.400
C32	...C29	2.762	C33	...C29	2.394
C30	...H291	2.051	H301	...H291	2.347
H311	...C30	2.024	C32	...C30	2.368
C33	...C30	2.751	C31	...H301	2.015
H311	...H301	2.317	H321	...C31	2.036
C33	...C31	2.401	C32	...H311	2.041
H321	...H311	2.342	H331	...C32	2.045
C33	...H321	2.041	H331	...H321	2.346
F2	...F1	2.280	F4	...F1	2.180
F5	...F1	2.24	F6	...F1	2.214
F3	...F2	2.185	F5	...F2	2.271
F6	...F2	2.232	F4	...F3	2.248

F5	...F3	2.173	F6	...F3	2.155
F5	...F4	2.175	F6	...F4	2.178

Intermolecular:

F1	...H21a	2.622	F6	...C3b	3.026
F6	...H31b	2.420	F2	...H41b	2.508
F4	...H131c	2.623	F5	...H181d	2.614
F6	...H231a	2.655	F4	...H261d	2.669
F3	...H291b	2.496	F5	...H321f	2.627

Key to symmetry operations relating designated atoms to reference atoms at (x, y, z):

(a) x, 1.0=y, z

(b) -x, 1.0-y, -z

(c) -x, 2.0-y, 1.0-z

(d) -x, 1.0-y, 1.0-z

(e) -1.0+x, 1.0+y, z

(f) -1.0+x, y, z

X-ray data for complex **7**.

Table 7.1 Fractional atomic co-ordinates ($x10^4$) and equivalent isotropic temperature factors ($Å^2 x10^3$).

Atom	x	y	z	U
Re1	891	7428	2173	30
Br1	1861(1)	8849	1928	48
C1	1628(6)	6101(4)	2187(4)	51(2)
C2	2723(6)	6609(4)	2045(4)	55(2)
C3	2989(6)	7103(5)	2765(5)	58(3)
C4	2084(6)	6919(4)	3361(4)	56(3)
C5	1229(6)	6305(4)	3006(4)	51(2)
C6	-51(5)	7131(3)	1108(3)	35(2)
C7	-964(5)	7690(3)	1436(3)	29(2)
C8	-1166(5)	7467(3)	2338(3)	30(2)
C9	-592(5)	8114(3)	2897(3)	32(2)
C10	-21(5)	6697(3)	299(3)	35(2)
C11	1162(6)	6495(4)	-38(4)	55(3)
C12	1160(7)	6081(4)	-798(4)	63(3)
C13	5(7)	5875(4)	-1242(4)	60(3)
C14	-1162(6)	6070(4)	-928(4)	56(2)
C15	-1184(6)	6480(4)	-162(3)	42(2)
C16	-1523(5)	8440(3)	1008(3)	31(2)
C17	-939(6)	8805(3)	331(4)	43(2)
C18	-1530(7)	9469(4)	-111(4)	58(3)
C19	-2701(8)	9769(4)	119(5)	66(3)
C20	-3299(7)	9430(4)	785(5)	62(3)

C21	-2705(6)	8751(4)	1229(4)	45(2)
C22	-2056(5)	6787(3)	2533(3)	29(2)
C23	-2056(5)	6001(3)	2153(3)	38(2)
C24	-2991(6)	5417(4)	2301(4)	44(2)
C25	-3956(6)	5579(4)	2826(4)	46(2)
C26	-3976(5)	6339(4)	3213(4)	43(2)
C27	-3059(5)	6943(4)	3059(3)	37(2)
C28	-398(5)	8118(4)	3840(3)	35(2)
C29	89(5)	8837(4)	4225(4)	44(2)
C30	395(6)	8866(5)	5099(4)	55(3)
C31	225(6)	8189(5)	5599(4)	57(3)
C32	-283(6)	7477(5)	5234(4)	55(2)
C33	-580(6)	7436(4)	4366(4)	44(2)

Table 7.2 Fractional atomic co-ordinates ($x10^4$).

	x	y	z
Re1	891	7248	2173
Br1	1861(1)	8849	1918
C1	1628(6)	6101(4)	2187(4)
C2	2723(6)	6609(4)	2045(4)
C3	2989(6)	7103(5)	2765(5)
C4	2084(6)	6919(4)	3361(4)
C5	1229(6)	6305(4)	3006(4)
C6	-51(5)	7131(3)	1108(3)
C7	-964(5)	7690(3)	1436(3)
C8	-1166(5)	7467(3)	2338(3)
C9	-592(5)	8114(3)	2897(3)
C10	-21(5)	6697(3)	299(3)
C11	1162(6)	6495(4)	-38(4)
C12	1160(7)	6081(4)	-798(4)
C13	5(7)	5875(4)	-1242(4)
C14	-1162(6)	6070(4)	-928(4)
C15	-1184(6)	6480(4)	-162(3)
C16	-1523(5)	8440(3)	1008(3)
C17	-939(6)	8805(3)	331(4)
C18	-1530(7)	9469(4)	-111(4)
C19	-2071(8)	9769(4)	119(5)
C20	-3299(7)	9430(4)	785(5)
C21	-2075(6)	8751(4)	1229(4)

C22	-2056(5)	6787(3)	2533(3)
C23	-2056(5)	6001(3)	2153(3)
C24	-2991(6)	5417(4)	2301(4)
C25	-3956(6)	5579(4)	2826(4)
C26	-3976(5)	6339(4)	3213(4)
C27	-3059(5)	6943(4)	3059(3)
C28	-398(5)	8118(4)	3840(3)
C29	89(5)	8837(4)	4225(4)
C30	395(6)	8866(5)	5099(4)
C31	225(6)	8189(5)	5599(4)
C32	-283(6)	7477(5)	5234(4)
C33	-580(6)	7436(4)	4366(4)

Table 7.3 Anisotropic temperature factors (Å x10^3).

Atom	U11	U22	U33	U23	U13	U12
Re1	29	30	30	3	3	3
Br1	48	45	51	13	-3	-11
C1	47(4)	33(4)	73(5)	0(3)	-2(3)	14(3)
C2	40(4)	65(5)	64(5)	14(4)	18(3)	27(4)
C3	34(4)	62(5)	76(5)	9(4)	-12(4)	13(3)
C4	46(4)	70(5)	49(4)	14(4)	-15(3)	24(4)
C5	46(4)	54(4)	56(4)	22(3)	13(3)	15(3)
C6	36(3)	34(3)	36(3)	-1(3)	14(3)	-4(3)
C7	29(3)	35(3)	23(3)	1(2)	1(2)	-4(3)
C8	28(3)	31(3)	31(3)	-1(3)	4(2)	5(3)
C9	32(3)	26(3)	36(3)	0(3)	-3(3)	4(2)
C10	44(3)	32(3)	31(3)	-2(3)	13(3)	-1(3)
C11	42(4)	71(5)	54(4)	-16(4)	16(3)	-12(3)
C12	67(5)	64(5)	64(5)	-18(4)	35(4)	1(4)
C13	89(5)	50(4)	44(4)	-16(3)	21(4)	-13(4)
C14	56(4)	66(5)	46(4)	-16(4)	5(3)	-10(4)
C15	40(3)	48(4)	37(4)	-6(3)	12(3)	1(3)
C16	34(3)	31(3)	27(3)	0(2)	-9(2)	0(3)
C17	55(4)	35(3)	39(4)	4(3)	1(3)	-1(3)
C18	78(5)	50(4)	44(4)	15(3)	-11(4)	-11(4)
C19	82(6)	43(4)	66(5)	8(4)	-29(4)	3(4)
C20	49(4)	49(4)	85(5)	-3(4)	-11(4)	15(4)
C21	44(4)	42(4)	49(4)	2(3)	-2(3)	2(3)
C22	34(3)	34(3)	20(3)	2(2)	1(2)	2(3)

C23	43(3)	39(3)	33(3)	0(3)	14(3)	0(3)
C24	54(4)	31(3)	49(4)	-2(3)	11(3)	-10(3)
C25	41(4)	45(4)	53(4)	10(3)	12(3)	-10(3)
C26	34(3)	60(4)	38(4)	15(3)	16(3)	7(3)
C27	33(3)	43(4)	36(3)	-2(3)	6(3)	7(3)
C28	31(3)	42(4)	31(3)	-8(3)	0(2)	9(3)
C29	44(3)	47(4)	38(4)	-10(3)	-1(3)	6(3)
C30	44(4)	73(5)	48(4)	-26(4)	-4(3)	8(4)
C31	48(4)	90(6)	31(4)	-14(4)	1(3)	9(4)
C32	53(4)	76(5)	36(3)	10(4)	4(3)	13(4)
C33	48(3)	49(4)	37(3)	-2(3)	3(3)	3(3)

Table 7.4 Hydrogen fractional atomic co-ordinates (x 10^4) and isotropic temperature factors ($Å^2$ x10^3).

	x	y	z	U
H11	1228(6)	5696(4)	1802(4)	62(4)
H21	3199(6)	6611(4)	1546(4)	62(4)
H31	3680(6)	7506(5)	2842(5)	62(4)
H41	2055(6)	7166(4)	3912(4)	62(4)
H51	503(6)	6068(4)	3270(4)	62(4)
H91	-608(35)	8667(9)	2669(21)	7(10)
H111	1979(6)	6647(4)	263(4)	62(4)
H121	1976(7)	5934(4)	-1018(4)	62(4)
H131	16(7)	5594(4)	-1777(4)	62(4)
H141	-1969(6)	5920(4)	-1242(4)	62(4)
H151	-2007(6)	6616(4)	54(3)	62(4)
H171	-119(6)	8593(3)	169(4)	62(4)
H181	-119(7)	9717(4)	-576(4)	62(4)
H191	-3111(8)	10224(4)	-193(5)	62(4)
H201	-4112(7)	9653(4)	946(5)	62(4)
H211	-3125(6)	8503(4)	1689(4)	62(4)
H231	-1389(5)	5867(3)	1781(3)	62(4)
H241	-2962(6)	4883(4)	2031(4)	62(4)
H251	-4610(6)	5168(4)	2919(4)	62(4)
H261	-4632(5)	6456(4)	3598(4)	62(4)
H271	-3117(5)	7479(4)	3319(3)	62(4)
H291	214(5)	9323(4)	3887(4)	62(4)

H301	738(6)	9370(5)	5355(4)	62(4)
H311	456(6)	8215(5)	6199(4)	62(4)
H321	-435(6)	7002(5)	5583(4)	62(4)
H331	-916(6)	6926(4)	4118(4)	62(4)

Table 7.5 Bond lengths (Å).

Br1-Re1	2.538(4)	C1-Re1	2.264(8)
C2-Re1	2.316(8)	C3-Re1	2.333(8)
C4-Re1	2.305(7)	C5-Re1	2.244(8)
C6-Re1	1.931(7)	C7-Re1	2.188(7)
C8-Re1	2.145(7)	C9-Re1	2.260(7)
C2-C1	1.420(9)	C5-C1	1.426(9)
C3-C2	1.396(10)	C4-C3	1.404(10)
C5-C4	1.406(9)	C7-C6	1.414(8)
C10-C6	1.459(8)	C8-C7	1.499(8)
C16-C7	1.477(8)	C9-C8	1.458(8)
C22-C8	1.472(8)	C28-C9	1.486(8)
C11-C10	1.400(8)	C15-C10	1.390(8)
C12-C11	1.372(9)	C13-C12	1.367(10)
C14-C13	1.367(9)	C15-C14	1.379(8)
C17-C16	1.396(8)	C21-C16	1.381(8)
C18-C17	1.389(9)	C19-C18	1.369(10)
C20-C19	1.372(10)	C21-C20	1.410(9)
C20-C21	1.410(9)	C23-C22	1.400(8)
C27-C22	1.394(8)	C24-C23	1.376(8)
C25-C24	1.365(8)	C26-C25	1.368(9)

C27-C26	1.386(8)	C29-C28	1.381(8)
C33-C28	1.398(8)	C30-C29	1.391(8)
C31-C30	1.364(10)	C32-C31	1.366(10)
C33-C32	1.382(9)	H21-C2	0.960
H31-C3	0.960	H41-C4	0.960
H51-C5	0.960	H91-C9	0.960(2)
H111-C11	0.960	H121-C12	0.960
H131-C13	0.960	H141-C14	0.960
H151-C15	0.960	H171-C17	0.960
H181-C18	0.960	H191-C19	0.960
H201-C20	0.960	H211-C21	0.960
H231-C23	0.960	H241-C24	0.960
H251-C25	0.960	H261-C26	0.960
H271-C27	0.960	H291-C29	0.960
H301-C30	0.960	H311-C31	0.960
H321-C32	0.960	H331-C33	0.960

Table 7.6 Bond angles (°).

C1-Re1-Br1	135.8(2)	C2-Re1-Br1	99.7(3)
C2-Re1-C1	36.1(2)	C3-Re1-Br1	84.6(3)
C3-Re1-C1	59.3(3)	C3-Re1-C2	34.9(2)
C4-Re1-Br1	105.1(3)	C4-Re1-C1	60.2(3)
C4-Re1-C2	59.2(3)	C4-Re1-C3	35.3(2)
C5-Re1-Br1	140.7(2)	C5-Re1-C1	36.9(2)
C5-Re1-C2	60.3(3)	C5-Re1-C3	59.4(3)
C5-Re1-C4	36.0(2)	C6-Re1-Br1	105.0(3)
C6-Re1-C1	85.3(3)	C6-Re1-C2	97.7(3)
C6-Re1-C3	132.3(3)	C6-Re1-C4	144.7(2)
C6-Re1-C5	110.7(3)	C7-Re1-Br1	94.4(2)
C7-Re1-C1	117.4(3)	C7-Re1-C2	137.6(2)
C7-Re1-C3	171.4(2)	C7-Re1-C4	151.9(2)
C7-Re1-C5	123.5(3)	C7-Re1-C6	39.8(2)
C8-Re1-Br1	113.2(2)	C8-Re1-C1	110.8(3)
C8-Re1-C2	146.9(2)	C8-Re1-C3	147.2(2)
C8-Re1-C4	111.9(3)	C8-Re1-C5	93.4(3)
C8-Re1-C6	71.7(3)	C8-Re1-C7	40.5(2)
C9-Re1-Br1	85.9(2)	C9-Re1-C1	133.8(2)
C9-Re1-C2	154.7(2)	C9-Re1-C3	122.8(3)
C9-Re1-C4	95.5(3)	C9-Re1-C5	100.1(3)
C9-Re1-C6	104.6(3)	C9-Re1-C7	65.5(3)
C9-Re1-C8	38.5(2)	C2-C1-Re1	73.9(4)
C5-C1-Re1	70.8(4)	C5-C1-C2	107.3(7)
C1-C2-Re1	70.0(4)	C3-C2-Re1	73.2(5)

C3-C2-C1	107.7(7)	C2-C3-Re1	71.9(4)
C4-C3-Re1	71.3(4)	C4-C3-C2	109.2(8)
C3-C4-Re1	73.5(4)	C5-C4-Re1	69.7(4)
C5-C4-C3	107.8(7)	C1-C5-Re1	72.3(4)
C4-C5-Re1	74.4(4)	C4-C5-C1	108.0(7)
C7-C6-Re1	79.9(4)	C10-C6-Re1	146.9(4)
C10-C6-C7	132.9(5)	C6-C7-Re1	60.3(4)
C8-C7-Re1	68.2(3)	C8-C7-C6	109.8(5)
C16-C7-Re1	133.6(3)	C16-C7-C6	126.3(6)
C16-C7-C8	123.5(5)	C7-C8-Re1	71.3(4)
C9-C8-Re1	75.0(4)	C9-C8-C7	109.0(5)
C22-C8-Re1	129.4(5)	C22-C8-C7	120.8(5)
C22-C8-C9	129.1(5)	C8-C9-Re1	66.4(4)
C28-C9-Re1	117.8(4)	C28-C9-C8	128.7(6)
C11-C10-C6	121.6(6)	C15-C10-C6	120.1(6)
C15-C10-C11	118.4(6)	C12-C11-C10	120.3(7)
C13-C12-C11	120.4(7)	C14-C13-C12	120.3(7)
C15-C14-C13	120.3(7)	C14-C15-C10	120.3(6)
C17-C16-C7	121.3(6)	C21-C16-C7	119.8(6)
C21-C16-C17	118.7(6)	C18-C17-C16	120.8(7)
C19-C18-C17	119.6(7)	C20-C19-C18	121.2(7)
C21-C20-C19	119.2(7)	C20-C21-C16	120.5(7)
C23-C22-C8	124.0(6)	C27-C22-C8	119.3(6)
C27-C22-C23	116.3(6)	C24-C23-C22	121.3(6)
C25-C24-C23	121.4(7)	C26-C25-C24	118.6(7)
C27-C26-C25	120.9(6)	C26-C27-C22	121.4(6)
C29-C28-C9	117.3(6)	C33-C28-C9	125.4(6)

C33-C28-C29	117.2(6)	C30-C29-C28	120.6(7)
C31-C30-C29	121.2(7)	C32-C31-C30	119.2(7)
C33-C32-C31	120.2(7)	C32-C33-C28	121.5(7)
H11-C1-Re1	120.6(3)	C2-C1-H11	126.4(5)
C5-C1-H11	126.3(5)	H21-C2-Re1	122.6(3)
H21-C2-C1	126.2(5)	C3-C2-H21	126.0(5)
H31-C3-Re1	123.1(3)	H31-C3-C2	125.5(5)
C4-C3-H31	125.3(5)	H41-C4-Re1	122.5(3)
H41-C4-C3	126.1(5)	C5-C4-H41	126.1(5)
H51-C5-Re1	119.1(3)	H51-C5-C1	126.1(5)
H51-C5-C4	125.9(5)	H91-C9-Re1	104.7(25)
H91-C9-C8	116.2(23)	C28-C9-H91	111.6(24)
H111-C11-C10	119.9(4)	C12-C11-H111	119.8(5)
H121-C12-C11	119.8(5)	C13-C12-H121	119.8(5)
H131-C13-C12	119.7(5)	C14-C13-H131	120.0(5)
H141-C14-C13	119.8(5)	C15-C14-H141	120.0(5)
H151-C15-C10	119.9(4)	H151-C15-C14	119.8(5)
H171-C17-C16	119.5(4)	C18-C17-H171	119.7(5)
H181-C18-C17	120.2(5)	C19-C18-H181	120.2(5)
H191-C19-C18	119.3(5)	C20-C19-H191	119.4(5)
H201-C20-C19	120.4(5)	C21-C20-H201	120.4(5)
H211-C21-C16	119.8(4)	H211-C21-C20	119.8(5)
H231-C23-C22	119.4(4)	C24-C23-H231	119.3(4)
H241-C24-C23	119.2(4)	C25-C24-H241	119.3(5)
H251-C25-C24	120.6(5)	C26-C25-H251	120.8(4)
H261-C26-C25	119.6(4)	C27-C26-H261	119.6(4)
H271-C27-C22	119.3(4)	H271-C27-C26	119.2(4)

H291-C29-C28	119.8(4)	C30-C29-H291	119.6(5)
H301-C30-C29	119.4(5)	C31-C30-H301	119.4(5)
H311-C31-C30	120.3(5)	C32-C31-H311	120.5(5)
H321-C32-C31	119.9(5)	C33-C32-H321	119.9(5)
H331-C33-C28	119.2(4)	H331-C33-C32	119.3(5)

Table 7.7 Selected non-bonded distances (Å).

Intramolecular:

H11	...Re1	2.874	H21	...Re1	2.946
H31	...Re1	2.968	H41	...Re1	2.935
H51	...Re1	2.838	H91	...Re1	2.671
C10	...Re1	3.252	C16	...Re1	3.379
C22	...Re1	3.283	C28	...Re1	3.233
C3	...Br1	3.281	C9	...Br1	3.276
H91	...Br1	2.894	H21	...C1	2.133
C3	...C1	2.275	C4	...C1	2.290
H51	...C1	2.137	C6	...C1	2.852
C2	...H11	2.135	C5	...H11	2.139
H31	...C2	2.104	C4	...C2	2.282
C5	...C2	2.293	C3	...H21	2.109
H41	...C3	2.118	C5	...C3	2.270
C4	...H31	2.110	H51	...C4	2.117
C5	...H41	2.118	C8	...C6	2.392
C11	...C6	2.495	C15	...C6	2.468
C16	...C6	2.588	C9	...C7	2.406
H91	...C7	2.506	C10	...C7	2.643
C17	...C7	2.504	C21	...C7	2.472
C22	...C7	2.582	H91	...C8	2.069
C16	...C8	2.261	C23	...C8	2.536
C27	...C8	2.474	C28	...C8	2.653
C22	...C9	2.645	C29	...C9	2.450

C33	...C9	2.563	H151	...C10	2.045
C28	...H91	2.045	C29	...H91	2.518
H111	...C10	2.055	C12	...C10	2.404
C13	...C10	2.770	C14	...C10	2.402
H121	...C11	2.028	C13	...C11	2.377
C14	...C11	2.752	C15	...C11	2.396
C10	...H111	2.055	C12	...H111	2.028
H131	...C12	2.023	C14	...C12	2.371
C15	...C12	2.752	C13	...H121	2.023
H141	...C13	2.023	C15	...C13	2.382
C14	...H131	2.025	H151	...C14	2.035
C15	...H141	2.036	H171	...C16	2.047
C18	...C16	2.421	C19	...C16	2.779
C20	...C16	2.422	H211	...C16	2.035
H181	...C17	2.047	C19	...C17	2.383
C20	...C17	2.765	C21	...C17	2.388
C18	...H171	2.042	H191	...C18	2.020
C20	...C18	2.388	C21	...C18	2.770
C19	...H181	2.029	H201	...C19	2.033
C21	...C19	2.399	C20	...H191	2.024
H211	...C20	2.062	C21	...H201	2.069
H231	...C22	2.049	C24	...C22	2.420
C25	...C22	2.816	C26	...C22	2.425
H271	...C22	2.044	H241	...C23	2.026
C25	...C23	2.391	C26	...C23	2.738
C27	...C23	2.373	C24	...H231	2.027
H251	...C24	2.030	C26	...C24	2.351

C27	...C24	2.734	C25	...H241	2.017
H261	...C25	2.022	C27	...C25	2.396
C26	...H251	2.034	H271	...C26	2.035
C27	...H261	2.039	H291	...C28	2.036
C30	...C28	2.408	C31	...C28	2.801
C32	...C28	2.426	H331	...C28	2.046
H301	...C29	2.042	C31	...C29	2.400
C32	...C29	2.751	C33	...C29	2.371
H311	...C30	2.026	C32	...C30	2.355
C33	...C30	2.728	C31	...H301	2.016
H321	...C31	2.024	C33	...C31	2.383
C28	...C32	2.426	C29	...C32	2.751
H331	...C32	2.032	C33	...H321	2.037

Intermolecular:

C32	...H331	2.032